Politecnico di Milano

SCHOOL OF INDUSTRIAL AND INFORMATION ENGINEERING

Master of Science – Energy Engineering

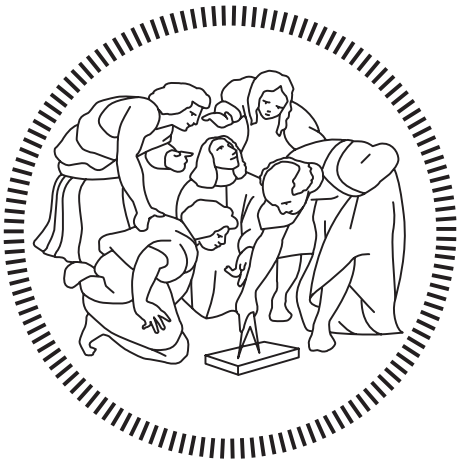

Techno-Economic Analysis of Biogas to Methanol Plants with Once Through Methanol Reactors

Supervisor

Prof. Matteo Carmelo ROMANO

Co-Supervisor

Dott. Riccardo RINALDI

Candidate

Emanuele CORSI – 913101

Academic Year 2019 – 2020

Ringraziamenti

Per quanto lungo possa sembrare il cammino un passo dopo l'altro ci si porta avanti. Ormai un percorso sta per giungere alla conclusione mentre un altro, molto più lungo, si intravede all'orizzonte. Prima di proseguire, è dal profondo del cuore che vorrei ringraziare la mia famiglia, per aver camminato al mio fianco tutto questo tempo.

Ringrazio mio fratello, per l'abbraccio che mi ha dato quella mattina di cinque anni fa, quando ho lasciato casa per andare a vivere a Milano. Non lo dimenticherò mai.

Ringrazio i miei nonni, tutti, per ogni volta che mi hanno pensato quando non c'ero e perché questo era assolutamente palese nei vostri occhi al mio ritorno.

Ringrazio i miei genitori, per aver reso possibile tutto questo. Un giorno vorrei essere in grado di dare quello che voi avete dato a me.

Grazie a tutti voi.

Sommario

Scopo del presente lavoro di tesi è di svolgere un'analisi tecnico economica su un impianto di produzione di metanolo di piccola taglia che sfrutta biogas proveniente dalla gestione di rifiuti. Oltre al tradizionale assetto di impianto che prevede il ricircolo di reagente nel reattore di sintesi è stata studiata la possibilità di adottare un reattore multistadio in configurazione once through.

Per entrambi i casi si è sviluppato un modello di impianto che adotta un reformer tubolare per la produzione del syngas necessario alla reazione di sintesi del metanolo. Particolare enfasi è stata data alla collocazione della sezione di separazione della CO_2: al fine di trovare il design ottimale sono state modellate varianti che praticano la cattura sia a monte che a valle del reformer. Vista la piccola taglia dell'impianto, non si è esclusa la possibilità di non praticare del tutto la separazione dell'anidride carbonica. Per la medesima ragione si è in prima istanza assunto che la purificazione finale del metanolo fosse praticata esternamente. Una sezione di purificazione a valle del processo è stata poi modellata per il solo assetto di impianto tradizionale ai fini di un confronto. Tutti i modelli di impianto sono stati realizzati tramite il software Aspen Plus®.

Analisi di sensibilità sul processo tradizionale hanno evidenziato come alti valori di ricircolo favoriscano la resa della reazione di sintesi e le prestazioni globali di impianto. In queste condizioni operative è possibile raggiungere elevate produttività anche adottando pressioni di sintesi minori, seppur sfavorevoli da un punto di vista termodinamico.

Circa il processo con reattore once through si è scoperto che adottare un raffreddamento marcato a cavallo di ogni stadio permette di estrarre maggiori quantità di prodotto utile e di migliorare le prestazioni dei singoli stadi di reazione.

L'assenza della separazione della CO_2 penalizza in ogni caso le prestazioni del reattore di sintesi in termini di resa e conversione del carbonio. Nel caso con reattore con ricircolo, una maggiore produttività ed efficienza globale del processo sono ottenute praticando la separazione a monte della reazione di reforming. Viceversa, nel caso di reattore once

through, risulta più conveniente collocare la sezione di separazione della CO_2 a valle del reformer.

I livelli di produttività del processo con reattore in configurazione once through sono del tutto comparabili con quelli del processo tradizionale con ricircolo.

Alla luce dei risultati tecnici delle simulazioni si è proceduto a valutare l'effettiva profittabilità degli impianti oggetto di studio tramite un'analisi economica. Dapprima sono stati valutati i costi di investimento relativi all'acquisto dell'apparecchiatura e i costi di produzione del metanolo, poi i principali indici economici di profittabilità (PBP, NPV e ROROI). Le funzioni di costo utilizzate per il reattore di sintesi sono state sviluppate in questo lavoro. Tutti gli assetti di impianto considerati risultano ampiamente profittevoli nell'arco di 25 anni di vita utile considerato, con NPV tra i 15 e i 21 M€. Le soluzioni più remunerative sono quelle che non praticano la separazione della CO_2 in virtù del risparmio sui costi fissi e operativi.

L'assetto ottimale per il processo BGTL in esame risulta essere quello che adotta un reattore con ricircolo senza ottimizzare la composizione del flusso reagente.

Si è infine riscontrato che l'introduzione di una sezione di purificazione del metanolo non ha effetti sulla reazione di sintesi ma migliora le prestazioni globali dell'impianto per via di un minore utilizzo di combustibile nel reformer. Ciò bilancia i costi aggiuntivi portando a risultati economici del tutto comparabili.

PAROLE CHIAVE: Methanol, Biogas, Once Through, Methanol Synthesis, CO_2 Separation, Economic Analysis, BGTL.

Abstract

Aim of the present thesis work is to perform a techno economic analysis of a small scale methanol plant processing biogas coming from waste treatment. Beside the traditional plant arrangement adopting unreacted feed recirculation, the possibility to adopt a multistage synthesis reactor in once through configuration has been studied.

Plant models developed for both cases provide the syngas necessary to perform the synthesis reaction by means of a tubular reformer. Emphasis has been given to the estimation of the optimal CO_2 separation section location: for this purpose plant variations adopting separation before and after the reforming reaction were modelled. Because of the small scale considered, the possibility to avoid this step at all was not excluded. For the same reason methanol purification has been assumed performed in an external purification hub. The impact of the integration of a purification section has been evaluated in a second moment only for the traditional arrangement. All plant models were realized through the Aspen Plus® software.

Results of the sensitivity analysis performed on the traditional arrangement confirmed that high values of recirculation favour the synthesis reaction yield and the overall plant performances. In such operating conditions significant production rates may be achieved even for lower and less favourable values of synthesis pressure. Concerning the once through alternatives, it has been discovered that a severe cooling between each stage operation allow to enhance reaction performances and to achieve higher amounts of product.

If CO_2 separation is not performed the synthesis reaction yield and carbon conversion are penalized by the non optimal syngas composition. With a traditional reactor, a higher productivity and process efficiency are obtained separating CO_2 before the reforming reaction. Vice versa CO_2 separation from produced syngas is more convenient if a multi stage once through reactor is adopted.

Recorded production rates for both the reactor configurations resulted to be comparable at all.

In the light of the technical results an economic analysis aimed to evaluate the effective plant profitability in each case of study. At first fixed investment costs and cost of methanol manufacturing have been computed, than the main profitability indexes (PBP, NPV and ROROI). Reactor cost functions adopted have been developed in this work. All the modelled plant arrangements resulted to be quite profitable in a life time of 25 years. NPV obtained range from 15 to 21 M€. The most profitable plant are the one avoiding CO_2 separation due to the fixed and operating cost saving.

The optimal layout for the considered BGTL process results the one adopting a traditional reactor without inlet syngas composition adjustment.

The introduction of a methanol upgrading section does not affect synthesis reaction but enhances the overall process performances due to a lower reformer biofuel consumption. The higher productivity mitigates the effect of the additional fixed and operating costs on plant economics.

KEY WORDS: Methanol, Biogas, Once Through, Methanol Synthesis, CO_2 Separation, Economic Analysis, BGTL.

Extended Abstract

1. INTRODUCTION

Diversification of energy sources plays a key role to reduce the dependence on fossil fuels in a scenario in which the primary energy demand is increasing worldwide. In the last years the shares of renewables and natural gas in the primary energy pool increased to record highs, making biogas an attractive sustainable carbon source. It can be used as fuel or in GTL processes to produce hydrocarbons or chemicals, like methanol. Because of its many uses, an annual growth rate of the global methanol market about 5.4% is forecast from 2019 to 2027, particularly in the eastern countries. Such chemical indeed is a key intermediate in the production of many synthetic materials and offers the possibility to turn waste CO_2 into a valuable product by hydrogenation. It can be also used as fuel or fuel additive.

The objective of this thesis work is to perform a techno economic analysis of a small scale methanol plant exploiting a sustainable biogas source. Beside the traditional plant arrangement adopting unreacted feed recirculation, the possibility to adopt a multistage synthesis reactor in once through configuration has been studied.

2. MODELLED PROCESS OVERVIEW

All the studied cases consider a 149.63 kmol/h inlet fresh biogas stream (CH_4 60% , CO_2 40%) coming from a biodigester. The process conceptual block flow diagram is reported in Figure 0.1.

Depending on the reformer heat requirement part of the inlet biogas stream is conveyed to the reformer furnace, where it is burnt as fuel with comburent air. If the CO_2 separation is adopted upstream the reformer operation, the main stream is moved towards an absorber using MDEA as solvent. This unit manages biogas composition in order to obtain a syngas stoichiometric module M equal to 2.1 at the synthesis reactor inlet. CO_2 rich solvent is regenerated in a stripper column while the purified biogas joins a pre heating line where it is heated up to 600°C by produced hot syngas.

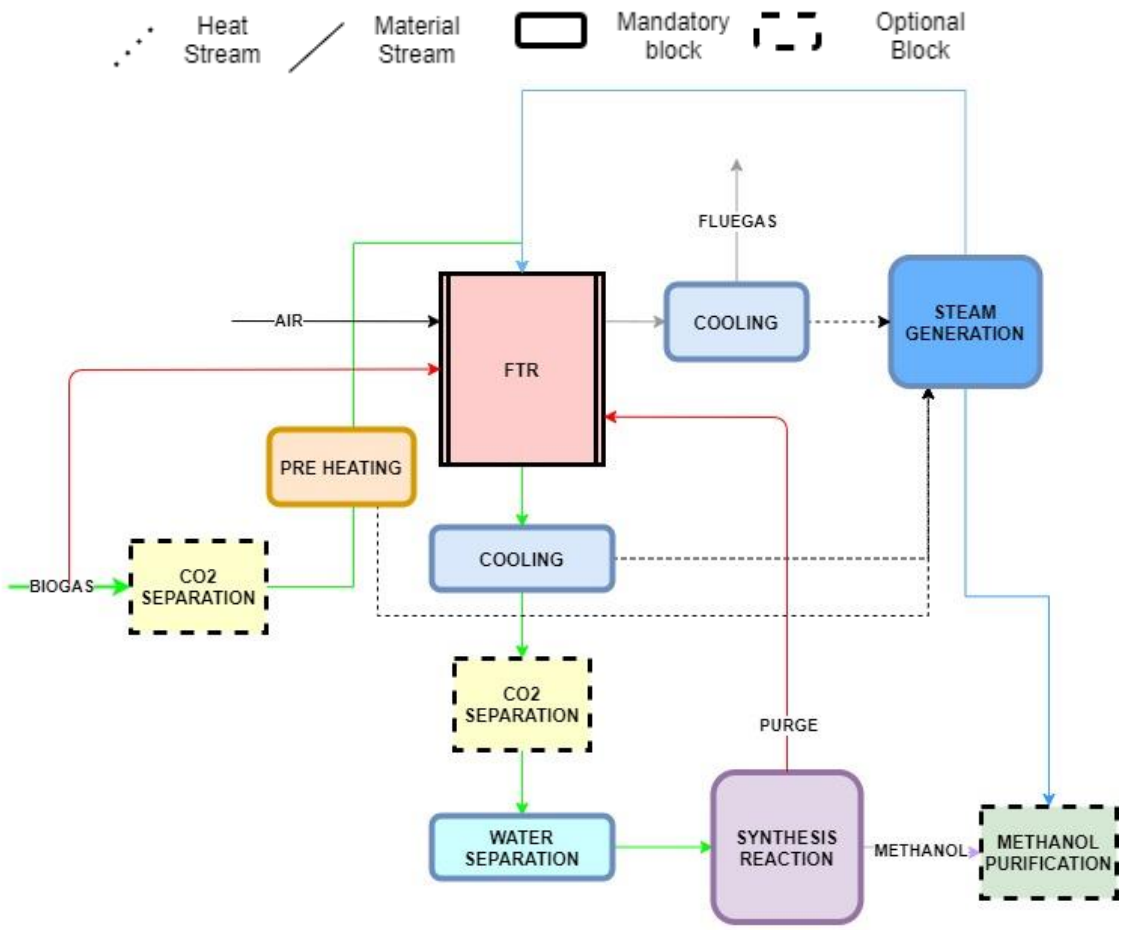

Figure 0.1: *process block flow diagram.*

Steam is added to the reformer inlet feed to perform the reaction with a S/CH_4 ratio equal to 3. Required steam is produced by thermal recovery from the hot sources available in the plant like produced syngas and reformer outlet flue gases, without further energy consumption. Both steam generation and biogas pre heating allow to cool down syngas temperature to 100°C. If CO_2 separation is performed downstream the reformer operation a further cooling using cold water is needed to reach lower temperatures, since high temperature operation promotes amines degradation. Excess water is separated by produced syngas in dedicated adiabatic flashes before the final compression to the synthesis reactor operating pressure.

The process described is analogous both when a traditional and a once through reactor configuration are adopted. Dealing with the traditional configuration, unreacted syngas is

separated from the synthesis reactor outlet stream after a partial cooling down to 30°C and then recirculated through a compressor. Part of the separator overheads are recycled as purge to the reformer furnace to reduce biofuel consumption. Produced crude methanol is obtained from the separator bottom liquid. A simple scheme is provided in Figure 0.2.

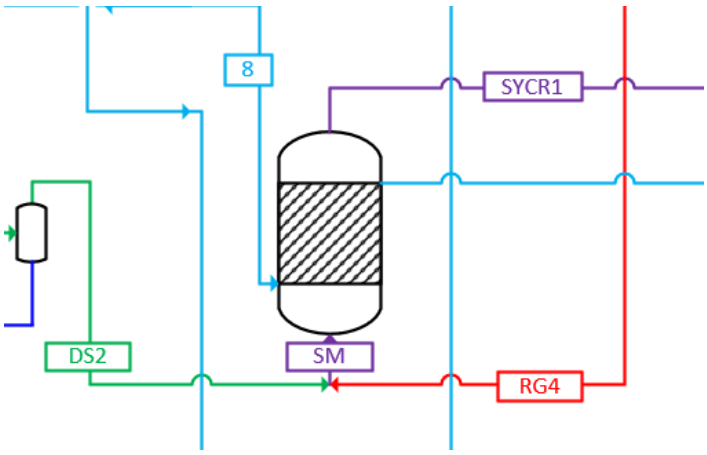

Figure 0.2: *scheme of the modelled traditional synthesis reactor with recirculation.*

As far as the once through configuration is concerned the synthesis is split in 4 stages. Between each stage, the reacting stream is cooled down to 30 °C, produced methanol is separated in an adiabatic flash and the unreacted syngas is fed to the following stage. A progressively reduced number of catalytic tubes is adopted due to the reducing flow rate. Produced crude from all the reaction stages is conveyed to a final flash where lighter components may be separated from the final product to be burnt in the reformer furnace as fuel. A scheme of the once through multi stage reactor is provided in Figure 0.3.

A total of 500 tubes is implemented in both the reactor configurations considered. The reaction heat release is controlled using boiling water as thermal fluid. Steam produced in this way is sent to the steam generation section where a certain degree of superheating is reached.

When a purification section is integrated, the produced crude stream is fed to a two distillation column system. In the first one, lighter component are separated at the top and conveyed to the furnace as further purge stream. The second is mainly devoted to water

separation. A 99% methanol purity is obtained in this section. Steam required from the columns bottom reboiler is provided from the steam generation section.

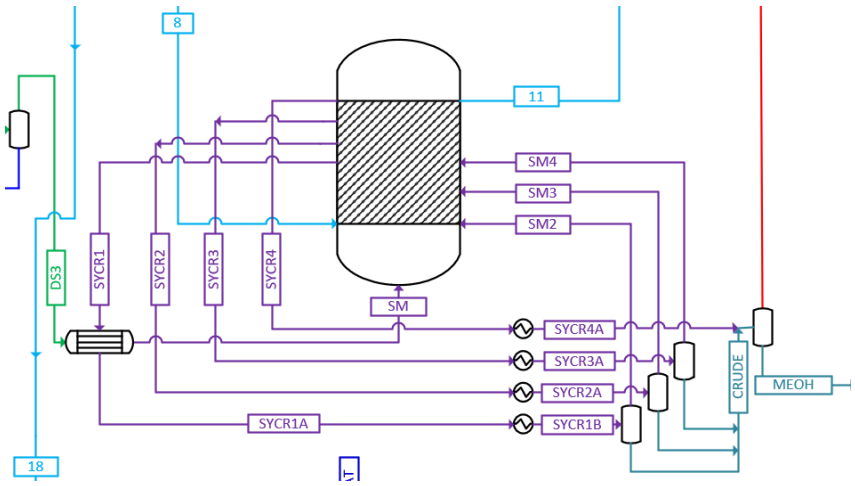

Figure 0.3: *scheme of the modelled once through multi stage synthesis reactor*

3. METHOD

Plant models and simulations have been performed using the Aspen Plus® software. As far as the thermodynamic model is concerned, a number of works for chemical equilibria in methanol synthesis from syngas indicate that the Redlich – Kwong – Soave (RKS) EoS gives best results in correcting non ideal gas behaviours [64, 65, 66]. This EoS has been chosen for the gas phase. Dealing with the liquid phase, the Non Random Two Liquid model equation (NRTL) was implemented. This model is suitable for the prediction of VLE and LLE for a wide range of hydrocarbon mixtures [68].

Plant performances have been evaluated mainly according to three indicators. The plant fuel efficiency quantifies the performance of the overall process. It can be defined as the ratio between outlet methanol thermal power and the plant inlet biogas one according to

$$\eta_{\text{fuel}} = \frac{\dot{n}_{\text{product}} \cdot x_{CH_3OH} \cdot LHV_{CH_3OH}}{\sum_{i=1}^{nc_{biog_{in}}} (\dot{n}_i \cdot LHV_i)}$$

Eqn. 0.1

Where $\dot{n}$ is a molar flow rate, x and LHV the molar fraction and the lower heating value of the specified species. Reaction performances have been evaluated mainly in terms of

reaction yield and carbon conversion. The reaction yield is computed as the methanol molar flow produced in a reference control volume over the available convertible carbon molar flow at the inlet. Depending on the control volume boundaries, this parameter may refer to the total reaction yield, η_{tot}, the single stage yield η_{stage} or to the contribution of a certain stage to the total yield $\eta_{\mathrm{tot}_{\mathrm{stage}}}$. In particular η_{stage} considers the amount of converted methanol respect to the available carbon at the stage inlet, while $\eta_{\mathrm{tot}_{\mathrm{stage}}}$ considers the available carbon at the beginning of the reaction. Similarly, the carbon conversion is defined as the amount of carbon converted respect to the available amount

$$\begin{cases} \eta_{\mathrm{tot/stage/tot_{stage}}} = \dfrac{\dot{n}_{\mathrm{CH_3OH}_{out}} - \dot{n}_{\mathrm{CH_3OH_{in}}}}{\dot{n}_{\mathrm{CO_{in}}} + \dot{n}_{\mathrm{CO_{2in}}}} \\ \varepsilon_C = \dfrac{(\dot{n}_{\mathrm{CO_{in}}} + \dot{n}_{\mathrm{CO_{2in}}}) - (\dot{n}_{\mathrm{CO_{out}}} + \dot{n}_{\mathrm{CO_{2out}}})}{\dot{n}_{\mathrm{CO_{in}}} + \dot{n}_{\mathrm{CO_{2in}}}} \end{cases}$$

Eqn. 0.2

Where the subscripts in and out are referred to the control volume boundaries and $\dot{n}$ the molar flow rate of the specified species.

The procedure to perform the economic analysis is suggested by Turton et al. [20]. According to the reference, when evaluating the economic feasibility of a certain plant at first fixed capital investment (FCI) and cost of manufacturing (COM) have to be computed. With these information it is possible to proceed with the profitability analysis, whose goal is to provide economic indicators as PBP, NPV and ROROI.

The overall fixed capital investment related to the equipment purchase mainly depends on each unit size. The impact of size on cost value may be expressed with an exponential law

$$\log\left(C_{\mathrm{p}}^{\mathrm{o}}\right) = K_1 + K_2 \cdot \log(A) + K_3 \cdot (\log(A))^2$$

Eqn. 0.3

Where the terms K represent fitting parameters proper of each component, A is the reference capacity and $C_{\mathrm{p}}^{\mathrm{o}}$ the purchased cost in base conditions. Such value requires to be updated to take into account also the effect of operating pressure and construction material. These

factors are strictly related to the considered piece of equipment such that and ad hoc correlations have to be adopted. When building a plant additional costs related to the component installation, unforeseen circumstances and fees should be accounted. By including all these cost contributions it is possible to achieve the plant grassroots cost. The last factor affecting the capital investment is inflation, which can be handled through the Chemical Plant Cost Index (CEPCI). Assuming to purchase the equipment in 2019

$$C_{2019} = C_{\text{ref}} \cdot \frac{I_{2019}}{I_{\text{ref}}}$$

Eqn. 0.4

Where I is the specific year CEPCI, C the grassroots and the subscript ref identifies a reference year. In the end the FCI results to be

$$FCI\ [\$] = \sum_{\text{i}=1}^{\text{n=n°of units}} C_{\text{i}_{2019}}$$

Eqn. 0.5

Particular attention has been dedicated to the synthesis reactor cost function, since, due to the small scale considered, it was challenging to find in literature a suitable one. The reactor chosen is of Lurgi kind, which basically consists of a shell containing catalysed tubes surrounded by thermal fluid. Thus, its configuration may be assimilated to a Shell&Tube heat exchanger [59].

With this assumption it has been possible to develop a further reactor model with Aspen EDR® software, which provided cost data for several values of heat exchange area. The resulting cost trend resulted to be linear, as for modular technologies, due to the dependence

on the number of tubes. From a linear regression it was possible to achieve several cost correlations for different reactor geometries and operating pressures in the form

$$C_{\mathrm{tot}} = C_{\mathrm{o}} + m \cdot A_{\mathrm{exch}}$$

Eqn.0.6

Tube lengths between 4 and 6 m, commercial tube diameters between 25 and 47 mm and pressure values from 50 to 93 bar have been considered. Figure 0.4 shows how a linear interpolation well suits achieved cost data.

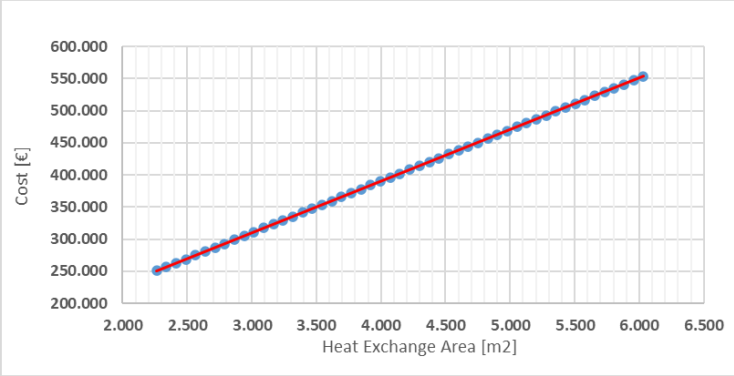

Figure 0.4: *linear interpolation of synthesis reactor cost data (tube length 6 m, tube diameter 42 mm, pressure 93 bar).*

As far as the cost of manufacturing is concerned, for the studied plant it may be computed according to

$$COM\ \left[\frac{\$}{year}\right] = 0.180 \cdot FCI + 2.73 \cdot C_{\mathrm{ol}} + 1.23 \cdot (C_{\mathrm{ut}} + C_{\mathrm{rm}})$$

Eqn. 0.6

Where C_{ol} is the operating labour costs, accounting for the operators salary, C_{ut} is the utility cost (in this case electricity and cooling water) and C_{rm} the raw material cost. This latter accounts for catalyst and MDEA replacement and fresh water consumption. Biogas cost is assumed to fully recovered from the incomes of the waste treatment.

By knowing plant productivity and costs it is possible to assess its profitability. This may be done according to three possible criteria, each corresponding to an economic index which

focuses on different aspects. Revenues from methanol retail have been computed assuming a selling price equal to 500 €/tons$_{MeOH}$ [10].

- Interest Rate Criterion

$$RORO I\ [\frac{\%}{year}] = \frac{\sum_{\text{working period}} \cdot CF_{\text{k}}}{(k_{\text{end wp}} - k_{\text{end bp}}) \cdot (FCI - S)}$$

Eqn. 0.7

Where $k_{\text{end wp}}$ and $k_{\text{end bp}}$ are the end of life year and the end of building phase year. S is the assumed salvage value. According to such criterion, the higher is the *ROROI*, the more profitable is the investment.

- Cash criterion

$$NPV\ [M€] = \sum_{\text{k=0}}^{\text{k=k}_{\text{end wp}}} CF_{\text{Discounted}_{\text{k}}}$$

Eqn. 0.8

Where CF is the yearly discounted cash flow. The higher is the NPV, the more profitable is the investment.

- Time criterion

$$PBP = \left(k^* - k_{\text{end bp}}\right) + \frac{C_{\text{land}} + WC}{NPV_{\text{k}^*} - NPV_{\text{k}^{*-1}}}$$

Eqn. 0.9

Where *WC* is the working capital, C_{land} the land cost and k^* the last year of negative cumulative cash flow (NPV). The shorter is the PBP, the more profitable is the investment

4. RESULTS

In terms of performances, the optimal location of the CO_2 separation section resulted different depending on the reactor configuration adopted. With a traditional reactor the best reaction performances were achieved by separating CO_2 after the reformer

operation, with a 98.2% of reaction yield. However the higher biogas consumption and purge stream necessary to sustain the reformer reaction penalized the overall productivity and fuel efficiency (respectively 21906 tons/year and 65.2%). Therefore the best design choice resulted the CO_2 separation upstream the reformer operation with a reaction yield of 96.6%, a fuel efficiency of 65.7%, and a yearly production of almost 23000 tons/year. Table 0.1 shows a summary of the recorded main results for this arrangement.

	Post Reformer CO_2 Separation	***Pre Reformer CO_2 Separation***	***No Separation***
Total reaction yield η_{tot} [%]	98.2	96.6	77.7
Fuel efficiency η_{fuel} [%]	65.2	65.7	65.3
Biofuel to the furnace [%]	31	29	34
Methanol yearly production [tons/year]	21906	22968	22821

Table 0.1: *reaction performances and overall plant efficiencies comparison for the traditional configuration.*

As for the once through reactor configuration, according to the main results reported in Table 0.22 the best reaction performances are coherently obtained when the CO_2 separation is performed downstream the reformer. In this case the H_2 richer purge stream recycled to the reformer furnace reduces the biogas consumption in the reformer burners, such that the effect of a more efficient reaction results in higher productivity levels and overall plant fuel efficiency (22836 tons/year and 65.4%).

		Post Reformer CO_2 Separation	***Pre Reformer CO_2 Separation***	***No Separation***
Single stage yield η_{stage} [%]	Stage 1	69.6	61.8	52.6
	Stage 2	63.9	46.7	44.5
	Stage 3	53.6	45.5	35.9
	Stage 4	69.6	61.8	52.6
Total yield contribution $\eta_{tot_{stage}}$ [%]	Stage 1	69.6	61.8	52.6
	Stage 2	11.7	10.6	11.8
	Stage 3	2.6	4.3	3.4
	Stage 4	1.3	2.7	2
Total reaction yield η_{tot} [%]		84.8	77.9	69.0
Fuel efficiency η_{fuel} [%]		65.4	64.7	64.7

Biofuel to the furnace [%]	14	21	26
Methanol yearly production [tons/year]	22836	22608	22596

Table 0.2: *reaction performances and overall plant efficiencies comparison for thee once through arrangement.*

Focusing on the single stage performances the first stage is the one with the highest reaction yield and produced methanol amount. This is related to the fact that it is fed with the highest syngas flow rate in optimal conditions (stoichiometric module equal to 2.1). Due to product separation the following stages inlet feed is progressively reduced, together with the converted methanol amount. CO_2 consumption during the synthesis reaction and CO_2 entrainment in the separated product stream strongly reduce carbon availability in the following stages, affecting their performances.

As the reaction proceeds a certain reduction in the single stage yields may be noticed except for the last stage, where the lack of available carbon brings to an apparent performance improvement according to Eqn. 0.2. However looking at the total yield contribution per stage, it is evident that only a minimum amount of methanol is converted in the last steps, such that adopting more than four stages will be useless.

The non-optimal syngas stoichiometric module is detrimental for the synthesis reaction independently of the location of the CO_2 separation. However, due to the small scale considered, the fixed investment and operating costs saving related to the absence of the separation section have a significant economic impact on plant profitability. Yearly cash flows are higher despite the lower productivity, resulting in ROROI over 30% , PBP around 2 years, and NPV greater than 19 M€. A global summary between all the studied cases is reported in Figure 0.6 and Figure 0.5.

Both adopting traditional and once through reactors obtained results are comparable, confirming the latter as a potential valid alternative.

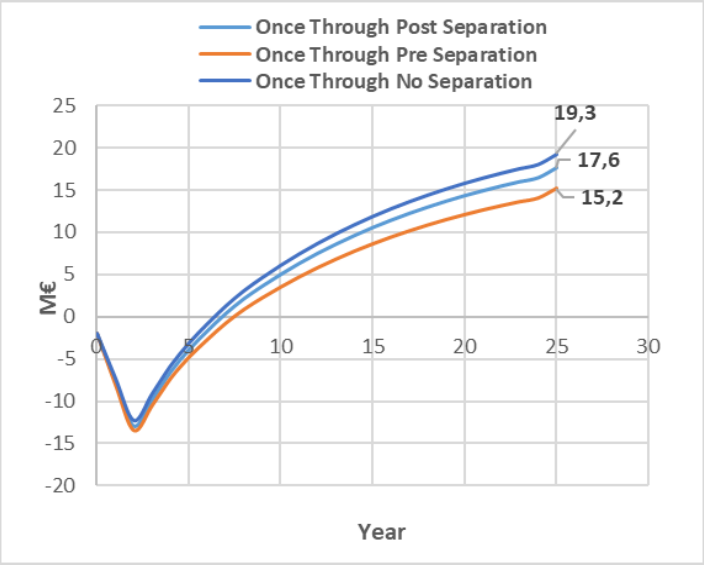

Figure 0.6: *once through configuration NPV comparison.*

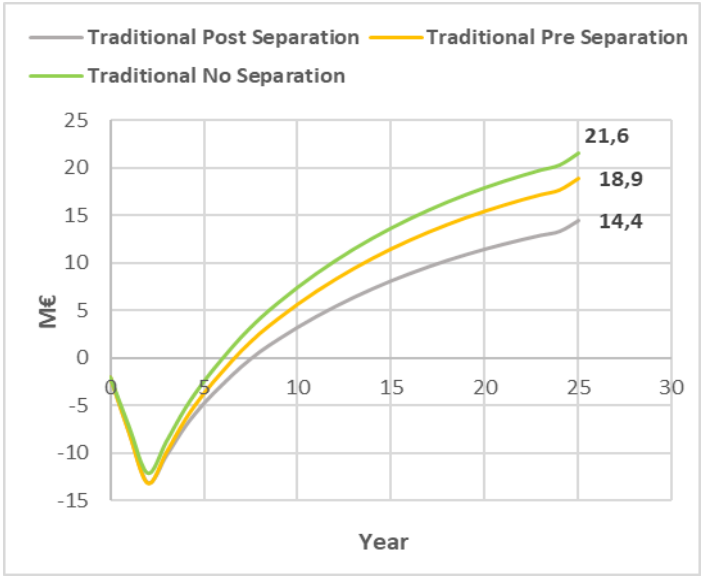

Figure 0.5: *traditional configuration NPV comparison.*

An important consideration about the once through reactor arrangement has to be highlighted. From the temperature profile reported in Figure 0.7 it can be noticed that before reaching the reaction temperature, the first stage reacting fluid has a temperature peak about 320 °C, detrimental for the catalyst resistance. Moreover, it exceeds the upper limit of the adopted kinetic model validity range (280°C). This phenomenon interests only the first stage since the greatest part of the conversion takes place there, with a consequent much more intense reaction heat release to be handled.

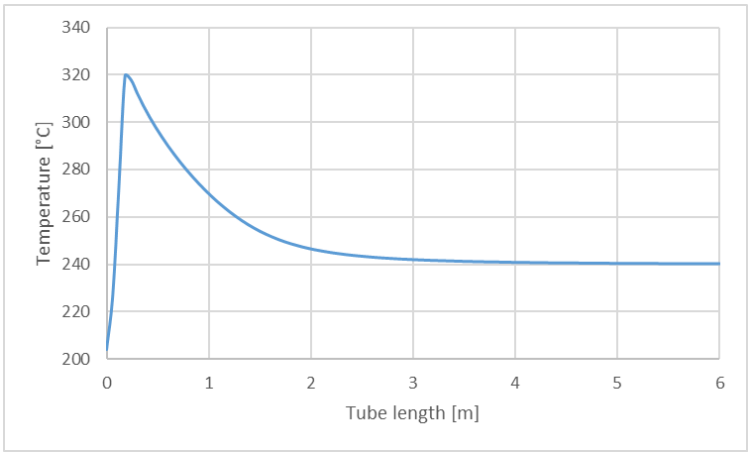

Figure 0.7: *first reaction stage reacting fluid temperature profile.*

Aiming to mitigate the temperature peak the effect of an enhanced reactor heat exchange coefficient has been studied. Even doubling the reactor heat exchange coefficient from 600 to 1200 W/m^2K the temperature peak decreased only by 16 °C. If smaller tubes are adopted, the surface to volume ratio will increase, augmenting the available heat exchange area. This is helpful to obtain a further peak reduction, but a temperature decrease only about 23 °C was achieved, still not sufficient to respect the kinetic model limit.

5. CONCLUSIONS

The CO_2 separation section affects plant performances and its optimal location in the plant depends on the reactor configuration adopted. In terms of profitability, due to the small scale considered, it is always better avoiding the investment for the CO_2 separation section. A small technical and economic convenience has been noticed implementing traditional reactors with recirculation but the once through configuration resulted to be a valid alternative. Further developments could aim to improve this solution.

Index

List of Figures

List of Tables

1. INTRODUCTION

It is well known that the primary energy demand is increasing worldwide together with the economic growth of emergent countries. Indeed, a strict relation between GDP, primary energy consumption and CO_2 emissions does exist. Rapid industrialization and modernization have amplified energy demands, exacerbating critical social issues like global warming and climate change, due to the use of fossil fuels for energy supply [3]. In 2015 the Paris Agreement was ratified, setting out the common goal to limit global warming and the increase in the global average temperature to well below 2°C, pursuing efforts to limit it to 1.5°C. Figure 1.1 shows the trend of the primary energy world consumption per energy source which rises continuously with the exception of the 2008 economic crisis. A further negative peak, even worse than the 2008 one, has been recorded in the first quarter of 2020 due to the Covid-19 pandemic crisis: the impact on global economy in fact brought to a decline of 3.8% of the global primary energy demand, with the forecast CO_2 emission decreasing by 8% [46].

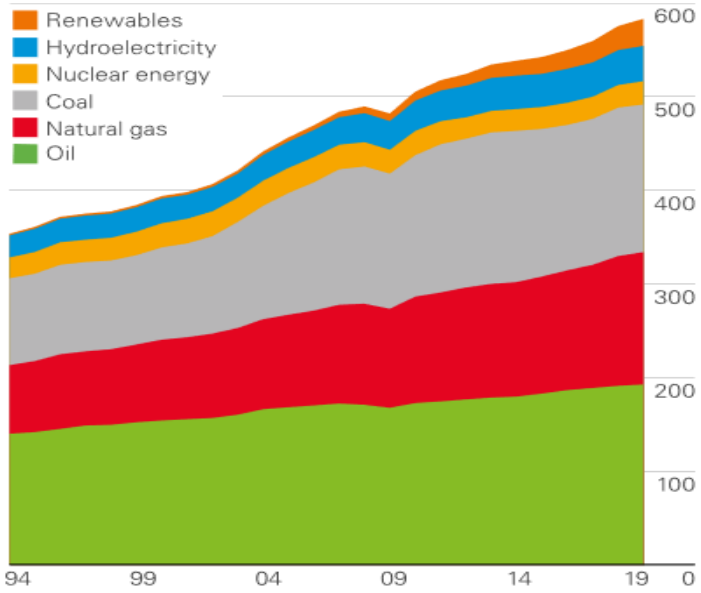

Figure 1.1: *Primary energy world consumption in Exajoule* [27].

Looking in particular at 2019 data, primary energy consumption rose by 1.3%, below its 10-year average rate of 1.6% per year, and it is weaker than the 2.8% growth seen in 2018. By region, consumption fell in North America, Europe and CIS and was below average in South & Central America. Demand growth in Africa, Middle East and Asia was roughly in line with historical averages. China was by far the biggest individual driver of primary energy growth, accounting for more than three quarters of net global growth. India and Indonesia were the next largest contributors, while the US and Germany posted the largest declines in energy terms [27].

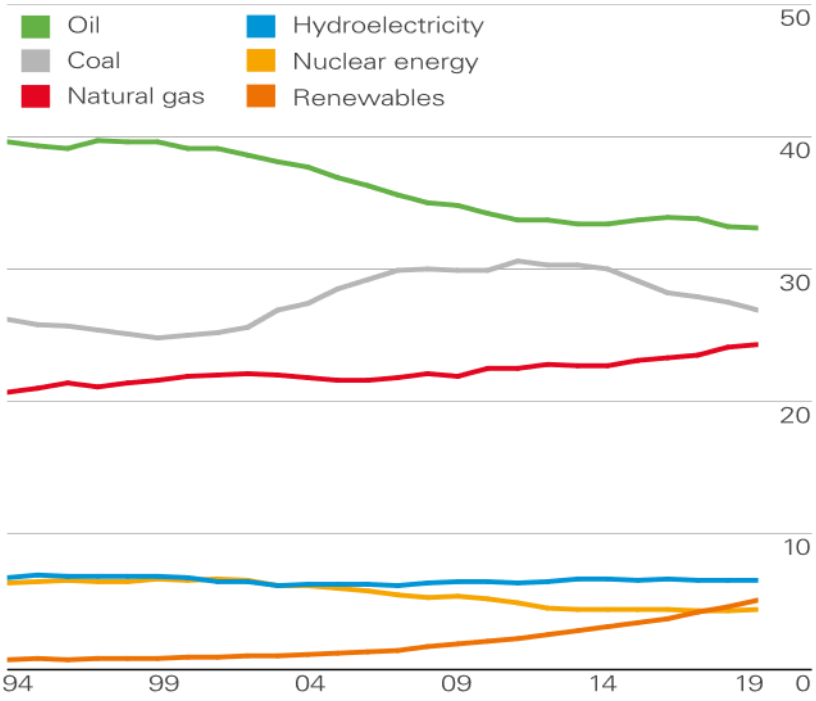

Figure 1.2: *Shares of global primary energy consumption by fuel* [27].

The greatest part of the world primary energy demand is still satisfied by fossil fuels due to many reasons, like for instance high energy density and chemical stability or immediate availability. In spite of this aspect, the key to reduce the dependence on fossil fuels and consequently GHG emissions is diversification of energy sources [26]. Looking at energy by fuel in Figure 1.2, 2019 growth was driven by renewables, followed by natural gas, which together contributed over three quarters of the net increase. The share of both renewables and natural gas in primary energy increased to record highs. Meanwhile, coal consumption declined, with its share in the energy mix falling to its lowest level since 2003 [27].

The combination of slower growth in energy demand and a shift in the fuel mix away from coal and toward natural gas and renewables led to a significant slowdown in the growth of carbon emissions [25]. Actually, progressing toward a more sustainable use of energy resources essentially requires a higher share of renewable sources into the energy pool, with the exploitation of new different options for energy vectors and alternative fuels which can guarantee a high energy density and easy long-term storage [3].

In this context biogas is an attractive renewable carbon source and its exploitation would be advantageous from both economic and environmental points of view [3]. Given the favourable perspective of the conversion of biomass residues and other organic materials into bioenergy, it comes as no surprise that the production of biogas is constantly growing. The number of biogas installations currently exceeds 35 million [28], mostly comprised of household installations in Asian countries like China and India. Larger farm digesters are mostly found in industrial countries in the Europe and North America. Production of bioenergy is projected to increase significantly to reach 108 exajoules (EJ) in 2030. This is twice the current level and it would represent 20% of the total primary energy supply and 60% of the final renewable energy use [28].

Biogas Source	Compound Content				CH_4/CO_2
	CH_4 (%vol)	CO_2 (%vol)	H_2S (ppm)	Other (%vol)	
Landfills gas recovery plants	45–55	30–40	n.a.	5-15 N_2	1.1–1.8
Municipal landfills (Finland)	47–62	37–41	27–32	n.a.	1.1–1.7
Wastewaters treatment plants	60–70	30–40	10–2000	<1% N_2	1.5–2.3
Municipal solid waste treatment plant (South Korea)	62	37	1300	n.a	1.7
Hurma wastewater treatment plant (Turkey)	61–67	33–39	n.a.	n.a.	1.6–2.1
Agricultural and industrial waste co-digestion plants:					
40% Fatty sludge from biodiesel production, 45% glycerine, 15% Cattle manure (Germany)	55–67	32–41	268–3174	0.1–0.7 N_2 0.1–0.2 O_2	1.3–2.1
87% biowaste, 10% green and brunch, 3% husk (Germany)	44–60	32–44	11–1572	0.1–19 N_2 0.1–2.9 O_2	1.0–1.9
Grass and Maize (Germany)	56–65	38–40	500–1000	n.a.	1.4–1.7

Table 1.1 *Chemical composition of biogas from different sources* [3].

Biogas is generally produced in different environments by anaerobic digestion of organic waste, such as livestock manure, sewage sludge, industrial and municipal refuses [56]. Its

composition strongly varies depending on the process adopted and on the chemical properties of the feedstock, as reported in Table 1.1 [30].

Such variability in terms of composition represents the main problem related to the direct use of biogas in internal combustion engines and gas turbines, essentially due to toxic emissions and low efficiency [31]. A promising alternative therefore consists in the production of syngas by reforming process in order to obtain a mainly H_2-CO based mixture which can be used directly as a fuel or also be further treated. Usually, the syngas obtained by biogas reforming may be applied to Gas-to-Liquid processes to produce liquid hydrocarbons or to synthesize chemicals, like methanol [31].

During the last years the interest in this chemical in particular has grown, such that an annual growth rate of the global methanol market about 5.4% is forecast from 2019 to 2027 [35]. Methanol is indeed one of the first building blocks in a wide variety of synthetic materials that make up many modern products and is also used as a fuel and a fuel additive. It offers also a convenient solution for an efficient energy storage and the possibility to turn CO_2 waste from industry into a valuable product by hydrogenation [2,6]. In the end, methanol production could be an important outlet for enhancing the value of natural gas and biogas and for the shift toward alternative and more sustainable energy sources [10].

Aim of this thesis work is to evaluate the techno-economic feasibility of a small scale Biogas-to-Liquid plant producing just methanol. Several plant arrangements have been simulated in different operating conditions with the purpose to establish the best case. Particular attention has been dedicated to the methanol synthesis reactor with the purpose to establish a realistic value of cost despite the unusual small size.

1.1 THESIS OUTLINE

The following chapter will provide more details concerning methanol and its applications, with some hints about methanol market and the state of art of methanol production processes from biogas. Chapter 3 deals with the description of the studied processes and the implemented plant variations, with a focus on the modelling details adopted in Aspen Plus. In Chapter 4 the main technical Key Performance Indicators and the whole procedure of the economic analysis are described. Particular emphasis has been dedicated to the achievement of suitable cost correlations for the synthesis reactor. A discussion on the choice of the EoS to be adopted in the simulation is also reported. Technical results are entirely discussed in Chapter 5 while economic considerations are reported in Chapter 6 . Chapter 7 provides a summary of the conclusions achieved in the present thesis work and suggests some possible further developments.

2. METHANOL PRODUCTION PROCESSES FROM BIOGAS

2.1 METHANOL

2.1.1 General Aspects and Properties

Methanol, or methyl alcohol, is an organic compound whose chemical structure is CH_3OH. It one of the simplest alcohols and it has been produced and used for millennia. The ancient Egyptians, for instance, produced it through pyrolysis and the main application was in the embalming process. However, it was not until 1661 that Robert Boyle produced pure methanol through further distillation, and only in 1834 was the elemental composition determined by Jean-Baptiste Dumas and Eugene Peligot [6].

The chemical structure and some of the main properties of this molecule may be appreciated in Table 2.1

Fuel	Methanol
Structure	CH_3OH
Molecular weight	32.04
O_2 (wt%)	50
LHV[a] (MJ/L)	15.8
Stoichiometric air/fuel ratio	6.46
Boiling point (°C)	64.7
RON	109
MON	89
ΔH_{vap} (kJ/kg from 25 °C)	1168
Solubility in water at 25 °C, wt%	Miscible
Specific gravity at 20 °C	0.792

Table 2.1 *Methanol properties* [32].

The presence of the hydroxyl group implies a low calorific value when compared to methane and due to the oxygen/hydrogen bound and its polarity it appears liquid at ambient temperature. Looking at the high Research Octane Number a certain predisposition to be used as anti – knock additive or directly as fuel in internal combustion engines may be noticed. It in fact allows to compress more the air/fuel mixture with less risk of autoignition in the chamber [33, 34].

As far as potential safety problems are concerned flammability and toxicity of methanol must be reported. Methanol indeed presents an ignition temperature about 470 °C and a saturated vapor pressure at 20 °C about 128 kPa. Methanol vapor is flammable at concentrations from 5,5 vol% to 44 vol%. A saturated air-methanol mixture is thus flammable over a wide temperature range. Storage facilities must be provided with fire-extinguishing equipment such as powder, carbon dioxide, foams or Halon. Water is unsuitable as extinguishing agent in presence of large amounts of methanol because it is miscible with the compound. Moreover, formaldehyde and carbon monoxide form when methanol burns with lack of oxygen, exacerbating the risk of toxic inhalations [47].

2.1.2 Methanol Applications

As already introduced methanol could be used both as an intermediate product in the production chain of a wide range of chemicals and synthetic materials or as a fuel or fuel additive. Some of the most common applications are reported in Figure 2.1 and a brief description for each one has been provided.

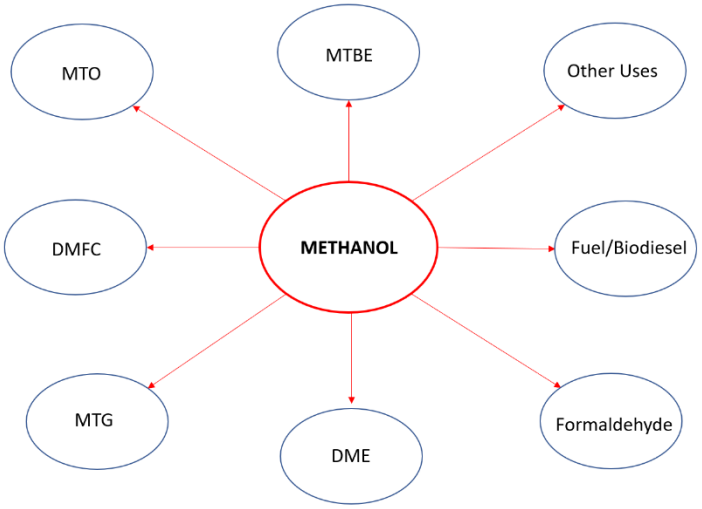

Figure 2.1 *Some methanol applications.*

1. **MTBE:** Methyl tert-butyl ether (MTBE), also known as tert-butyl methyl ether, is an organic compound with a structural formula $(CH_3)_3COCH_3$. MTBE is a volatile, flammable, and colourless liquid that is sparingly soluble in water. Primarily used as a fuel additive, MTBE is blended into gasoline to increase knock resistance and reduce unwanted emissions. However, mainly due to groundwater contamination concerns MTBE was banned in several U.S. states and gradually phased out of the country. Other countries that have banned MTBE include Japan and Canada, but its use has continued unhindered in much of the rest of the world, with China being its largest market [36].
2. **FORMALDEHYDE:** Formaldehyde is a colourless poisonous gas synthesized by the oxidation of methanol and used as an antiseptic, disinfectant, histologic fixative, and general-purpose chemical reagent for laboratory applications. Formaldehyde is readily soluble in water and is commonly distributed as a 37% solution in water; formalin, a 10% solution of formaldehyde in water, is used as a disinfectant and to preserve biological specimens. Environmentally, formaldehyde may be found in the atmosphere, smoke from fires, automobile exhaust and cigarette smoke. Small amounts are produced during normal metabolic processes in most organisms, including humans. Its production is one of the largest applications of methanol [41].

3. **DME:** DME (or Dimethyl Ether) and bio-DME have a number of uses in products and are most commonly used as a replacement for propane in liquid petroleum gas (LPG), but can also be used as a replacement for diesel fuel in transportation. Diesel fuel contains more energy per gallon than the gasoline adopted in most passenger cars, and where pure methanol would not be able to power a diesel engine with the same effectiveness, DME can. Today DME is primarily produced by converting hydrocarbons via gasification to synthesis gas. Synthesis gas is then converted into methanol in the presence of catalyst (usually copper – based), with subsequent methanol dehydration in the presence of a different catalyst (for example, silica-alumina) resulting in the production of DME. Besides being able to be produced from a number of renewable and sustainable resources, DME also holds advantage over traditional diesel fuel because of its high cetane number, which measures the combustion quality of diesel fuel during compression ignition. By combusting more thoroughly, an engine tailored to run on DME can achieve higher efficiencies, better mileage and emissions reductions [8,37].
4. **MTG:** MTG stands for methanol to gasoline process. It was developed in response to the 1970's energy crisis when oil and its derivative prices rose dramatically. Basically, once dehydration of methanol into DME is performed, it is promoted its conversion into light alkenes and gasoline range hydrocarbons. Interest in MTG decreased when oil prices dropped again, yet due to the need for alternative fuels a renewed interest recently grew [38,43].
5. **MTO:** MTO stands for methanol to olefins process. It was developed by Exxon Mobil in 1977 and it aims at producing mostly propylene and butylene with high octane gasoline as side product. The olefins can be reacted to produce polyolefins, which are used to make many plastic materials [39].
6. **DMFC:** In such application liquid methanol is used as hydrogen carrier in direct methanol fuel cells, generally used to power portable devices like phones or laptops. Methanol has high energy storage density and that is why a lot of research proceeds concerning these devices to develop an alternative to lithium ion batteries [40].
7. **FUEL:** Methanol can be used in different blends together with gasoline resulting in lower carbon emissions. The most promising blends are M15, M56, M85 and M100,

each corresponding to the own volume percentage of methanol in the gasoline/methanol blend.

In Table 2.2, a comparison between traditional 95 RON gasoline and an M85 powered vehicle is shown. It is possible to notice a significant reduction in unburnt hydrocarbon emissions from. The comparison has been made running both the engines in the same efficiency conditions.

Fuel type	95 Octane Petrol	105 Octane M85
Air-Fuel Ratio	14,0:1	7,6:1
Fuel energy MJ/l	32,2	18,2
Performance		
Max. power	68 hk	73 hk
Max. torque	97 Nm	102 Nm
MJ/km	1,63	1,62
km/l	19,8	11,8
Car efficiency	15%	15%
Engine efficiency	25%	25%
Emissions		
CO2, g/km	118	118
CO, g/km	1,4	0,4
NOx, g/km	0,4	0,6
Pn, G#/km	234	259

Table 2.2: *Summary of performance with M85 compared to gasoline on Peugeot 107* [5].

Concerning M100, practically the engine runs on neat methanol, but this can result in cold-starting issues because the vapor pressure would be too much low. M15 is popular because modern cars can usually run it without engine changes [5].

In China, M15 is the largest utilization of fuel methanol and Israel has recently concluded promising M15 tests. In 2014 the consumption in China of methanol blends with gasoline grew to 7 million tons. Sadly, M15 is not allowed in the EU. Only fuels with less than 3 vol% and more than 30 vol% methanol are allowed since methanol could have damaging effects on vehicles engines due to its corrosivity. [5]

2.1.3 Methanol Market

Methanol is one of the chemicals/fuels with the largest growth rate in the last decade, with its demand increasing from about 5 Mt in 2005 to more than 70 Mt in 2015. The compound

annual growth rate (CAGR) nearly doubled in the last five years compared to the average in the decade before and an additional 5,4% growth is forecast from 2019 to 2027 [35, 42].

The global methanol market can be geographically divided into the regions of North America, Europe, Asia-Pacific, Latin America and the Middle East & Africa.

In 2018, the Asia-Pacific region was the dominant region in the global methanol market, and it is projected to further continue its course of growth trajectory throughout the forecasting period [42].

Growth in Asia-Pacific's chemical sector was also supported by the dynamism in emerging countries of industries such as electronics, textiles, construction, leather and plastics processing. The developing countries in Asia-Pacific are striving to become global leaders in these sectors, which are important end-users of chemicals [44]. The world methanol consumption shares per country in 2019 reported in Figure 2.2 confirm the Asian countries consumption of such chemical.

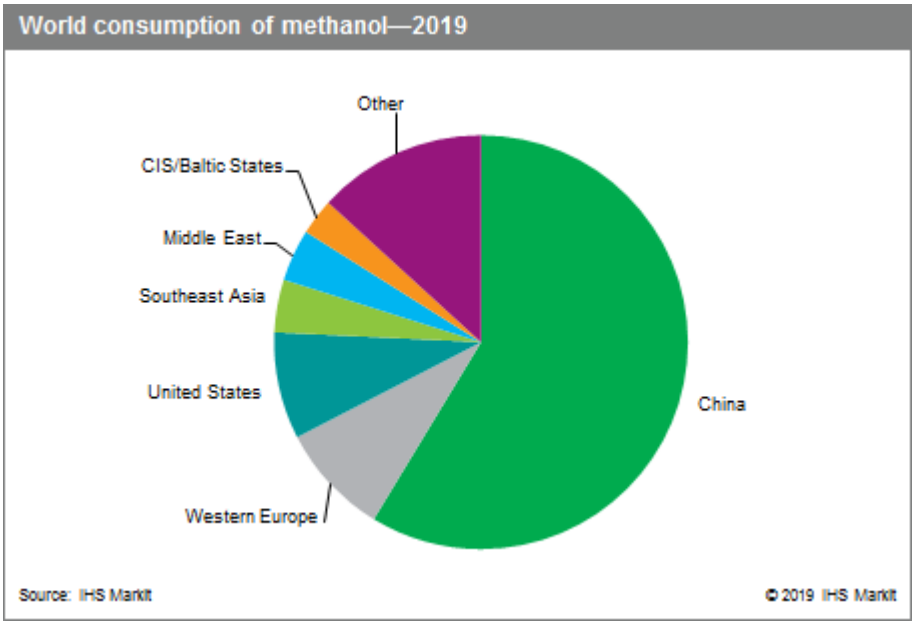

Figure 2.2: *World methanol consumption per country in 2019* [43].

Among the key drivers responsible for the growth of the methanol market it is possible to find the increased acceptance of the MTO technology, the rise in the demand for petrochemicals, the need for conventional transportation fuels and the promotion of methanol as an alternative fuel by governments [35]. A representative example is reported

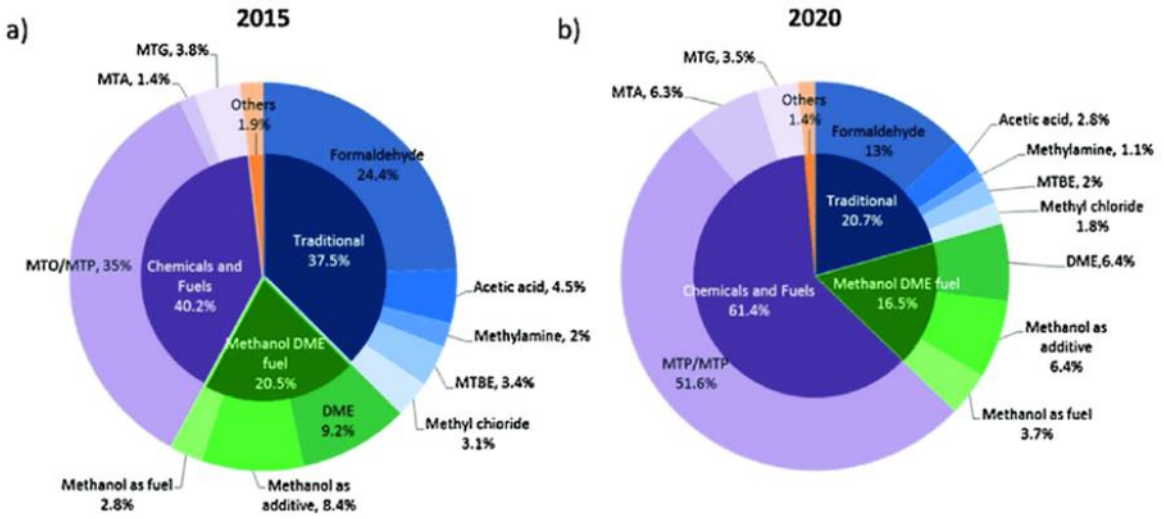

Figure 2.3: *China's methanol production in 2015* ***(a)*** *and 2020* ***(b)*** *(projected) and its sharing ratio in each derivative* [45].

in Figure 2.3 which shows a comparison between 2015 and 2020 methanol utilization shares in China. Fast-rising fuel demand in China, as well as the development of unconventional chemical production plants (MTO/MTP) have primarily driven methanol consumption. A growth about 11,4% concerning chemicals and fuels production field may be noticed, thanks to the opportunity for China to diversify away from conventional naphtha cracking to produce olefins [43]. The use of methanol as a pure fuel increased despite a global percentage reduction in this field, while the share adopted in formaldehyde production has strongly decreased even if it is one of its largest applications.

The methanol market also faces challenges such as unstable methanol prices, economic slowdown hindering the demand for methanol and strict regulations and policies. Such prices oscillations may be appreciated in Figure 2.4, representing the last years global methanol pricing fluctuations.

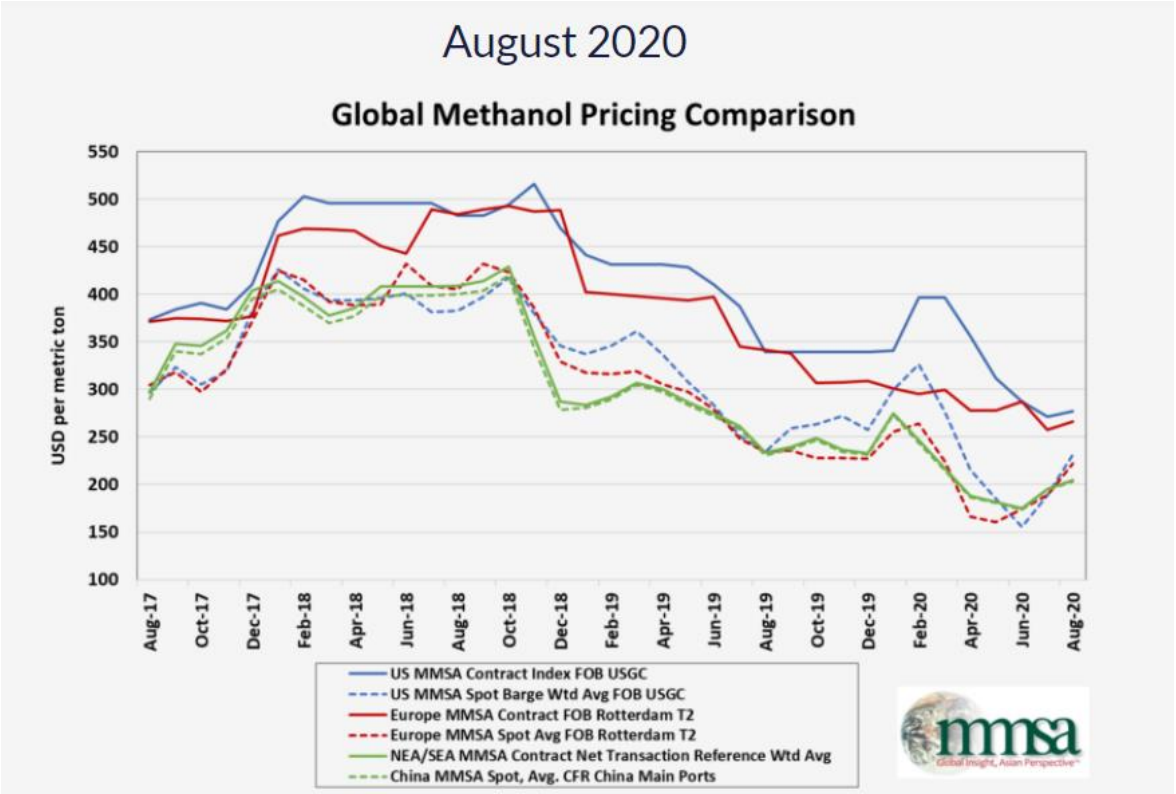

Figure 2.4: *Global methanol pricing comparison from 2017 to 2020* [37].

Such fluctuations are generally assumed to be driven by the upstream natural gas price. Anyway, beside the relation with natural gas pricing, a further factor to be taken into account is the influence of the strong demand in eastern countries [44].

In the end, beside the reported applications, there are also other outlets that could be exploited to expand methanol market. The increase in the demand for bio-based products, development in technology for biorefining and the application of methanol as a marine fuel are some of the opportunities that can be leveraged by this market in order to propel further growth [42].

2.2 METHANOL PRODUCTION PROCESS FROM BIOGAS

This section will focus on methanol production process before the introduction of the adopted methods and the investigated plant configurations. As previously mentioned,

methanol is produced by a catalytic reaction of carbon monoxide (CO), carbon dioxide (CO_2) and hydrogen (H_2) [59]. These gases, together called synthesis gas, are generally produced from natural gas. Yet, syngas may be obtained also from other organic substances, such as biomass, like in this case of study.

A train of processes to convert biomass to required gas specifications precedes the methanol reactor. These processes include pre-treatment, biomass gasification or anaerobic digestion (AD), gas cleaning and gas conditioning. Finally, a purification section following the synthesis reactor is required to meet methanol purity specifications. [60, 58]

Since a wide range of biomass substrates may be used (sewage, sludge, agriculture crops, organic and municipal waste or even algae), the pre – treatment depends on the feed characteristic and, clearly, on the following process. This study considers an inlet clean fresh biogas feed coming from a biodigester. Therefore, some hints will be provided about the anaerobic digestion process and to the reforming reaction, while particular attention has been dedicated the synthesis reaction. In the end some information about the capable methanol synthesis reactors and the final upgrading section precedes the chosen plant configurations and methods description.

2.2.1 Anaerobic Digestion, AD

Anaerobic digestion to convert organic compounds into biogas is a complex process that involves a series of microbial metabolism. The process can be divided into four main steps: hydrolysis, acidogenesis, acetogenesis, and methanogenesis [56]. Each of the four steps involves different biochemical reactions with different substrates and microorganisms. A summary of them is provided in Figure 2.5.[57]

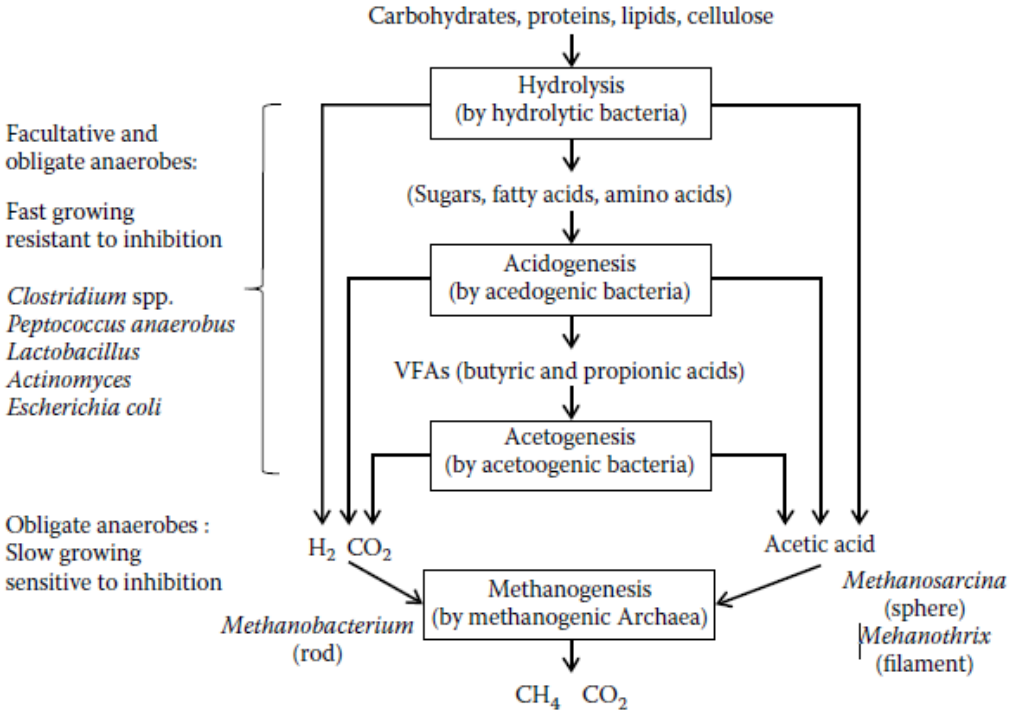

Figure 2.5: *A schematic diagram of anaerobic degradation of organic compounds to biogas (methane and carbon dioxide).*

Hydrolysis: Original organic waste materials usually contain mainly large – molecule compounds such as carbohydrates, proteins, lipids, and celluloses. These organic compounds are hydrolysed by facultative (active in both environments with and without oxygen) and obligate (active only in the environment without oxygen) anaerobic bacteria to mainly smaller molecules, such as sugars, fatty acids, amino acids, and peptides, as well as a small amount of acetic acid, hydrogen, and carbon dioxide. During the hydrolysis, the energy

reserved in the original large-molecule organic compounds is redistributed as 5% to hydrogen, 20% to acetic acid, and 75% to smaller molecule organic compounds. [56, 57]

Acidogenesis: The sugars, fatty acids, amino acids, and peptides are fermented by the anaerobic bacteria to volatile fatty acids (VFAs) such as propionic and butyric acids during the acidogenesis. Similar to the hydrolysis process, acidogenesis also produces a small amount of acetic acid, hydrogen, and carbon dioxide. In acidogenesis, 10% of the energy is released in the form of hydrogen, 35% in the form of acetic acid, and the rest reserved in the VFAs. [56, 57]

Acetogenesis: The VFAs are completely degraded into acetic acid, hydrogen, and carbon dioxide during acetogenesis. At this step, 17% of the energy is transferred to acetic acid and 13% to hydrogen. [56, 57]

Methanogenesis: The whole anaerobic digestion process is complete when both hydrogen and acetic acid are converted to methane during the methanogenesis. The conversion of hydrogen to methane involves a biochemical reaction of hydrogen and carbon dioxide to form methane [56]:

$$4H_2 + CO_2 \rightarrow CH_4 + 2H_2O$$

Eqn. 2.1

The conversion of acetic acid to methane is a degradation of acetic acid into methane and carbon dioxide [56]:

$$CH_3COOH \rightarrow CH_4 + CO_2$$

Eqn. 2.2

Anaerobic digestion can be performed at different temperatures and may exploit different kinds of biomass substrates. It generally has three categories based on temperature:

psychrophilic (low-temperature), mesophilic (medium temperature), and thermophilic (high-temperature) anaerobic digestion processes. [56]

- **Psychrophilic** anaerobic processes are normally operated at a temperature range of 10° C - 25° C. These anaerobic systems are simple and relatively economical in construction and operation because no heat exchange units are involved. They can be used for treating a variety of waste materials containing high carbohydrates. An issue is that anaerobic microbial activities are low. High residence time or large volume of digesters is necessary for efficient degradation of organics and biogas production.[56]
- **Mesophilic** anaerobic processes are the most commonly used ones for the treatment of a variety of industrial and municipal organic wastes for biogas production. They are usually operated at moderate temperatures of 30°C–37°C. They are popular because they are easy to start up, stable in performance, and relatively high in microbial activities.[56]
- **Thermophilic** anaerobic microbes grow well at elevated temperatures (50°C–65°C). Thermophilic anaerobic digestion (TAnD) has been commonly applied for the treatment of animal, industrial, and municipal organic wastes. Because of their high digestion rates, thermophilic anaerobic digesters can be highly compact in size. An issue is the slow and difficult start up.[56]

2.2.2 Biogas Purification

Biogas composition may cover a wide range of values depending on the biomass feed and the process applied. In Table 2.3 some typical values are reported.

Component	%
Methane (CH_4)	50–80
Carbon dioxide (CO_2)	20–40
Nitrogen (N_2)	0–5
Hydrogen (H_2)	0–1.0
Hydrogen sulfide (H_2S)	0.05–1.0
Ammonia (NH_3)	0.02–0.5
Oxygen (O_2)	0–0.5

Table 2.3: *Example of typical ranges of biogas composition* [56].

Among the components, methane is the only one that can generate energy through combustion. CO_2 does not change during the combustion, but its existence dilutes the energy density of the methane and consumes energy during the combustion for the increase of the temperature. Hydrogen sulphide is oxidized into sulphur dioxide and water, which forms sulfuric acid. Sulfuric acid is a very strong and corrosive acid. Hydrogen sulphide itself can also be corrosive to the metals. It can form its own electrolyte and absorb directly onto the metal to cause corrosion. If the hydrogen sulphide concentration is very low, the corrosion will be slow. However, if the concentration of hydrogen sulphide in the biogas is greater than 100 ppm, it may cause pitting corrosion, which is a severe corrosion form. Moreover, since in the methanol production process a reforming section is following, it is crucial to remove H_2S. Catalysts used in the reforming reaction are indeed quite sensitive to H_2S poisoning. [23-26]

There are currently several methods to remove H_2S from the biogas, including precipitation by reaction with metal ions, physical adsorption with activated carbon or zeolites, chemical absorption, and biological oxidation via sulphur oxidizing bacteria. [56]

As previously mentioned, the investigated plants consider an inlet purified fresh biogas feed. Its molar composition consists of 60% methane and 40% carbon dioxide. The next chapters will deal with gas conditioning to achieve the required conditions to perform methanol synthesis.

2.2.3 Syngas Requirement

It has to be highlighted that methanol synthesis requires syngas with suitable H_2/CO and H_2/CO_2 molar ratios. These may be achieved if the syngas module M ranges from 2-3. Such parameter may be defined as:

$$M = \frac{x_{H_2} - x_{CO_2}}{x_{CO} + x_{CO_2}}$$

Eqn.2.3

Where x stands for the molar fraction of each component. Values of M greater than 2 indicate an excess of H_2 in the feed gas, while on the other hand values smaller than 2 an excess of carbon. If only CO_2 and H_2 are present in the feed, a ratio of H_2/CO_2 about 3:1 ensures M=2, which is well known as optimal value [6, 3]. An M about 2 also limits H_2O formation and prevents catalyst deactivation [49].

Syngas composition at the outlet of the reforming section may be managed by downstream processes like water gas shift, WGS, and/or pressure swing absorption, PSA, able to remove both H_2 and CO_2. CO_2 separation may also be performed using amines like MEA or MDEA in a system of distillation columns (absorber and stripper). Distillation is indeed one of the most used separation process in the chemical industry. [26, 58]

Anyway, by producing syngas under the following particular reforming conditions, it is possible to directly process the feed gas avoiding the syngas upgrading steps [3]:

- Reforming of natural gas or biogas with high methane content (CH_4/CO_2= 2.3). Natural gas or biogas with lower methane content produce CO_2 rich syngas that is not suitable for the direct conversion;

- Dry Reforming in the temperature range 650-900 °C. These conditions satisfy the request of H_2-CO-CO_2 composition, ensuring a CH_4 conversion always higher than 80%. However, carbon formation in this case needs to be considered;
- Steam Reforming for S/CH_4 molar ratio from 0.1 to 3 in the temperature range 650-900 °C. The increasing in steam content dramatically reduces or eliminates carbon deposition and favours the WGS equilibrium, increasing the H_2 and CO_2 content. However, higher amount of steam means higher energy requirements, lowering the overall process efficiency;
- Oxy – Steam Reforming only with low amount of oxygen ($O_2/CH_4 \leq 0.1$) and at low S/CH_4 ratio ($\leq$ 0.1) at temperature comprised between 650 and 750 °C. The feasibility range results significantly reduced. Indeed, the simultaneous presence of steam and oxygen leads to high CO_2 concentration in the gaseous products, due to the WGS equilibrium and total oxidation reaction, respectively. Moreover, low quantity of steam and oxygen can be partially overcome the problem of energy requirements, but the carbon deposition phenomena still remain a potential drawback of the process.

In the processes under study, CO_2 separation is performed upstream the reforming section in order to achieve the mentioned stoichiometric module at the rector inlet equal to 2.1 and perform the direct process without the other upgrading steps of WGS/PSA. Anyway, also plant designs with the reformer downstream CO_2 separation have been investigated and compared in order to identify the optimal configuration.

Dealing with a small scale application, the direct process without syngas composition conditioning has been considered. This clearly implies a certain penalization on the performances, due to the stoichiometric module M different form the optimal value at the synthesis reactor inlet. Nevertheless, because of the effect of economies of scale, the absence of the CO_2 separation section may be remunerative under the economic point of view.

2.2.4 Reforming Process

Production of syngas from natural gas or biogas is achievable via Reforming process. This process may be carried on in several ways, for instance among the basic ones it is possible

to include Partial Oxidation, Steam Reforming (SR) or Dry Reforming (DR). It is also possible to combine different techniques: SR+DR or Tri Reforming (TR) are only some of the possible solutions [50]. In these lines some of the most relevant will be presented.

2.2.4.1 Steam Reforming

Steam Reforming or Steam Methane Reforming (SMR) is the most common reforming technique. It is a catalysed process performed in a reformer operating at high temperatures, about 800-900°C, and moderate pressure, about 30 bar. SMR is often followed by the WGS reaction to improve hydrogen production and adjust syngas composition. [50]

$$SMR: CH_4 + H_2O \leftrightarrow CO + 3H_2 \qquad \Delta H_{298K} = 206\frac{kJ}{mol}$$

Eqn. 2.4

$$WGS: CO + H_2O \leftrightarrow CO_2 + H_2 \qquad \Delta H_{298K} = -41.1\frac{kJ}{mol}$$

Eqn. 2.5

It is evident that SMR is strongly endothermic, thus, favoured at high temperatures and requires a certain heat load to be satisfied. Moreover, it is enhanced by low pressures having an increasing number of moles; in spite of this, a moderate pressure around 30 bar is commonly adopted both to downsize reactors and because usually the resultant syngas is further processed at moderate-high pressures depending on the application. Hydrogen production, methanol production or direct exploitation in gas turbines are just some possible examples [26].

These considerations may be appreciated also by looking at the expression of the SMR equilibrium constant:

$$lnK_{\mathrm{p}} = -\frac{27106}{T} + 30.420$$

Eqn. 2.6

Where T is the temperature expressed in Kelvin. Such relation is valid in a temperature range between 600 and 1500 K [51]. In Figure 2.6 a graphical representation is provided, confirming that high temperatures are required to obtain an appreciable reaction yield.

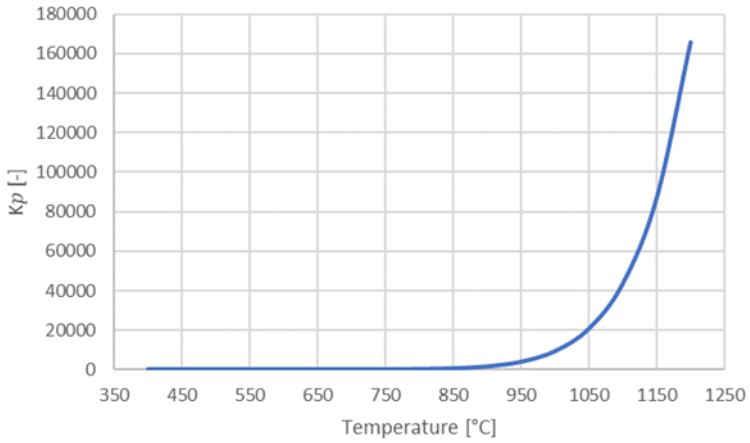

Figure 2.6: *SMR Equilibrium constant as function of T.*

By expressing the equilibrium constants as function of species partial pressure some more considerations may be done:

$$p_{\mathrm{i}} = P \cdot \mathrm{x_i}$$

Eqn. 2.7

$$K_{\mathrm{p}} = \frac{p_{\mathrm{H2}}^{3} \cdot p_{\mathrm{CO}}}{p_{\mathrm{CH4}} \cdot p_{\mathrm{H2O}}} = P^{2} \cdot \frac{x_{\mathrm{H2}} \cdot x_{\mathrm{CO}}}{x_{\mathrm{CH4}} \cdot x_{\mathrm{H2O}}}$$

Eqn. 2.8

Where P represents the total pressure, while x_{i} and $\mathrm{p_i}$ the molar fraction and the partial pressure of the $\mathrm{i^{th}}$ species. For a certain value of the equilibrium constant, a higher steam content moves the equilibrium towards products. Hence, high values of the Steam to Carbon ratio (S/C) are desirable to increase the reaction yield. Anyway, both upper and lower limits for the value of the S/C ratio do exist and they vary depending on the technology adopted. Concerning the upper limit, it has to be reminded that steam acts also as an inert, therefore

an excess of H_2O may increase too much the energy requirement and penalize the efficiency of the process. The lower limit, instead, deals with the carbon content: an excess of carbon may favour carbon deposition in the reactor, with the risk of catalyst poisoning and deactivation [26]

Typically, SR is carried on in a Fired Tubular Reformer, FTR, which consists of a furnace providing the requested heat load and several catalysed tubes in which the reacting gas flows. An example is shown in Figure 2.7. Often Ni is used as active metal due to the low cost, even if also other noble metals may be used, like Co, Ru or Rh for instance. These metals have a higher activity per unit area respect to Ni, yet the higher costs represent a limit for large scale applications [52].

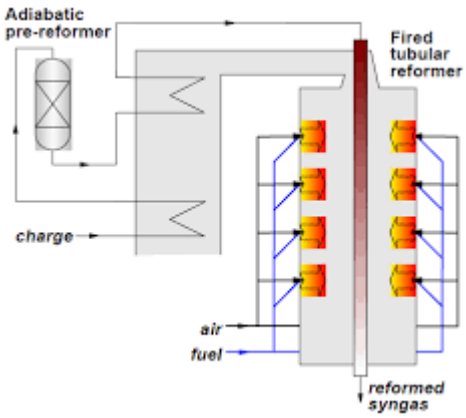

Figure 2.7: *Scheme of a Fired Tubular Reformer.*

Depending on the feed, a pre-reforming section may be adopted to break bonds of the heavier hydrocarbons, aiming to avoid carbon deposition in the reformer tubes. Beside catalyst poisoning, a further issue for this technology is that carbon deposits have a different heat exchange coefficient, such that local overtemperature in hotspots along reactor tubes may occur, compromising in the end the system integrity. For this kind of reactors values of the St/C ratio between 2.7 and 4 on molar basis are strongly suggested [26].

A further valid and common technology to perform SMR is the Auto-thermal Reforming, ATR. Basically, in the auto-thermal reformer the heat load to sustain the reaction is provided by partial oxidation of the fresh charge with a sub stoichiometric amount of O_2. The overall

reaction is in the end adiabatic, meaning that there is no need of an external heat source. For this technology a St/C value below 2 is suggested since H_2O is formed in the combustion chamber due to the partial oxidation reaction. Feed gas and comburent oxygen or air are usually supplied from the top of the reactor. [26]

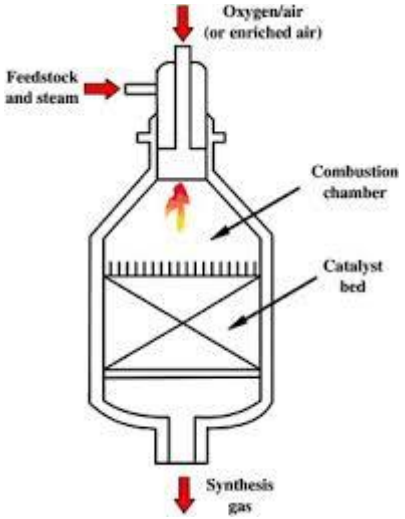

Figure 2.8: Scheme of an Auto-Thermal Reformer.

As it is shown in Figure 2.8, a catalysed bed follows the combustion chamber promoting the SR reaction. The obtained syngas flows out from the bottom of the system. Due to the internal combustion higher temperatures respect to the FTR technology may be expected. The outcoming flux temperature, indeed, is about 200°C higher, with a value of almost 1100°C. Moreover, because of the same reason temperature in the combustion chamber approaches values above 2500°C, such that refractory shields are in general adopted to allow the use of cheap construction materials like carbon steel [26,53].

2.2.4.2 Dry Reforming

In the last decades interest in CO_2 methane reforming, i.e. dry reforming, has grown, being it a possible way to exploit the captured carbon dioxide from other processes [50]. The reaction considered is the following:

$$DR:\ CH_4 + CO_2 \rightarrow 2CO + 2H_2 \qquad \Delta H_{298K} = 260.5\ \frac{kJ}{mol}$$

Eqn. 2.9

This reaction is quite endothermic and favoured by high temperatures and low pressure.

Pt group metals are the best solution to be used as catalysts, yet again Nickel based ones are preferred due to the lower costs and the high availability. However, a serious issue for this reforming technique is the rapid carbon deposition on the catalyst, in particular if Ni is used. Notable efforts have concentrated on exploring new catalysts, which are resistant to carbon formation. Sulphur passivated nickel catalysts and noble metals have been shown to exhibit resistance to carbon formation. But the low activity of sulphur passivated nickel, and the high costs and limited availability of the noble metals have limited their application [50,54].

Catalytic coking may be limited also by performing SR together with DR, or even by an accurate temperature control in the optimal range of 600-1040 °C. Carbon deposition in fact takes place according to the Boudouard Reaction:

$$2CO \rightarrow CO_2 + C \qquad \Delta H_{298K} = -172\ \frac{kJ}{mol}$$

Eqn. 2.10

Such reaction is exothermic and may be limited in the mentioned operating condition [50]. Figure 2.9 shows the beneficial effect of higher temperatures on chemical equilibrium. In the reported example a ratio CH_4/CO_2 of 1.5 and a pressure of 1 atm are considered. It can be observed that products molar fraction increases strongly as well as C formation is, at least in part, hindered.

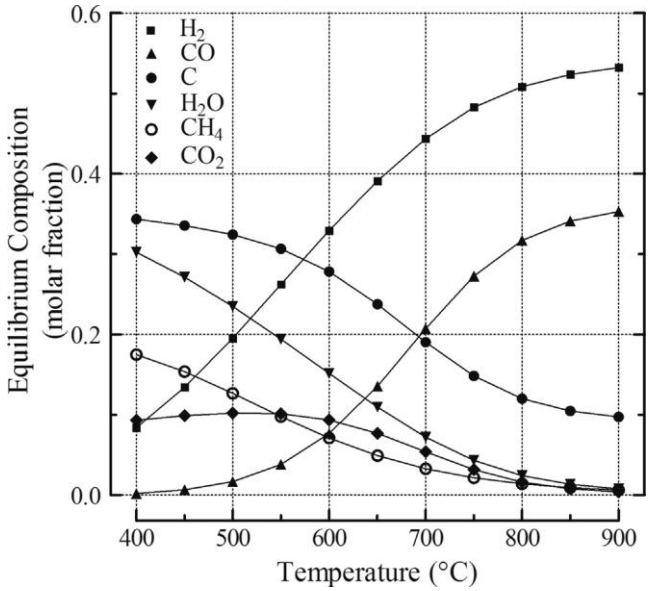

Figure 2.9: *Dry Reforming of biogas (CH4/CO2=1.5 M, P=1 atm): effect of temperature on thermodynamic equilibrium composition* [3].

As for the reactors, several are the alternatives. Fluidized bed reactors appear to be suitable for the process in terms of conversion and catalytic activity. However, application on commercial scale is still a challenge due to the expensive costs [54].

2.2.4.3 Tri-Reforming

The Tri-Reforming process is a synergic combination of CO_2 Reforming, Steam Reforming and Partial Oxidation of Methane. The Tri-Reforming concept represents a new way of thinking both for conversion and utilization of CO_2 in flue gas without CO_2 separation, and for production of industrially useful synthesis gas with desired H_2/CO ratios using flue gas and natural gas. Beside Eqn. 2.9 and Eqn. 2.5 also the methane exothermic partial and complete oxidation reactions take place with the aim to provide heat for the process [55]:

$$CH_4 + \frac{1}{2}O_2 \rightarrow CO + 2H_2 \qquad \Delta H_{298K} = -35.6\ \frac{kJ}{mol}$$

Eqn. 2.11

$$CH_4 + 2O_2 \rightarrow CO_2 + 2H_2O \qquad \Delta H_{298K} = -880\ \frac{kJ}{mol}$$

Eqn. 2.12

Thanks to partial autothermal reaction related to oxidation reactions, the process energy efficiency is increased, yet this is not the only advantage. Such integration dramatically reduces or eliminate the issue of carbon formation on the catalyst related to Dry Reforming, augmenting catalyst lifetime [55]. TR is a valid solution also because it exhibits relatively low operating costs and reduced capital investment in comparison with SR of natural gas. Even when an ASU is required for TR, the reformer cost is considerably lower than the one for SR [49].

2.2.5 Methanol Synthesis Reaction

As well known, methanol synthesis reaction exploits a syngas feed containing mainly H_2, CO_2, CO and traces of other inert elements like unconverted methane from the reforming section. A proper syngas composition is crucial to obtain suitable yields from the synthesis reaction, whose pathway consists in the following reactions [59]:

- *CO hydrogenation:*

$$CO + 2H_2 \leftrightarrow CH_3OH \qquad \Delta H_{298K} = -90.77\frac{kJ}{mol}$$

Eqn.2.13

- *Reverse Water Gas Shift:*

$$CO_2 + H_2 \leftrightarrow CO + H_2O \qquad \Delta H_{298K} = 41.2\ \frac{kJ}{mol}$$

Eqn.2.14

- *CO_2 hydrogenation:*

$$CO_2 + 3H_2 \leftrightarrow CH_3OH + H_2O \qquad \Delta H_{298K} = -49.16\frac{kJ}{mol}$$

Eqn.2.15

Where CO_2 hydrogenation is the result of a linear combination between the first two reactions. According to thermodynamics, only the reverse water gas shift reaction (RWGS) is endothermic, while hydrogenation reactions are exothermic. The overall process is exothermic, thus the temperature increase has a negative impact on equilibrium and the higher yields are achieved for lower temperatures. Considering the decreasing number of moles, a high pressure is also beneficial for chemical [6,3]. It is possible to express the equilibrium constant per each reaction according to: [6]

$$\begin{cases} ln\ K_{\mathrm{a}} = 9.8428 \cdot \dfrac{10^4}{RT} - 29.07 & K_{\mathrm{a}}[atm^{-2}] \\ ln\ K_{\mathrm{b}} = 4.3939 \cdot \dfrac{10^4}{RT} + 5.639 & K_{\mathrm{b}}[-] \\ ln\mathrm{K_c} = K_{\mathrm{a}} \cdot K_{\mathrm{b}} & K_{\mathrm{c}}[atm^{-2}] \end{cases}$$

Eqn.2.16

Where $R = 8.314\ [\frac{J}{molK}]$ and each subscript a, b, c stands for CO hydrogenation, RWGS and CO_2 hydrogenation respectively. Such correlations are based on fugacity values expressed in [atm]. For values of K in [Pa^{-2}] the equations turn to:

$$\begin{cases} ln\ K_{\mathrm{a}} = -52.096 + \dfrac{11840}{T} & K_{\mathrm{a}}[Pa^{-2}] \\ ln\ K_{\mathrm{b}} = -\dfrac{5285}{T} + 5.639 & K_{\mathrm{b}}[-] \\ lnK_{\mathrm{c}} = K_{\mathrm{a}} \cdot K_{\mathrm{b}} = -46.457 + \dfrac{6555}{T} & K_{\mathrm{c}}[Pa^{-2}] \end{cases}$$

Eqn.2.17

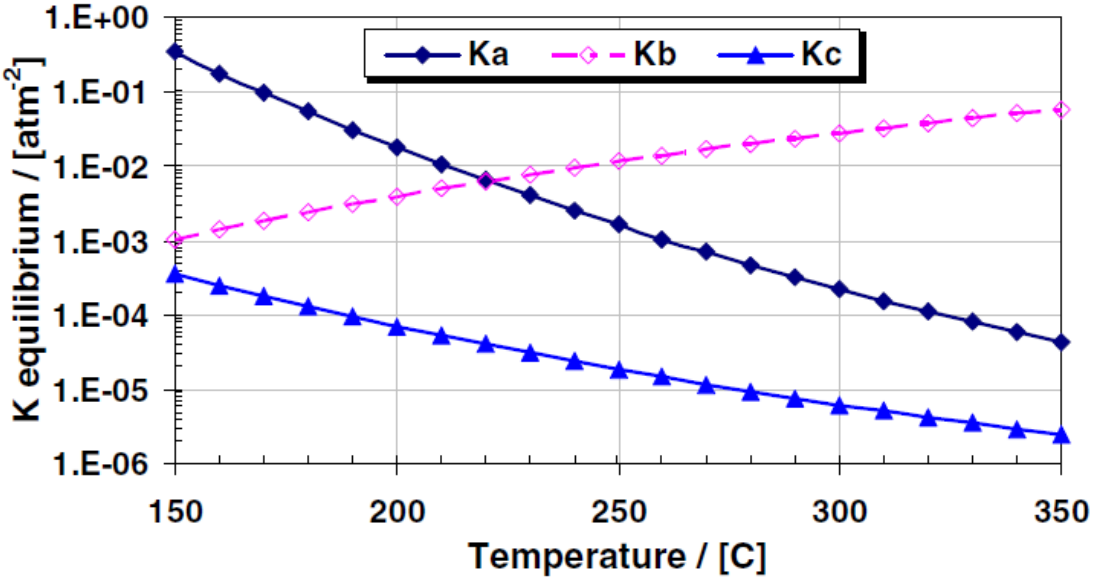

Figure 2.10: *Temperature impact on equilibrium.* ***a)*** *CO hydrogenation;* ***b)*** *RWGS;* ***c)*** *CO_2 hydrogenation* [6].

From Figure 2.10 one can state that the optimal temperature interval for a suitable yield ranges from 150 to 250 °C. Such statement considers that the reactions require a catalyst whose activation is favoured by high temperatures. Lower temperatures would be prohibitive for catalyst activation even if the equilibrium constant of the overall reaction is greater than one at 135°C, while higher temperatures lead to a too low equilibrium constant [6].

2.2.6 Catalysts

The described process working according to Eqn.2.13, Eqn.2.14 and Eqn.2.15 is promoted by proper catalysts. Historically, the first industrial process based on catalytic synthesis starting from syngas was the BASF process. The BASF process operated at above 300 atm and 300 – 400°C, using a zinc chromite (Cr_2O_3–ZnO) catalyst developed by Alwin Mittasch. Such high pressure was employed to ensure a proper conversion despite the quite unfavourable temperature needed to keep the catalyst active [2].

These catalysts have been largely replaced by formulations based on copper/ zinc oxide/ alumina. These catalysts are active at much lower temperatures and hence can be operated at lower pressure for the same level of conversion as the older formulations, usually around 90 bar; they are generally known as low – pressure catalysts. Because they are able to operate at lower temperature and pressure, the low-pressure catalysts produce far less by – product than the high-pressure process [8]. In particular, Table 2.4 shows a comparison between high pressure and low pressure tendency to form by-products, where it is quite evident the convenience of the latter.

By-product	High pressure (ppm (w/v))	Low pressure (ppm (w/v))
Dimethyl ether	5000–10 000	20–150
Carbonyl compounds	80–220	10–35
Higher alcohols	3000–5000	100–800
Methane	2% of input carbon	None

Table 2.4: *Comparison between high pressure and low pressure catalysts tendency to form by products* [8].

The formation of other by-products is influenced by the presence of impurities in the catalyst. Alkalis promote the formation of higher alcohols and acids (such as silica) promote the formation of waxes which block the catalyst. Many impurities are transported onto the

catalyst during operation. For instance, nickel and iron can be transported in the gas phase as the metal carbonyls which are formed in up-stream operations when synthesis gas interacts with finely divided metal. These impurities promote the formation of methane, paraffins and waxes in the methanol synthesis loop. Other impurities such as sulphur and chlorine can contaminate the synthesis gas and can permanently decrease the activity of the catalyst [2,8].

2.2.7 Methanol Synthesis Reactors

The most important part of the methanol synthesis process is the methanol reactor. Because the synthesis reaction is strongly exothermic, heat removal is an important step, and so temperature control is important. A high heat flux leads to fewer tubes, smaller furnaces, and thus reduced costs. The reactor technologies used extensively in commercial settings fall into two broad categories [59]:

- multiple bed reactors;
- single bed converters;

A short overview of the state of art of these reactors is provided in the following lines.

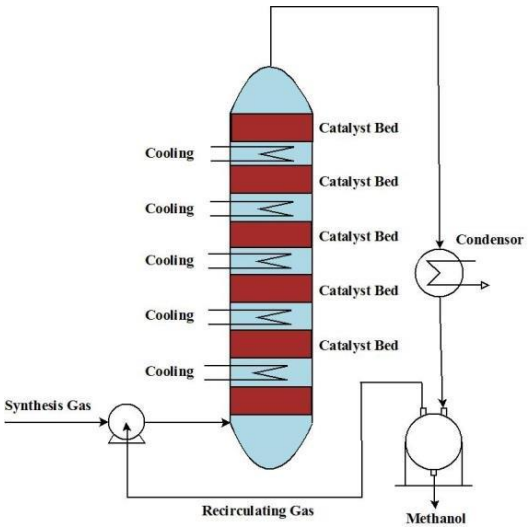

Figure 2.11: *Simple scheme of a multiple bed methanol reactor.*

Multiple catalyst bed reactors, as the one shown in Figure 2.11, control the reaction temperature by separating the catalyst mass into several sections with cooling devices placed

between the sections. Bed sizes are generally designed to allow the reaction to reach equilibrium conditions. Among the main multiple bed reactors it is possible to report [59]:

- **Kellog, Brown, and Root's adiabatic reactors in series**: in these reactors, which are displaced in series, each catalyst layer is accommodated in a separate reactor vessel with intercoolers between each reactor. The feed gas enters directly into the first reactor, which increases the kinetic driving force for the reaction.
- **Toyo Engineering Corporation's MRF-Z reactor**: this reactor is a multistage radial flow reactor with intermediate cooling. This indirect cooling keeps the temperature close to the path of the maximum reaction rate curve (when the methanol concentration is plotted against temperature). Maximum, or close to maximum, conversion per pass is then achieved.

In single bed reactors, heat is continuously removed from the reactor by its transfer to a heat removing medium, so the reactor runs effectively as a heat exchanger. In most commercial methanol production today, gas-phase reactor technology, which is a two-phase, gas-solid reactor, is in use. Recently, a three-phase, gas-solid-liquid technology was introduced: the reaction is performed with a solid catalyst suspended in a liquid medium that efficiently removes the reaction heat. Consequently, the reaction temperature in this type of reactor can be controlled more easily than in an ordinary solid reactor, and it has a higher single pass conversion. Through the simplicity of their converter design, these liquid-phase technologies are reducing costs in the methanol industry. The following are the main kind of single bed reactors [59]:

- **Linde isothermal reactor**: in this reactor's design, helically coiled tubes are embedded in the catalyst bed, which is very similar to LNGs (liquefied natural gas heat exchangers) with the catalyst around the tubes. The Linde isothermal reactor allows for up to 50% more catalyst loading per unit of reactor volume. Compared to reactors with the catalyst inside the tubes, the heat transfer on the catalyst side is significantly higher for a Linde isothermal reactor. As a result, the cost of materials is less because less cooling area is required.

- **Lurgi Methanol Reactor**: the Lurgi Methanol Reactor, also shown in Figure 2.12, is much like a heat exchanger in that it has a vertical shell and tube heat exchanger with fixed tube sheets. The catalyst in the tubes rests on a bed of inert material. Steam is generated by the heat of reaction and drawn off below the upper tube sheet. To achieve precise control of the reaction temperature, steam pressure control is applied. Operating at isothermal conditions enables high yields at low recycles, since recirculation is commonly adopted. In addition, the amount of by-products is minimized. This kind of reactor is the one chosen for this work. Beside the traditional arrangement with feed recirculation, in this work has been studied the Once Through alternative, with several Lurgi reactor in series.

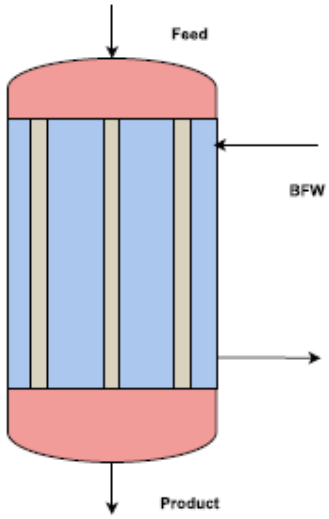

Figure 2.12: *Simple scheme of a Lurgi single bed reactor.*

2.2.8 Methanol Purification

Crude methanol from low pressure process approximately consists of 68% methanol and 31% water (on molar basis), the rest are higher alcohols. Depending on the application, a certain methanol grade is required, such that a separation process to increase its purity is necessary [8,69]. As mentioned, distillation is the most widely used separation technique in the chemical process industries. In methanol production, indeed, distillation is the standard

separation method, and typically in the low pressure methanol process a two columns system is adopted.

A schematic example is given in Figure 2.13: in a first column lighter components are separated in a light end flux which has a certain LHV depending on its composition. Such flux may be burned where needed to increase the overall energy efficiency of the process. In the second column methanol is mainly separated from waste water [58,69].

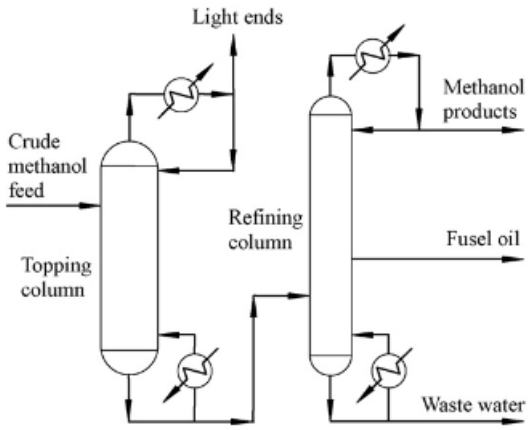

Figure 2.13: *Scheme of a two distillation columns methanol purification system* [58].

However, the comprehensive energy consumption of this step is high, accounting for about 20 % of the total energy consumption in methanol production. This issue is mainly related to the reboiler consumption [58]. Many efforts have been pursued to find energy saving alternatives to the standard two columns scheme. A number of these alternatives involve the split of the refining column into several separate columns operating at different pressure: in this way the overheads of higher pressure columns may be used in the reboiler of the lower pressure ones [58, 61].

The simplest example is the Lurgi three column double effect scheme, reported in Figure 2.14, which is made up by a pre – run column, a higher pressure column and an atmospheric column. In the first light ends are removed from the top while the bottom liquid is fed to the pressurized column. Overhead vapours of the pressurized column have a higher temperature respect to the bottom liquid of the atmospheric one, therefore they are used as reboiler heat

source. In this way it is possible to reduce the overall steam requirement and energy consumption [58].

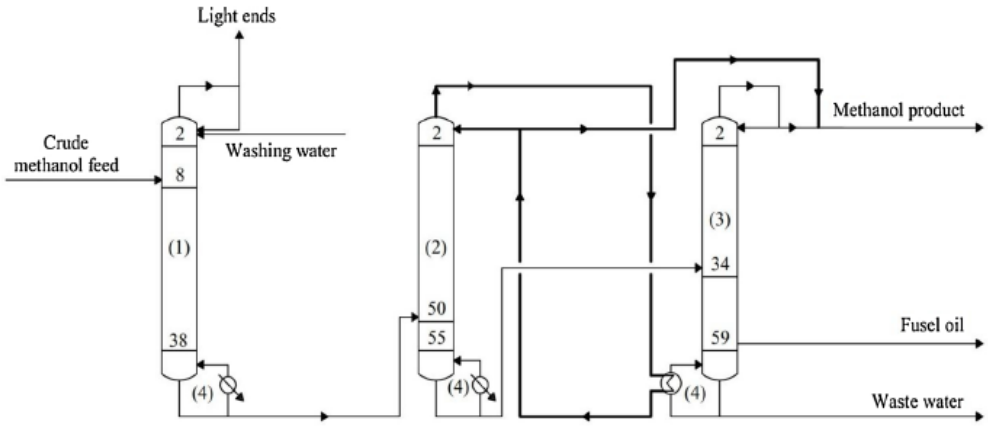

Figure 2.14: *Lurgi's three distillation columns double effect scheme* [61].

Other systems are mainly based on the improvement of the three columns arrangement or on the adoption of more columns, even four or five. From Figure 2.15 it is possible to appreciate a three columns triple effect scheme, where overheads of the higher pressure column are exploited in the reformer of both light end and atmospheric columns. An energy saving roughly about 20% respect to the double effect system may be noticed [61].

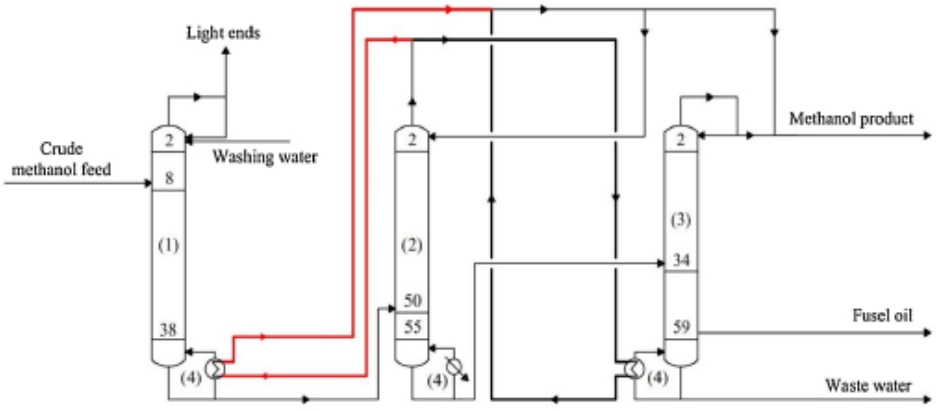

Figure 2.15: *Three distillation columns triple effect scheme* [61].

The adoption of more intermediate pressure columns leads both to a more complex design and to higher investments costs. On the other hand, such multi column schemes may offer significative energy savings: the five columns arrangement shown in Figure 2.16 may save energy around 39% respect to a traditional two column system. This fact suggests a certain convenience to adopt such solutions on large scale applications [58, 61].

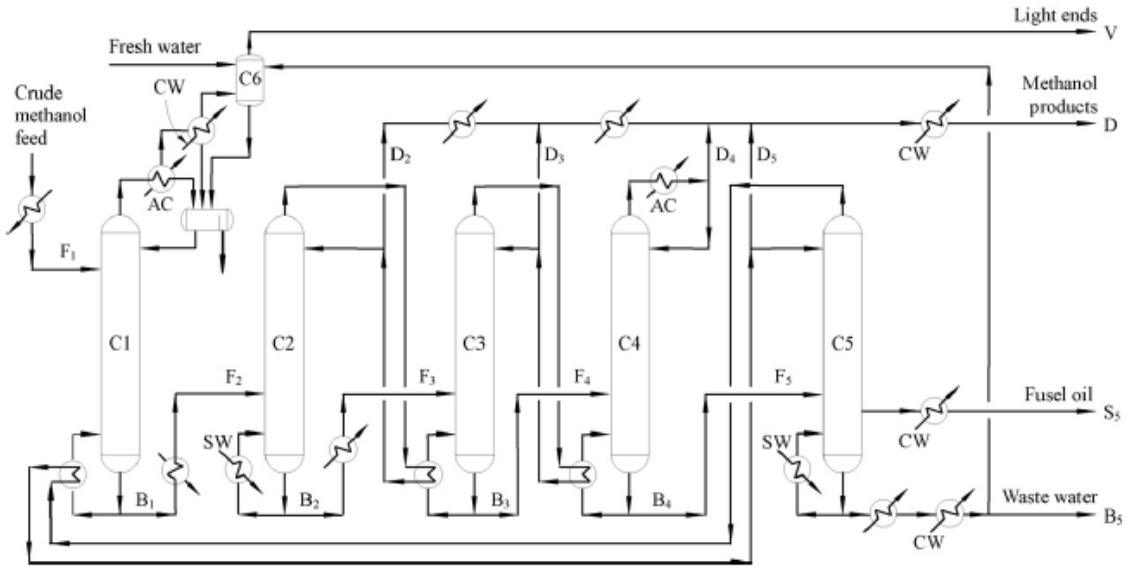

Figure 2.16: *Five columns multi effect scheme* [58].

2.2.9 Product Quality

Traded methanol is generally analysed by the methods described in ASTM D1152 of the International Methanol Producers and Consumers Association (IMPCA).

There are several grades of methanol; the key parameters for these grades are given in Table2.5:

- **Fuel methanol** can be produced in a single column due to the lower purity required. This product has water content reduced to <1%. Since the presence of higher alcohols is not a problem with fuel grade, the product contains some ethanol.

	Fuel	Grade A	Grade AA	IMPCA
Methanol (min wt%)	>95%	>99.85%	>99.85%	>99.85
Specific gravity (20°/20°)		0.7928	0.7928	0.971–0.973
Distillation range† (°C)		1	1	1
Water (max wt%)	<1%	0.15	0.10	0.10
Acetone + aldehydes (ppm)		<30	<30	
Acetone (ppm)		<30	<20	<30
Ethanol (ppm)			<10	<50
Residue (mg/L)		<10	<10	
Chloride (mg/kg)				0.<0.5
Sulphur (mg/kg)				0.<0.5
Acidity (acetic acid; mg/kg)		<30	<30	<30
Permanganate (@ 15 min)		>30	>30	>60

†Must contain 64.6 °C +/– 0.1 °C at 760 mm

Table 2.5: *General specifications for traded methanol* [8].

Higher alcohols are favoured by high temperature synthesis, and since higher alcohols have higher energy content, this could be advantageous for some end uses. There have been proposals to produce fuel methanol with several percent higher alcohol (particularly butanol) content. The use of this grade as an intermediate for the immediate production of another product such as gasoline. [5, 8]

- **Federal Grade A** methanol can be produced in a two-column system. This grade is used when certain specifications in the AA grade are not critical, e.g. for the production of formaldehyde. [8]
- **Federal Grade AA** is the grade generally traded. It has a high specification, particularly on the ethanol and acetone content. This grade could be produced by a two, three or four-column distillation system. [8]

3. PLANT CONFIGURATIONS

In this chapter a detailed description of the investigated plant configurations modelled through the Aspen Plus® software is provided. Beside the traditional process including recirculation, the possibility to perform methanol synthesis via once through reactors has also been considered.

Being steam required in the process, steam generation has been integrated in all the plants by means of thermal recovery from sources like hot produced syngas, reformer flue gases and MeOH reaction heat release. Each plant configuration considers an inlet fresh biogas stream coming from a biodigester. Since typically such systems are integrated, part of the biodigester duty, assumed to be 10% of the inlet biogas available thermal power (ca. 2 MW), is provided by the methanol plant thanks. This is done by means of thermal recovery from hot sources which provide the thermal power to heat up water required by the biodigester from 60 to 80 °C . The inlet biogas stream properties are reported in Table 3.1.

Species	***Molar fraction [-]***
CH_4	0.6
CO_2	0.4
Mole Flow [Kmol/h]	149.63
Mass Flow [kg/s]	1.13
Temperature [°C]	20
Pressure [bar]	1

Table 3.1: *inlet fresh biogas stream properties.*

For a better understanding of the studied cases, plant schemes with explicit stream names are also provided. Beside the real processes description, details about their modelling using Aspen Plus® software are provided. A final section reports plant variations implemented to perform a critical comparison between several arrangements with techno – economic optimization purposes.

3.1 Traditional Arrangement Adopting Recirculation

In this section the methanol production process plant involving unreacted syngas recirculation is presented. A plant scheme provided with stream names is reported in Figure 1.1.

As first step of the process, part of the inlet fresh biogas stream BG1 is sent through a blower to the reformer furnace, where it is burnt as fuel to provide the heat required for the endothermic reforming reaction. The main stream, instead, is mixed with syngas recovered from further separation processes before being fed to a three intercooled stages compressor Condensation formed during the cooling process is extracted from the unit. At the outlet of the third stage a pressure of 12.65 bar is achieved, which, except for the head loss relative to the following units, coincides with the reforming operating pressure.

The stream BG4 enters then the CO_2 separation section consisting of an absorber and a stripper unit, both equipped with five stages. The goal of this section is to remove enough carbon dioxide to obtain a stoichiometric module M equal to 2 at the reactor inlet by means of MDEA as solvent. The rigorous M definition is provided by Eqn.2.3. The liquid solvent diluted in water solution is fed from the top of the absorber, while the inlet biogas enters the unit at the bottom, on the fifth stage.

The CO_2 rich bottom liquid, R1, requires to be regenerated to minimize amine consumption. This is done in the stripper unit after a first pre – heating with the hot regenerated amine stream up to 45°C. Flux R2 is then fed on the column first stage, where CO_2 is removed from the amine: the stripping process is exothermic. As the reboiler is approached, regeneration is performed thanks to the heat flux which provides energy to break bonds between amines and CO_2. After cooling down to 30°C amines are mixed with a make up stream and fed to the absorber top, since a perfect regeneration is not achieved in the stripper column. Separated gases, mainly CO_2 and traces of other compounds are vented to the atmosphere.

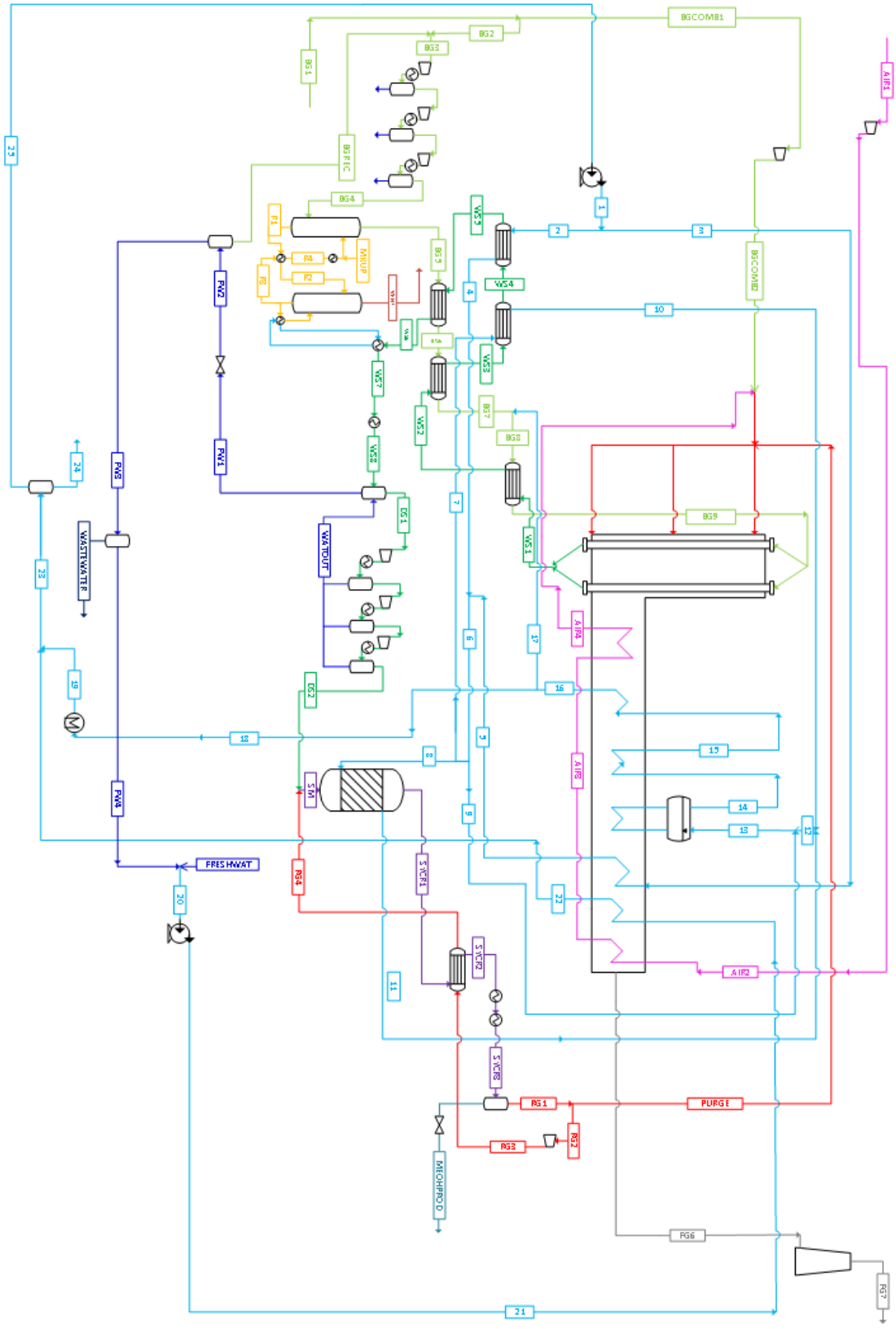

Figure 3.1: *Plant configuration adopting recirculation of unreacted syngas.*

The reboiler heat duty is provided by hot syngas coming from the reformer as form of energy saving. To do so, a water loop is adopted as intermediate mean between heat source and liquid solvent.

The purified biogas BG5 leaves the absorber top to join a pre – heating line before the reforming reaction. It consists of three counter current heat exchangers exploiting hot syngas coming from the reformer as heat source. In the first unit a biogas temperature around 200°C is achieved using syngas at lower temperature already exploited to produce steam. Being indeed steam required during operation, its generation has been coupled with thermal recovery from hot sources available in the plant, like syngas, to avoid an additional energy consumption. The last part of biogas pre – heating is carried on in a couple of exchangers fed by hotter syngas exiting from the reformer reactor. In section 2.2.4.1 it has been explained how a certain excess of steam may enhance the reforming reaction conversion. For this purpose, before entering the third pre – heater, biogas is mixed with produced steam at 255°C to obtain a S/CH_4 ratio equal to 3 on molar basis, an optimal value for the following reforming reaction [26]. A rigorous definition of this parameter is given by:

$$\begin{cases} \dfrac{S}{CH_4} = \dfrac{\dot{n}_{\text{steam}}}{\dot{n}_{\text{CH}_4}} \\ \dot{n}_{\text{steam}} = \dot{n}_{\text{BG9}} \cdot x_{\text{H}_2\text{O}} \\ \dot{n}_{\text{CH}_4} = \dot{n}_{\text{BG9}} \cdot x_{\text{CH}_4} \end{cases}$$

Eqn. 3.1

Where $\dot{n}$ represents a molar flow rate and *x* the molar fraction of the specified component. In the end a temperature for the stream BG9 about 600 °C is achieved at the Fired Tubular Reformer inlet.

The reforming reaction is endothermic, thus, a certain heat requirement has to be satisfied to sustain the reaction. To do so, the furnace of the FTR is fuelled with part of the fresh biogas separated from the main stream at the start of the process, together with a purge flux coming from the methanol synthesis reactor. The latter is recycled to the furnace since it contains oxidable compounds like residual CO and H_2 or traces of entrained methanol. In this way it is possible to reduce fresh fuel consumption. Comburent air is fed to ensure complete

combustion with an excess of O_2 in the flue gas about 4% on molar basis. The flue gas stream FG1 leaves the combustion chamber at 950°C, thus thermal recovery can be performed to cool down its temperature before injection in environment.

Figure 3.2 provides details about the hot source cooling and the processes involved. At first it is possible to recognize air pre – heating, which is practised since the higher is the combustion reactants temperature, the lower will be the irreversibility related to the reaction. Aiming to perform the heat exchange with the smaller possible temperature difference between hot and cold fluid, air pre – heating has been partitioned in a couple of units: one uses colder gases to rise air temperature from ambient conditions to 139 °C, while a second exploits hotter gases from the reformer outlet to set the final temperature to 450 °C. Between them, it may be noticed that the great part of the flue gas thermal power is employed in the steam generation process. An economizer heats the liquid water up to the evaporation temperature of 240 °C and moves it towards a collector where a VLE between liquid water

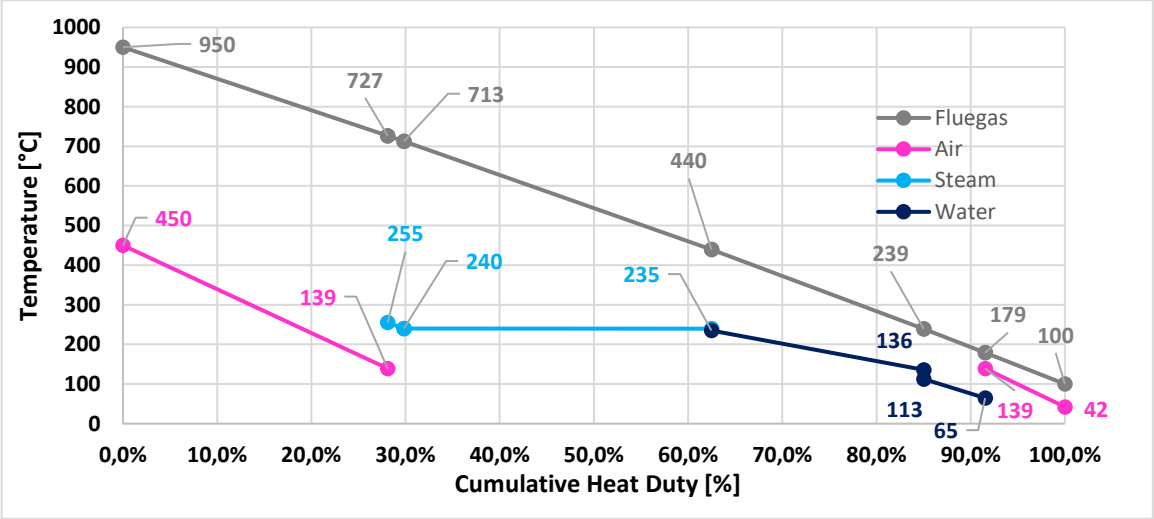

Figure 3.2: *Flue Gas T – Q diagram.*

and produced steam takes place: liquid water joins an evaporator while saturated vapour is fed to a superheater, which sets its final temperature to 255 °C. In this condition it is mixed with the main biogas stream. Even if part of the injected steam is recovered by further separation processes, a certain water consumption takes place due to the reforming reaction

and a make up stream is required. Fresh water is heated up by reformer flue gases in a heat exchanger until a temperature about 113 °C is achieved.

It has to be highlighted that since this arrangement does not consider the methanol purification section, steam is only required to enhance the reforming conversion. Excess of generated steam (flux 18 in Figure 3.1) is condensed and then fed together with the pre – heated fresh water stream to an adiabatic flash drum, where undesired incondensable species are vented in air. Before joining again the steam production process, the resultant water stream 25 is managed by a pump able to rise its pressure to the evaporation pressure of 43.67 bar.

As mentioned, thermal recovery may also be performed from the produced syngas exiting the reformer at 850 °C. The T – Q diagram reported in Figure 3.3 shows details about the whole syngas cooling process. Beside biogas pre – heating, it has been anticipated that part of the syngas thermal power is devoted to steam generation: this is done by means of an economizer and an evaporator working between 136 and 240 °C as for the flue gas cooling. Produced saturated steam is sent to the common collector before the superheating step. At the outlet of the biogas pre – heating line the syngas stream WS6 is exploited by two more heat exchangers where liquid water is adopted as cold side fluid. The first aims at providing the reboiler heat requirement while the other produces hot water at 80 °C for the associated biodigester operation.

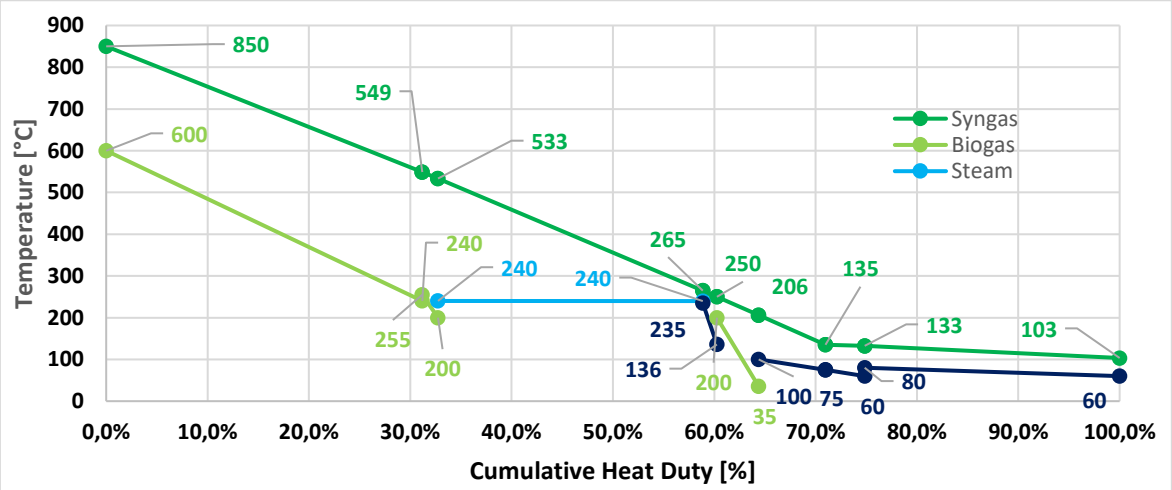

Figure 3.3: *Syngas T – Q diagram.*

Once thermal recovery from hot syngas is completed, the resultant stream WS8 at 99 °C is fed to an adiabatic flash drum to perform water separation and to adjust the final composition. The unit bottom residue is processed in a further flash unit to separate lighter entrained components: the syngas purge BGREC is mixed with the inlet fresh biogas, while the heavier water stream joins a last separator. As result wastewater is extracted from the system while the recovered stream FW4 is mixed with the fresh inlet water make up stream to take part again in the steam production process. Syngas with the desired stoichiometric module may now approach the methanol production island. The final compression is operated by a three intercooled stage compressor rising the stream DS2 pressure up to 95.65 bar. Condensation formed is again extracted from the unit and recycled to the previous water separator. The compressed stream DS3 is mixed with recirculated unreacted feed before entering the methanol synthesis reactor at 202 °C.

The methanol synthesis reactor is a multi – tubular Lurgi reactor equipped with 500 tubes through which the reacting gas flows. Tubes are loaded with zinc oxide based catalyst and as far as the geometrical features are concerned, a standard commercial diameter about 42 mm and a tube length of 6 m have been chosen. Considering that such reactor requires an accurate temperature control [59], boiling water at 240 °C has been adopted as thermal fluid surrounding the equipped tubes. In this way the synthesis reaction occurs almost under isothermal conditions. The water stream comes from the economizers operation while the outlet steam produced due to the reaction heat release, stream 11, is mixed with the other saturated steam fluxes and sent to the afore mentioned collector. In a single passage only a limited amount of fresh feed is converted, such that separation of unreacted syngas from produced methanol is necessary to allow its recirculation in the reactor. To do so, the outlet stream SYCR1 has to be properly cooled: a first regenerative heat exchanger manages its temperature from 242.2 °C, the reactor outlet temperature, to 106.6 °C using the recycled separated stream RG3 as cold side fluid; a further cooler produces hot water at 80 °C for the interaction with the biodigester operation, while a last exchanger brings SYCR3 temperature down to 25 °C. In this condition unreacted feed separation from produced crude methanol is performed in an adiabatic flash unit.

Lighter compounds extracted from the top of the separator, having a certain heating value, are partially recycled to the reformer furnace as purge flux. The great part of the stream is recirculated to the methanol synthesis reactor according to a reflux ratio about 6 on molar basis. It may be defined as the ratio between the recycled stream and the inlet fresh feed molar stream expressed on molar basis:

$$RR = \frac{\dot{n}_{\text{recycled feed}}}{\dot{n}_{\text{fresh feed}}}$$

Eqn. 3.2

A devoted compressor restores a pressure value of 95.65 bar for the stream RG2, previously dropped due to the passage in the reactor and in the following exchangers. Finally, the recycled flux RG3 is pre – heated to 212 °C by the hot reactor outlet stream and then mixed with the incoming fresh syngas.

As for the produced heavier crude, it is extracted at the bottom of the separator at 25 °C and laminated down to 5 bars in a valve. Stream MEOHPROD in these conditions is sent to an external purification hub where the methanol grade specification could be met. Such value of pressure has been chosen since typically methanol distillation is operated a nearly ambient pressure, while a temperature of 25 °C is suggested as a suitable value for methanol storage [59,62].

3.2 Once Through Configuration

Recirculation of the methanol reactor feed is commonly adopted in industrial plants to maximize the synthesis reactor conversion and yield, which would be dramatically low in a single passage. This alternative configuration aims at performing the methanol synthesis reaction in a multistage once through Lurgi reactor operating without adopting recirculation. Unreacted feed from the first stage will react in the following ones, enhancing the global reaction yield.

Initially, the plant behaviour is analogous to the one described in the previous section: the inlet biogas stream is split depending on the reformer requirements before entering the CO_2 separation section. Purified biogas is preheated and mixed with the correct amount of superheated steam to perform the reforming reaction. Thermal recovery is performed both from hot syngas and from reformer flue gases producing steam or providing heat for sub processes like air and biogas pre – heating or amines regeneration. After water separation produced syngas with the desired stoichiometric module about 2.1 is compressed to the synthesis operating pressure. It is reminded that M is computed according to Eqn.2.3. The plant layout keeps unchanged in all these steps as it is shown in Figure 3.4.

Differences may be noticed as the compressed syngas approaches the synthesis reactor. For a better comparison with the traditional arrangement the reactor geometry features as tube diameter and length have been kept unchanged (42 mm, 6 m respectively). The total number of implemented catalysed tubes as well has not been modified, yet it has been partitioned between four reaction stages. Each of them basically consists of three steps: methanol conversion, outlet stream cooling and produced crude extraction.

The number of tubes per stage is set in order to have a Gas Hourly Space Velocity (GHSV) about 4000 h^{-1}, which ensures a sufficient residence time and an acceptable conversion. The GHSV may be defined according to:

$$\begin{cases} GHSV = \dfrac{\dot{n}_{\text{in}} \cdot v_{\text{o}}}{V_{\text{reatt}}} \ [h^{-1}] \\ v_o = \dfrac{R \cdot T}{P} \ [\dfrac{m^3}{Kmol}] \\ V_{\text{reac}} = \dfrac{\pi \cdot D_{\text{reac}}^2}{4} \cdot n^{\circ}_{\text{tubes}} \cdot L_{\text{tubes}} \end{cases}$$

Eqn. 3.4

Where $\dot{n}_{\text{in}}$ is the stage inlet feed mole flux, v_o the specific volume calculated according to the ideal gas equation of state in normal conditions (0°C, 1 atm), R the universal gas constant and V_{reac} the reactor volume. Considering that most of the produced crude is extracted from

the main reacting stream before it joins the succeeding stage, a reduction of $\dot{n}_{in}$ occurs during operation. As consequence, according to Eqn. 3.4 the GHSV would drop unless the reactor volume is managed to decrease. This is done by adopting a progressively reduced number of tubes per stage: the first is equipped with 280 catalysed tubes, while the others implement 100, 70, 50 tubes, respectively.

Temperature control in the reactor is pursued again using boiling water coming from the economizers operation, such that the outlet streams exiting the unit have a temperature about 240 °C. The cooling step is mandatory to achieve a consistent product separation, since in general terms the lower is the temperature of the stream fed to the separator, the higher the liquid fraction will be. In particular, each stream is processed by a couple of water coolers: the first heats up water from 60 to 80 °C as ideal interaction with the biodigester, while the other manages the hot fluid temperature down to 30 °C with the cold side fluid operating between 20 and 25 °C. This target value has been established as result of an optimization discussed in Chapter 5. Concerning the first stage outlet stream, it may be noticed the presence of a further heat exchanger beside the mentioned coolers. This unit exploits incoming fresh syngas as cold side fluid to reduce the cooling duty of the following exchangers as form of energy saving.

Cooled streams with the desired temperature (SYCR1B, SYCR2A, SYCR3A, SYCR4A) are fed to adiabatic flashes where produced crude is separated from the unreacted syngas. Except for the last stage, all the gaseous overheads are sent to the following reactor stage while the extracted bottom liquid fluxes are conveyed to the fourth stage flash unit to perform a final separation. Lighter components in this case are recycled to the reformer furnace to reduce fresh fuel consumption as in the previous arrangement, while produced crude methanol is laminated to 5 bars in a valve.

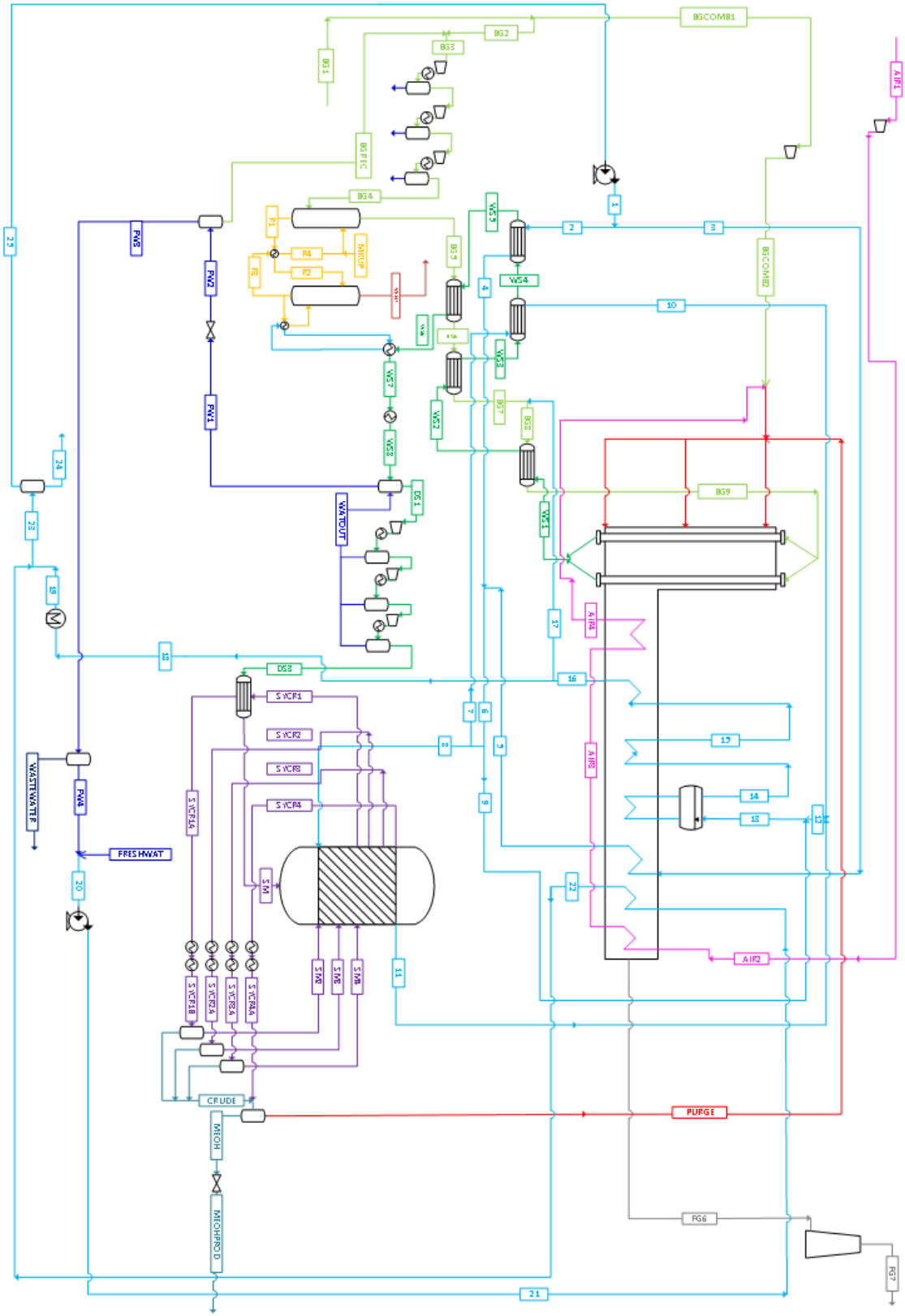

Figure 3.4: *Plant configuration adopting a Once Through reactor.*

Even if the separator inlet temperature is about 30°C, the evaporation process taking place inside the unit reduces the outlet temperature down to 15°C, an acceptable value for methanol storage. Stream MEOHPROD in these conditions consist mainly of water, methanol and CO_2, and it should be sent to an external purification hub to meet the grade requirements.

3.3 Aspen Plus Modelling Details

This section aims to provide more details about the Aspen Plus® models and the Design Specs implemented to simulate the real process behaviour. A summary of them is reported in Table 3.2 together with their task in the simulation and the configuration in which they are active. Being the two plant arrangements quite similar, these considerations are valid for both except when differently specified. For sake of completeness full Aspen Plus flowsheets are reported in Appendix together with tables of implemented calculators and adopted units and streams.

Desing Spec	*Task*	*Configuration*
DS-AIR	Set the amount of comburent air for a complete combustion with a 4% O_2 excess.	Recirculation/Once Through
DS-BGCOMB	set the amount of fresh biogas to be burnt to sustain the reforming heat requirement (QRES = 0)	Recirculation/Once Through
DS-CO2R	set the amount of CO_2 to be separated to obtain a syngas stoichiometric module to 2.1.	Recirculation/Once Through
DS-HXT1	set outlet reformer flue gas temperature to 100°C.	Recirculation/Once Through
DS-LIWAT	set the amount of water to equal the heat duty of the stripper reboiler and the syngas heat exchanger.	Recirculation/Once Through
DS-LOOP1	set cooling water outlet temperature to 80°C. (syngas cooling)	Recirculation/Once Through
DS-LOOP2	set cooling water outlet temperature to 80°C. (crude methanol cooling)	Recirculation/Once Through
DS-LOOP3	set cooling water outlet temperature to 80°C. (second stage cooling)	Once Through
DS-LOOP4	set cooling water outlet temperature to 80°C. (third stage cooling)	Once Through
DS LOOP5	set cooling water outlet temperature to 80°C. (fourth stage cooling)	Once Through
DS-REB	set HCO_3, CO_2, CO_3^- to 8%vol. in R3 stream.	Recirculation/Once Through

DS-SPL3	set the amount of steam to be injected for a S/CH_4 ratio equal to 3.	Recirculation/Once Through

Table 3.2: *implemented Design specs.*

A first remark deals with the reforming process: since a unit to represent a Fired Tubular Reforming does not exist in Aspen, its behaviour has been modelled with the auxilium of two RGibbs reactor units as shown in Figure 3.5. RGibbs units in Aspen are reactor blocks which can take many input or output streams and optional heat streams. Calculations for this kind of unit are based on minimizing the Gibbs energy for the system. The reactor COMB performs the combustion reaction, while REF the reforming one. Interaction between the two lies in the heat stream QREF representing the reforming heat requirement to be satisfied. Heat losses are taken into account with the heat stream QLOSS.

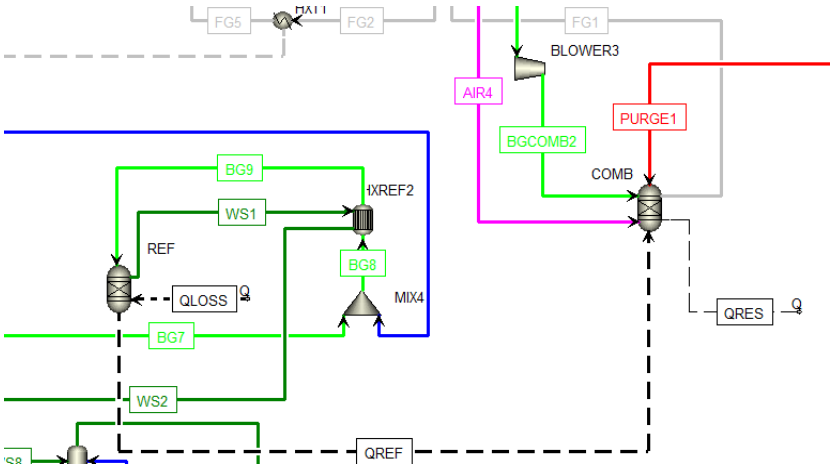

Figure 3.5: *Detailed reforming modelling.*

The overall behaviour is regulated by two design specs, DS-AIR and DS-BGCOMB, which respectively set the amount of comburent air and the amount of fresh fuel to be separated from the main inlet biogas to respect the thermal balance applied to the system. In other terms the heat release from the combustion reaction should satisfy the reformer heat duty expressed by QREF considering also the heat losses QLOSS. QRES models the residual heat from the thermal balance and it is set to 0 thanks to the DS operation.

The auxilium of even three Deign Specs is required to govern the CO_2 separation section performances: DS-LIWAT manages the interaction between syngas cooling and stripper reboiler operation depending on the result of DS-REB, which establishes the required reboiler duty to limit impurities in the regenerated amines stream. More challenging under the computational point of view is the task of DS-CO2R which controls the amount of fresh amines fed to the absorber. Indeed, it aims to obtain syngas with the desired stoichiometric module at the synthesis reactor inlet by removing enough carbon dioxide from the raw biogas even before the reforming reaction.

Concerning the interaction with the biodigester, coolers devoted to hot water production are modelled with water loops operating with cold fluid temperature between 60 °C and 80 °C as shown in the examples provided by Figure 3.6:

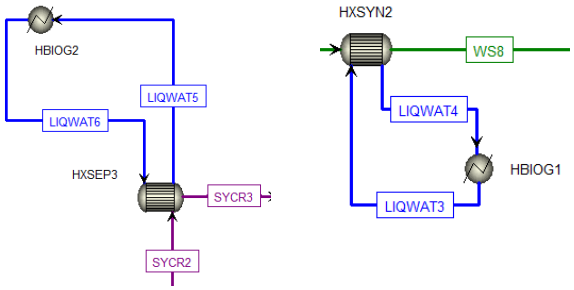

Figure 3.6: *Examples of water loops modelling.*

Each loop is governed by an own DS-LOOP Design Spec varying the amount of water to satisfy the specified duty fraction with a water outlet temperature of 80 °C. In the traditional arrangement the biodigester duty is shared between just two water loops, while in the once through configuration more units are involved, since a water loop is assigned to every reaction stage cooling step. This fact may be appreciated in Figure 3.6 representing how the methanol production island has been modelled in the software for this arrangement. It should be highlighted that because of the reducing feed per stage, also the biodigester duty fraction is progressively reduced and the greatest part is covered by the first stages.

Remarkable is the fact that several RPlug units have been used to model conversion in each stage. RPlug blocks are able to perform more rigorous reactor simulations respect to RGibbs

ones. They offer the possibility to set up the catalyst used and to implement the desired reaction kinetics.

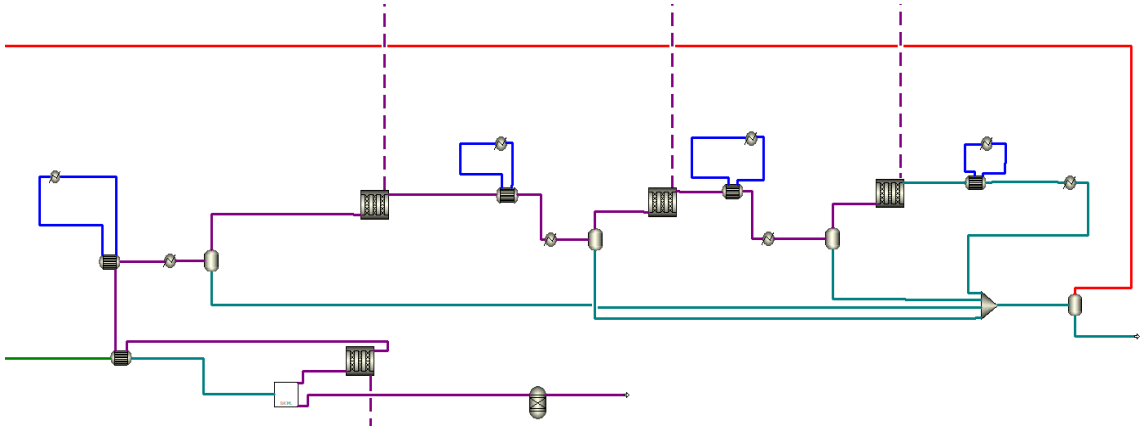

Figure 3.7: *Once Through reactor modelling in Aspen Plus®.*

Differences between the adopted blocks in Figure 3.7 consist only in the specified number of tubes, since in the real process syngas conversion takes place in a single multi stage Lurgi reactor. A RGibbs ideal reactor is present in both the plant configurations to evaluate the equilibrium synthesis conversion; of course, it has not a corresponding unit in the real process.

As for the adopted reactor kinetics in RPlug blocks, the main lines in the conversion mechanism of a CO, CO_2 and H_2 based feed into methanol over a $CU/ZnO/Al_2O_3$ catalyst have been widely studied during past years. Several are the reaction rate expressions available in literature as reported in the work of Bussche and Froment [71]. Relying on literature reaction schemes and experiments, such work proposes a steady state kinetic model which seemed to be suitable for this study purposes, being it extensively tested and sufficiently accurate respect to publications or plant data [71,72].

Two are the reactions considered in the model, RWGS and methanol synthesis. The eventual side reaction of ethanol synthesis has been considered negligible respect to the primary ones. The reaction kinetics suggested has been implemented in the simulation software using the

GENERAL reaction form, where reaction rates are defined according to the LHHW (Langmuir-Hinshelwood-Hougen-Watson) equation for heterogeneous catalyst:

$$r = \frac{K_{\mathrm{f}} \cdot Dr_{\mathrm{f}}}{K_{\mathrm{ads}}}$$

Eqn. 3.5

K_{f} represents the kinetic factor, Dr_{f} the driving force and K_{ads} the adsorption term, all derived by the software itself once provided the required input taken from the reference steady state model.

A final consideration is about the steam production process which has been detached by the main plant model and designed a part. Basically, the interaction between them is represented by material and heat streams. Among the material stream it is possible to include recovered water from produced syngas and the superheated steam required by the reforming reaction. Heat streams, instead, come from the synthesis reaction heat release and from hot sources cooling, i.e. reformer flue gas and syngas. Such streams take part in the sub process detailed in Figure 3.8 which is provided with own Design Specs. All of them are required to rule the heat exchange with the various sources.

Starting from the economizers operation, the incoming compressed fresh water is fractioned according to a first DS to exploit all the remaining available thermal power from the syngas source in the unit ECO1. The rest is dispatched towards the other exchanger, ECO2, fed by the reformer flue gas thermal power. Outlet water at 240 °C is collected in a single stream before the evaporation step, which is more complex to handle since three are the heat sources to be considered. The synthesis reaction heat release is only involved this step, therefore a DS establishes the amount of water to fully exploit this source in the exchanger EVA2.

Another Spec acts instead on the evaporator fed by hot syngas, EVA1, to obtain a minimum internal approach temperature of 25 °C varying the amount of cold side boiling water. The collector behaviour has been modelled by a flash drum governed by a further DS. Its task is to find the amount of liquid water to be supplied to the evaporator fed by the reformer flue

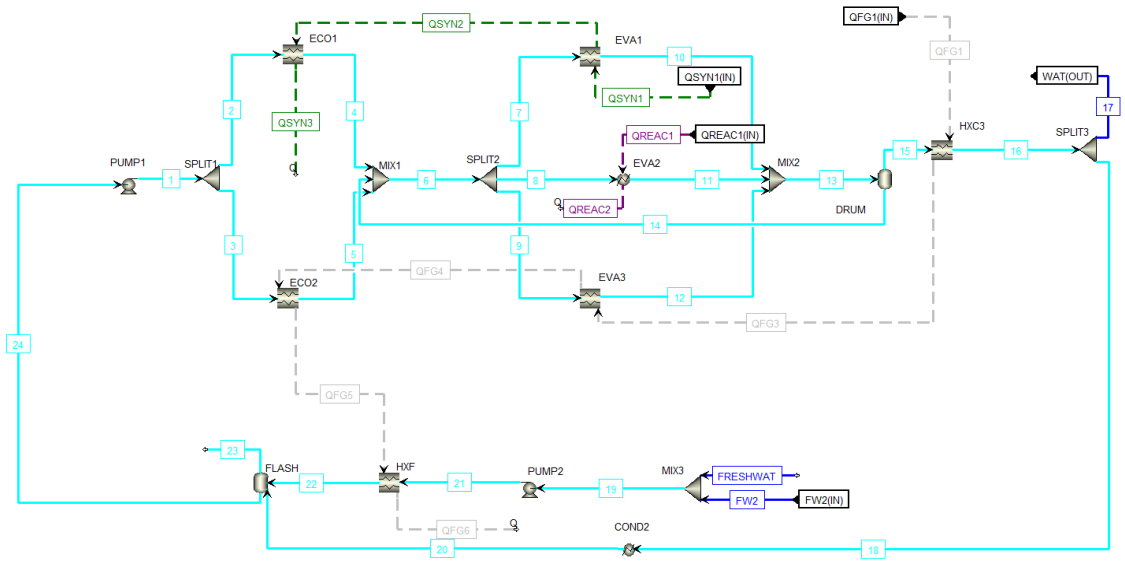

Figure 3.8: *steam generation from heat recovery.*

gas heat stream in order to obtain a minimum internal approach temperature of 200 °C . On the other hand, saturated steam is processed in the superheater where it is able to reach 255 °C. The amount of superheated steam mixed with the reformer inlet biogas is established by the DS-SPL3 operating in the main plant. The excess steam, as mentioned, is condensed and recycled to the incondensable separator before the beginning of a new cycle. Fresh water and recycled water from the main process as well are sent to the separator after being pre – heated by the remaining flue gas thermal power.

A summary of all the implemented Design Specs implemented in the sub process is available in Table 3.3.

Desing Spec	***Task***
DS RECY	Set water required to get a minimum internal approach temperature of EVA3 to 200 °C.
DS SPL1	Set water required to exploit all the syngas remaining thermal power in the heat flux QSYN2.
DS SPL2E	Set water required to get a minimum internal approach temperature of EVA1 to 25 °C.
DS SPL2R	Set water required to exploit all the methanol reactor thermal power.

Table 3.3:*Summary of design specs implemented in the heat recovery section.*

3.4 Plant Configuration Variations

These sections focus on the modifications implemented to the base plants to perform a critical analysis with optimization purposes. Base cases for both the traditional and the once through arrangements adopt a CO_2 separation section upstream the reformer, whose aim is to achieve the desired stoichiometric module at the reactor inlet. Anyway, alternatives as the CO_2 separation performed on the reformed syngas or the direct process without separation have been studied. The aim was to establish the optimal location of the separation section.

Crude methanol distillation is an energy intensive separation process and contributes significantly to the cost of methanol production [58]. Dealing with a small scale plant the presence of the distillation section has been neglected, assuming purification performed in an external purification hub. In this way it has been possible to save both fixed and operating costs related to this process. Anyway, the effect on plant performances and costs related to the integration of the purification section has been also considered with a comparative approach. For this purpose, a traditional two columns system has been modelled and implemented in the traditional plant configuration

3.4.1 Post reformer CO_2 separation

This variation has been implemented both in the once through and in the traditional arrangement aiming to find the optimal location of the CO_2 separation section. Modifications described are common in both cases.

The fresh biogas feed follows a path analogous to the one previously described towards the first multi stage compressor. Then, after being compressed, the main stream directly flows through the pre – heating line to approach the reformer with a reduced pressure drop and the same inlet temperature of 600 °C. This is related to the fact that fresh biogas has been managed by less units. Steam is added from the heat recovery section to obtain the desired S/CH_4 ratio before the reforming reactor in the FTR, whose methane conversion is expected to increase due to the abundance of CO_2 promoting the Reverse Water Gas Shift reaction (RWGS):

$$RWGS: CO_2 + H_2 \rightarrow CO + H_2O \qquad \Delta H_{298_K} = +41.1 \frac{kJ}{kmol}$$

Eqn. 3.6

Water formed in this way during the process may take part in the steam reforming reaction0 enhancing methane conversion.

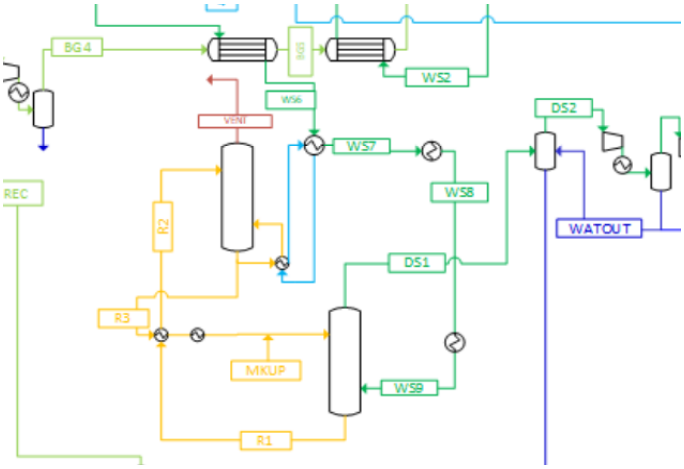

Figure 3.9: *Post - Reformer CO_2 Separation process.*

The CO_2 rich reformer outlet syngas follows the same cooling path, feeding part of the steam generation process and the biogas pre – heaters, together with the stripper reboiler and the water cooler associated with the biodigester operation. Anyway, syngas temperature at the end of the cooling process is about 75°C for the traditional arrangement and 80 °C for the once through case. It is still too elevated to be exploited in a separation system based on amines: high temperatures indeed promote amines degradation, compromising the separation process [26]. A further cooler is needed to cool down the syngas temperature to 30 °C at the absorber inlet, the same feed temperature chosen for the separation located upstream the reformer reactor. From Figure 3.9 it is possible to appreciate the new design of the CO_2 separation section with the presence of the additional cooler between streams WS8 and WS9. Such plant variation is common to both the studied configurations, whose full modified plant scheme is reported in Appendix.

No appreciable differences have to be reported concerning the behaviour of the separation section, which is still governed by the same three Design Specs. The difference with respect

to the pre – reformer configuration concerns the composition of the main stream to be purified which is now dependent on the reforming reaction. The effect on cost and performances has been deeply evaluated in the following chapters. From this point on plants do not present other changes respect to their base case configuration, compressed syngas with the desired stoichiometric module approaches the synthesis reactor where the process proceeds depending on the specific configuration.

3.4.2 Direct process without CO_2 separation

Typically, large scale applications may afford to face higher fixed investment costs for the equipment exploiting the positive effect of economies of scale and a greater productivity. Since in this study a small scale methanol production plant is concerned, it seemed to be reasonable to consider the effect of the direct syngas processing without CO_2 separation. In this way it is possible to save the investment cost related to the purchase of several heat exchangers and the two columns, absorber and stripper, needed for the process. Also operating costs are expected to decrease, because there is no need to satisfy the stripper reboiler heat requirement or to reintegrate fresh amines. On the other hand, by performing direct processing of the assumed biogas feed it will not be possible to reach an optimal stoichiometric module at the reactor inlet, thus a certain penalization of performances follows. Such aspects have been evaluated in detail in the techno economic analysis.

This variation has been considered both for the once through and the traditional arrangement; except for the absence of the whole separation section, the behaviour of each plant keeps unchanged.

3.4.3 Addition of a methanol purification section

It has been anticipated that crude methanol upgrading is an energy intensive and costly process needed to meet the product grade requirements. Due to the small scale application considered, purification performed in an external hub has been assumed. Anyway, with the aim to evaluate the possible impact on plant performances and cost, a simple two complete distillation columns system has been integrated in the traditional plant adopting recirculation aiming to obtain a methanol purity about 99% (grade AA) [8]. Even if more columns would

have reduced the reboilers steam requirement, the two columns system appeared to be the most reasonable choice in terms of investment costs for the specific case.

Figure 3.10 provides a complete scheme of the plant including the integrated methanol upgrading section. Once the unreacted syngas has been separated from the produced crude, this latter is laminated down to the first column operating pressure of 10 bar. Before being processed in the column, it is fed to a couple of regenerative pre – heaters. The first rise the crude temperature to 67 °C using purified AA methanol as heat source. The other exploits hot wastewater coming from the bottom of the atmospheric column and it is able to achieve a crude temperature about 74 °C. The crude stream in these conditions is supplied on the light column fifth stage. A total of 14 stages have been adopted to perform separation of light ends from heavier compounds like water and methanol, which are collected at the bottom of the unit. A partial reboiler recirculate part of the bottom vapours inside the distillation column where they ascend and condense in the trays in contact with colder liquids. More volatile components will continue to ascend in the gas phase to be extracted from the top.

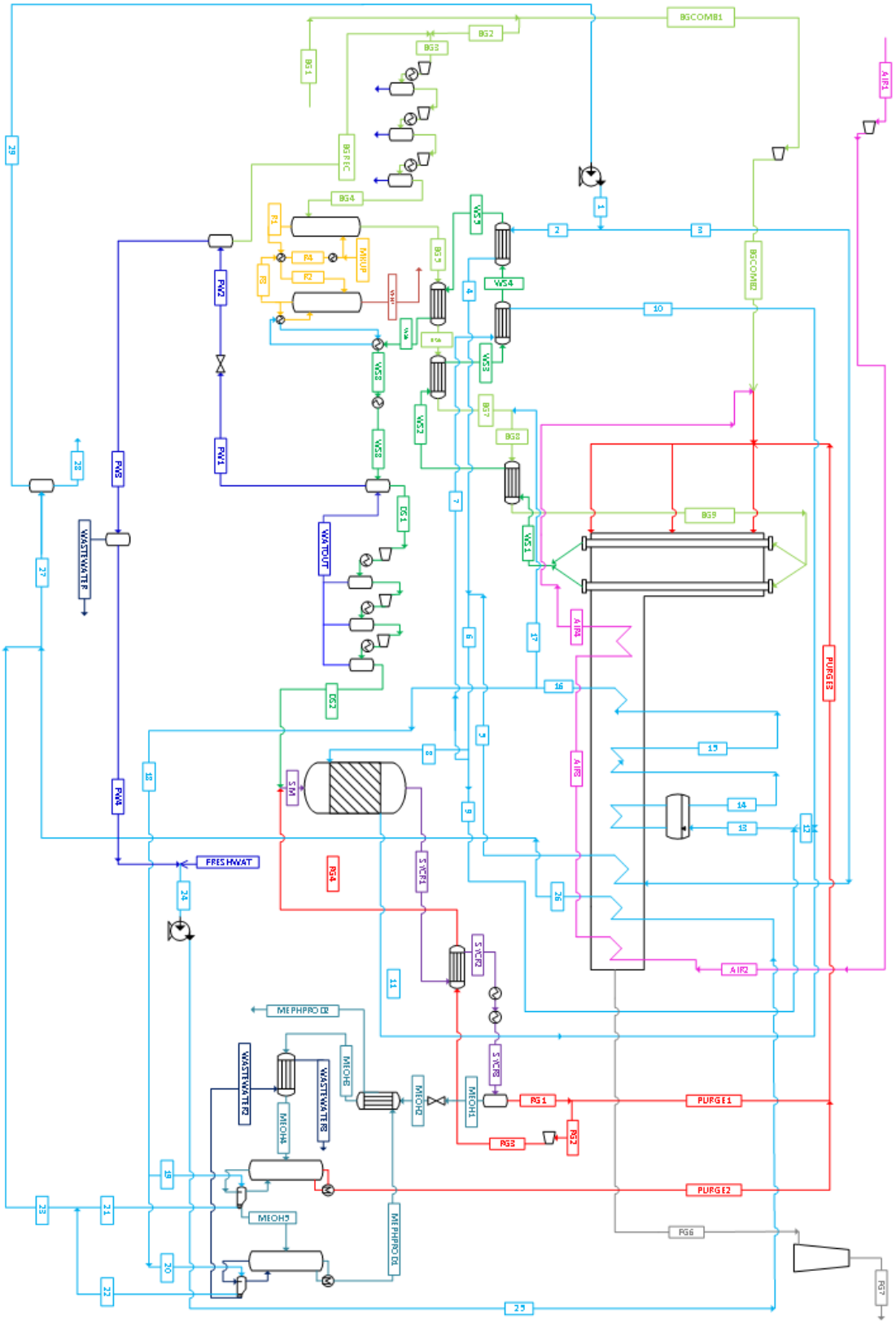

Figure 3.10: *Complete methanol production process including methanol upgrading.*

Since the overhead stream contains oxidable compounds like CO and traces of methanol, it is recycled to the reformer furnace as a further purge flux to reduce the amount of required biogas. Part of the distillate is anyway recycled in the system through a total condenser according to a reflux ratio about 0.257. The reflux ratio may be defined as the ratio between the distillate molar flow rate ($\dot{n}_{distillate}$) and the recirculated molar flow rate ($\dot{n}_{reflux}$):

$$R_r = \frac{\dot{n}_{\text{distillate}}}{\dot{n}_{\text{reflux}}}$$

Eqn. 3.6

Due to the contact with hotter vapours, the recycled stream will evaporate again during operation. Globally, respect to the inlet feed, the column operates with a distillate to feed ratio of 0.054 on molar basis:

$$D_f = \frac{\dot{n}_{\text{distillate}}}{\dot{n}_{\text{feed}}}$$

Eqn. 3.7

Where again $\dot{n}$ represents the molar flux.

The liquid outlet stream leaves the bottom reboiler at 141 °C to enter the following atmospheric column on the 16th stage, where heavier water may be separated from produced methanol. A total of 20 stages have been equipped. The working principle is the same, condensed heavier species leave the system from the bottom while the lighter gas phase from the top. This unit operates with a D_f about 1.027 and a R_r about 0.76 on molar basis. Respect to the previous it is evident a net difference in the values of the mentioned design parameters. This is coherent with the initial stream composition since impurities and water covered only about the 30% of the stream MEOH1 on molar basis. Both the outlet streams leave the system at high temperature and may be exploited in the crude preheaters. Purified overheads have a temperature about 81 °C at the outlet of the top condenser, while separated wastewater exits the column bottom reboiler at 118 °C. Due to the small portion of entrained methanol

or lighter components, it should be properly treated in a wastewater treatment section before injection in environment. Thanks to this two column distillation system, a methanol purity of 99% for the stream MEOHPROD2 is achieved.

Particular emphasis should be given to the fact that both the distillation column reboilers are fed by superheated vapour generated by thermal recovery from hot sources (streams 19, 20). In the simulation the amount of steam delivered is established to fully satisfy the reboilers heat requirement by a devoted Design Spec. It has to be highlighted that even if in the simulated operating condition a S/CH_4 ratio about 3.02 is achieved at the FTR inlet, this parameter is not anymore controlled by a Design Spec due to the constraint on the reboilers duty. In other terms steam not required by the distillation section is mixed with the biogas stream to enhance the reforming reaction. Moreover, streams 19 and 20 fed to the column reboilers condense during operation such that a condenser is not required before the incondensable separation.

No significant changes have been made on the adopted Design Spec, with the exception of the mentioned updating of DS-SPL3 that now controls the reboilers steam requirement instead of the reformer inlet S/CH_4 ratio.

4. METHODS

This chapter describes the criteria and methods adopted to perform a techno – economic analysis of the presented methanol plant configurations. At the beginning a brief discussion about the Equations of State (EoS) adopted in the simulation is reported. As a second step the description of the utilized methodology and criteria to perform plants economic analysis are presented. Particular emphasis has been given to the methanol synthesis reactor: due to the small scale considered it was challenging to find in literature a suitable cost correlation as function of the reactor size for the economic evaluation of the component. Considering that a Lurgi reactor basically consist of a shell inside which catalysed tubes are surrounded by thermal fluid, its configuration may be assimilated to a Shell&Tube heat exchanger [59]. With this assumption it has been possible to develop a further reactor model with the auxilium of the Aspen EDR® software, thanks to which several cost correlations valid for different reactor geometries and operating conditions have been achieved. A final section deals in the end with the presentation of the main technical Key Performance Indicator (KPI) according to which plant performances have been evaluated in the next chapter.

4.1 Equations of State

In general terms, the choice for the more suitable EoS to adopt in the simulation of a real reacting system is quite challenging. Each component, indeed, may show a different behaviour from ideality. In the high pressure methanol synthesis, for instance, CO and H_2 represents nearly ideal gas behaviour, while methanol is far off from ideality [64].

A number of works for chemical equilibria in methanol synthesis from syngas indicate that the Redlich – Kwong – Soave (RKS) EoS gives best results in correcting non ideal gas behaviours [64, 65, 66]. This is a cubic EoS based on the Redlich – Kwong formulation: [67]

$$P = \frac{R \cdot T}{v - b} - \frac{a}{v \cdot (v + b)}$$

Eqn. 4.1

Where P is the pressure, R the gas constant, T the temperature and v the specific molar volume. The term b is a correction for the volume, while the term a takes into account attractive potential of molecules. When dealing with mixtures both a and b become composition dependent [67]

$$\begin{cases} a_{\mathrm{i}}(T) = \dfrac{0.42747 \cdot R^2 \cdot T_{\mathrm{ci}}^2}{P_{\mathrm{ci}}^2}\ \alpha_{\mathrm{i}}(T) \\ b_{\mathrm{i}} = 0.08664 \cdot \dfrac{RT_{\mathrm{ci}}}{P_{\mathrm{ci}}} \end{cases}$$

Eqn. 4.2

Where the subscript i stands for the mixture i[th] species, while T_c, P_c for the critical temperature and pressure.

In the RK model, beside composition, a is function of temperature due to the parameter $\alpha_i(T)$, while the Soave correction introduces the dependency on the molecule sphericity represented by the Pitzer acentric factor ω [65, 67]

$$\sqrt{\alpha_{\mathrm{i}}(T,\omega)} = 1 + m_i(\omega) \cdot \left(1 - \sqrt{T_{R_{\mathrm{i}}}}\right)$$

Eqn. 4.3

T_{R_i} is the reduced temperature respect the critical one and $m_i(\omega)$ a further parameter that can be expressed according to [65]

$$m_{\mathrm{i}} = 0.48508 + 1.55171 \cdot \omega_{\mathrm{i}} - 0.15613 \cdot \omega_{\mathrm{i}}^2$$

Eqn. 4.4

Mixing rules are to obtain the parameters a and b. For a better fit of the EoS binary interaction between components should be taken into account in the mixing rules. This could be done by means of binary interaction parameters $k_{ij,}$ empirically derived; the subscripts i and j identify a pair of components. In the original formulation of the mixing rule b is calculated without binary interaction parameters [65, 67].

$$\begin{cases} b = \sum_{i}^{n} x_i \cdot b_i \\ a_{ij} = \sqrt{a_i \cdot a_j}(1 - k_{ij}) \\ a = \sum_{i}^{n}\sum_{j}^{n} x_i \cdot x_j \cdot a_{ij} \end{cases}$$

Eqn. 4.5

Where *n* represents the total number of species and *x* their molar fraction.

As far as the liquid phase is concerned, the Non Random Two Liquid model equation (NRTL) can be applied in a wide variety of hydrocarbon mixtures for the prediction of VLE and LLE [68]. It basically provides an expression for the computation of each species activity coefficient γ_i depending on the local molar composition. For sake of completeness the general equation is reported without showing its details. Being i the central molecule surrounded by j molecules in a mixture of k elements [68]

$$\ln(\gamma_i) = \frac{\sum_j^n x_j \cdot \tau_{ij} \cdot G_{ij}}{\sum_k^n x_k \cdot G_{ki}} + \sum_j^n \left(\frac{x_j \cdot G_{ij}}{\sum_k^n x_k \cdot G_{kj}} \left(\tau_{ij} - \frac{\sum_k^n (x_k \cdot \tau_{kj} \cdot G_{kj})}{\sum_k^n (G_{kj} \cdot x_k)}\right)\right)$$

Eqn. 4.6

Several equations are available for the expression of the terms τ and *G* [68, 77, 78].

In the light of these considerations, among the proposed methods by the Aspen Plus database the RKS model has been applied to the methanol synthesis reactor, while the NRTL – RK for the rest of the plant. Such model implements the NRTL equation for the liquid phase and the RK for the gas phase. Concerning water separators, due to the presence of HCO_3^- and CO_3^{--} ions entrained in the water stream, it was necessary to adopt the ELECNRTL model (Electrolyte NRTL with RK EoS method), able to predict their behaviour in the solution. Basically, it is a modification of the NRTL method which add two more contributions to the calculation of the activity coefficient [78]

$$\ln(\gamma_i) = \ln(\gamma_i)^{PDH} + \ln(\gamma_i)^{BORN} + \ln(\gamma_i)^{NRTL}$$

Eqn. 18

Equations for the additional contributions are provided by Mondal et al. [78].

As further development of this work, the effect of the Mathias Jakobsen modification of the RKS could be evaluated [65]. This model has been adapted to better describe VLE in systems containing water and methanol, a fundamental mixture in methanol synthesis. Mathias modification basically introduces a polarity correction parameter, p_p, on the mentioned term $\alpha_i(T, \omega, p_p)$ to take into account behaviour of polar components. This model should predict a higher conversion at the end of the synthesis process [65]. Considering that it is not present in the Aspen Plus database by default, it should be modified manually from the RKS model.

4.2 Economic analysis method

The implemented method described in this section is suggested by Turton et al. [20]. According to the reference, when evaluating the economic feasibility of a certain plant at first plant economics should be computed. These consist in the fixed capital investment (FCI) related to the purchase of all the equipment and in the operating cost of manufacturing (COM). With these information it is possible to proceed with a profitability analysis, whose goal is to provide significant economic indicators.

The complete procedure to perform the economic analysis has been implemented in the Aspen simulation by means of an Excel calculator. In this way it was possible to automatically obtain results for each studied arrangement and investigated operating condition.

4.2.1 Capital Cost

When evaluating the capital cost to purchase the equipment the effect of several factors has to be taken into account: capacity, operating pressure, material, installation and inflation.

4.2.1.1 Capacity Effect

The cost of a certain component is dependent on the adopted size according to its cost function, which typically is a power law or an exponential equation:

$$C_{\mathrm{p}}^{\mathrm{o}} = C_{\mathrm{ref}} \cdot \left(\frac{A}{A_{\mathrm{ref}}}\right)^{\mu}$$

Eqn. 4.8

Where $C_{\mathrm{p}}^{\mathrm{o}}$ is the purchased cost in base conditions and *A* represents the component capacity or size. The subscript ref identifies a reference cost and size while μ the exponential factor for the considered unit. Such equation may be managed and expressed in function of proper empirical fitting parameters typical of each component cost curve, K_{i} , according to:

$$\log\left(C_{\mathrm{p}}^{\mathrm{o}}\right) = K_1 + K_2 \cdot \log(A) + K_3 \cdot (\log(A))^2$$

Eqn. 4.9

The term $C_{\mathrm{p}}^{\mathrm{o}}$ does not take into account the effect of the operating pressure or the building material. Such kind of equation has been used for almost all the unit adopted with the exception of the methanol reactor and the auxiliary cooling tower required to cool down utility water). For the cooling tower an investment cost of 125000$ has been assumed [22] while for the synthesis reactor a cost function has been derived with the auxilium of the software Aspen EDR.

Since this step requires information about a representative size or capacity parameter for each component considered in the plant, additional calculators have been developed to achieve them where they are not provided by the default software results. For instance, this is the case of separators volumes or exchangers heat exchange surface. A list of all the calculators implemented in the simulations is reported in Appendix.

The computed capacity or size of some units exceeded the validity range for the correlations provided by the main reference. In such cases fitting parameters have been taken from [10, 18, 73, 76].

4.2.1.2 Pressure and Material effect

To take the effect of both adopted material and operating pressure into account it is necessary to update the purchased cost in base conditions, C_p^o, into the bare module cost C_{BM}. Beside information about pressure and materials, such cost term takes also into account other expenses related to each specific component. Examples could be insulation expenses, fireproofing, auxiliary instrumentation and many other depending on the specific case. Calculation of this parameter, therefore, strongly depends on the unit considered and requires some intermediate factors.

In general terms the adoption of higher operating pressure brings to higher stresses to withstand. Reinforcements of the components structures are needed to allow operation under such more severe condition, resulting therefore in an increment of the investment cost. The effect of pressure may be synthesized by the parameter F_p , pressure factor, which has a different expression depending on the considered unit. For process vessels, both horizontal and vertical, the following equation is used:

$$F_{p_{vessel}} = \frac{\frac{P \cdot D_{vessel}}{2 \cdot (850 - 0.6 \cdot P)} + 0.00315}{0.0063}$$

Eqn. 4.10

Where P is the operating pressure and D_{vessel} the vessel diameter. For all remaining units the following exponential function is adopted:

$$log(F_p) = C_1 + C_2 \cdot \log(P) + C_3 \cdot (\log(P))^2$$

Eqn. 4.11

Again, P stands for the pressure and C_i are fitting parameters typical of each unit. If the F_p calculation returns a value less than 1 it has to be rounded to 1, meaning that the component operating pressure has no influence on the total fixed investment cost.

The effect of different building material is considered with the constant parameter F_m, the material factor. By combining F_p and F_m it is possible to compute the bare module factor F_{BM}, a multiplication factor that beside the information of pressure and material includes the effect of auxiliary the expenses proper of each unit

$$F_{BM} = B_1 + B_2 \cdot F_m F_p$$

Eqn. 4.12

B_1 and B_2 are tabulated coefficients. With this information it is possible to calculate the mentioned C_{BM}. All the adopted equations are reported in the following Table 4.1 together with the validity field:

Equations	***What for***	***n°***
$C_{BM} = C_p^o \cdot F_{BM}$	Heat exchangers, vessels, pumps, compressors, drivers and power recovery	***Eqn. 4.13***
$C_{BM} = C_p^o \cdot F_{BM} \cdot F_p$	Evaporators, vaporizers and fans	***Eqn. 4.14***
$C_{BM} = C_p^o \cdot F_{BM} \cdot F_p \cdot F_t$	Furnace and boilers.	***Eqn. 4.15***
$C_{BM} = C_p^o \cdot N \cdot F_{BM} \cdot F_q$	Trays and demister pads	***Eqn. 4.16***

Table 4.1: Adopted bare module cost equations and validity fields.

In some cases other factors beside the mentioned ones are involved. More precisely, in Eqn. it is reported the superheating correction factor, F_t. When evaluating boilers this term takes into account the produced vapour superheating degree, while for furnaces it is equal to 1. In Eqn. , instead, the term F_q represents the quantity factor, strictly dependent on the number of trays/pads, N:

$$\begin{cases} log(F_q) = 0.4771 + 0.08516 \cdot \log(N) - 0.3473 \cdot (\log(N))^2 & if\ N < 20 \\ F_q = 1 & if\ N \geq 20 \end{cases}$$

Eqn. 4.17

All the required coefficient to update the unit costs have been taken from [20].

4.2.1.3 Installation effect

When building a plant also some other costs have to be considered like contingency and fee costs and auxiliary facilities costs.

Starting from the first group, they account for unforeseen circumstances, unpredicted prices increase and taxation. The total module cost C_{TM} includes these costs and may be computed from the bare module cost. For well known systems it is reasonable to assume a surcharge about 15% for contingency costs and about 3% for fees, resulting in:

$$C_{TM} = 1.18 \cdot \sum_{i=1}^{n=n°of\ units} C_{BM_i}$$

Eqn. 4.18

Auxiliary facilities costs include costs for site development, auxiliary buildings and off – site utilities. These terms are generally unaffected by components operating pressure or construction materials and may be considered roughly about half of the plant global bare module cost. Adding these costs to the total module cost provide the grassroots cost C_{GR} :

$$C_{GR} = C_{TM} + 0.5 \cdot \sum_{i=1}^{n=n°of\ units} C^{o}_{BM_i}$$

Eqn. 4.19

Where $C^{o}_{BM_i}$ is the bare module cost of the ith component computed for a pressure factor equal to 1.

4.2.1.4 Inflation effect and FCI calculation

Costs are not constant in time since the value of money varies due to inflation/deflation. When depending on past records or published correlations for price information it is essential to update the cost value obtained taking these phenomena into account. This could be done by means of the Chemical Engineering Plant Cost Index, CEPCI. It is basically an index computed according to statistic analysis of price data [79]. Assuming all the equipment purchased in 2019 the actualized cost using the CEPCI result to be:

$$C_{2019} = C_{\text{ref}} \cdot \frac{I_{2019}}{I_{\text{ref}}}$$

Eqn. 4.20

Where *I* is the CEPCI for a certain year, *C* the cost to be actualized and the subscript ref identifies the reference year respect to which the actualization is performed. All the required CEPCI values have been taken from [79].

By summing all the actualized cost data per each adopted unit in the process, the total fixed capital investment to build the plant (FCI) is finally obtained:

$$FCI\ [\$] = \sum_{\text{i}=1}^{\text{n=n°of units}} C_{\text{GRi}_{2019}}$$

Eqn. 4.21

4.2.2 Operating Costs

The plant operating costs are related to the manufacturing process and are represented by the parameter *COM*, i.e. cost of manufacturing. For the studied plants model it may be computed according to:

$$COM\ \left[\frac{\$}{year}\right] = 0.180 \cdot FCI + 2.73 \cdot C_{\text{ol}} + 1.23 \cdot (C_{\text{ut}} + C_{\text{rm}})$$

Eqn. 4.22

It is evident the dependence on the *FCI* and other cost terms as C_{ol}, $C_{\text{ut}}, C_{\text{rm}}$ which respectively stand for labour, utility, waste treatment and raw material operating costs.

To evaluate these cost terms on a yearly basis, a stream factor SF equal to 0.96 has been assumed. SF is representative of the plant operating hours per year.

4.2.2.1 Utility Cost

Utilities considered in the plant model consisted in cooling water and electricity. Steam was not included as utility in this analysis since it is produced by the plant itself and no additional

cost have to be considered for its supply. Concerning cooling water, once known the volumetric yearly consumption v_{H20} it has been estimated according to:

$$C_{\text{cooling water}}\left[\frac{\$}{year}\right] = v_{\mathrm{H20}}\left[\frac{m^3}{year}\right] c_{\text{cooling water}}\left[\frac{\$}{m^3_{\mathrm{H_2O}}}\right] SF$$

Eqn. 4.23

While the cost of electricity requires to compute the global plant yearly electric energy requirement. Being *Pi* the electric power requirement of a certain component:

$$C_{\text{elec}}\left[\frac{\$}{year}\right] = c_{\text{elec}}\left[\frac{\$}{kWh}\right] \cdot SF \cdot\ 8760\left[\frac{h}{year}\right] \cdot \left(\sum_{\mathrm{i=1}}^{\text{n=n°powered units}} P_{\mathrm{i}}\,[kW]\right)$$

Eqn. 4. 24

The specific costs $c_{\text{cooling water}}$ and c_{elec} are provided by [20]. The term C_{ut} is computed from the sum:

$$C_{\mathrm{ut}}\left[\frac{\$}{year}\right] = C_{\text{elec}} + C_{\text{cooling water}}$$

Eqn. 4.25

4.2.2.2 Raw Material cost

This terms accounts for the raw material supply cost. Considering that inlet fresh biogas source is assumed to be waste treatment, its production cost has been considered negligible as paid back by the waste handling itself. It was instead evaluated the cost for fresh inlet water, make up amines and catalyst replacement:

$$\begin{cases} C_{\text{MDEA}}\left[\dfrac{\$}{year}\right] = m_{\text{MDEA}}\left[\dfrac{kg}{year}\right] \cdot c_{\text{MDEA}}\left[\dfrac{\$}{kg}\right] \\ C_{\text{fresh water}}\left[\dfrac{\$}{year}\right] = \ m_{\text{fresh water}}\left[\dfrac{kg}{year}\right] \cdot c_{\text{fresh water}}\left[\dfrac{\$}{kg}\right] \\ C_{\text{catalyst}}\left[\dfrac{\$}{year}\right] = \dfrac{\left(\dfrac{\pi \cdot D_{\text{tubes}}^2}{4} \cdot L_{\text{tubes}} \cdot n_{\text{tubes}}\right) \cdot [m^3]\rho_{\text{catalyst}}\left[\dfrac{kg}{m^3}\right] \cdot (1-\varepsilon) \cdot \ c_{\text{catalyst}}\left[\dfrac{\$}{kg}\right]}{t_{\text{replacement}}[year]} \end{cases}$$

Eqn. 4.26

Where m_{MDEA} and $m_{\text{fresh water}}$ are the plant yearly raw material requirements on mass base. It may be appreciated that the catalyst cost depends on the catalysed tubes total volume (computed once the number of implemented tubes and their geometrical features are known), the catalyst density ρ_{catalyst} and the reactor void fraction ε. Moreover, $t_{\text{replacement}}$ represents the fact that catalyst replacement should be performed every 4 years [10]. Specific cost data to account for MDEA and catalyst (c_{catalyst} and c_{MDEA}) are suggested by [10], while $c_{\text{fresh water}}$ is again provided by [20]. Again, the total cost of raw material is given by the sum:

$$C_{\text{rm}} = C_{\text{catalyst}} + C_{\text{fresh water}} + C_{\text{MDEA}}$$

Eqn. 4. 27

4.2.2.3 Operating Labour Cost

To compute this cost fraction at first it is necessary to estimate how many are the operators are required to run the plant (OP_{lab}). This is done by the correlation suggested by [20]:

$$\begin{cases} N_{\text{ol}} = \left(6.29 + 31.7P_{\text{solid}}^2 + \ 0.23N_{\text{np}}\right)^{0.5} \\ OP_{\text{lab}} = N_{\text{ol}} \text{ (rounded to the nearest integer)} \end{cases}$$

Eqn. 4.198

Where N_{np} is the number of non – particulate processing steps and P_{solid} the number of processing steps involving the handling of particulate solids (in this case equal to 0). The global operating labour cost C_{ol} is eventually evaluated according to :

$$C_{\mathrm{ol}} = 4.5 \cdot OP_{\mathrm{lab}} \cdot L_{\mathrm{w}}$$

Eqn. 4.209

L_{w} is the labour wage, assumed to be 69010 $/year according to [75]. Notice that OP_{lab} is the number of operators required to run the plant but it is multiplied by 4.5. This is related to the fact that a chemical plant is typically operative 24 hours per day but operators work is organized in shifts. The factor 4.5 takes into account shifts scheduling and potential vacations [20].

4.2.3 Profitability Analysis

With the information of the fixed capital investment and the manufacturing cost it is possible to proceed with the assessment of the economic feasibility of the plant through a profitability analysis. Some further assumptions are required to proceed with the calculation of yearly cash flows and useful economic indexes. These are reported in the following Table 4.2:

Profitability Analysis Assumptions
Land Cost : C_{land}= 2M€
Working Capital: WC= 20%FCI **
Tax Index: t = 0.45 **
Years allowed for equipment depreciation: n_{years} = 5 years **
Plant Lifetime: 25 years
Plant building phase: 2 years
Discount rate: i = 8%
Methanol selling price: p_{CH_3OH} = 500 €/tons [10]
FCI salvage value: S = 1M€ **
Euro-Dollar exchange rate: EURUSD = 1.12 (Jan. 2019)
** Taken from [20]

Table 4.2:*Profitability analysis assumptions.*

It has to be noticed that even if the *FCI* and the *COM* have been computed in dollars for compatibility with the manual correlations, results of the profitability analysis are provided in euros thanks to the Euro-Dollar exchange conversion.

Yearly cash flows during the plant building phase are negative (meaning that they represent an expenditure) and coincide with the cost related to the land purchasing, the working capital and the fixed capital investment to face. With the start of the working phase cash flows turns

positive due to the product sale on the market. Computation of the cash flows in this phase requires knowledge of the yearly revenues and the yearly equipment depreciation. Indeed, even if the land capital may be fully recovered at the end of the plant lifetime as a further revenue, it is not so for the equipment whose value decreases in time .

Concerning revenues, they may be easily calculated once known the tons of produced methanol per year ($m_{methanol}$) and the selling price ($p_{methanol}$):

$$Rev = p_{\text{methanol}}\left[\frac{€}{tons}\right] \cdot m_{\text{methanol}}\left[\frac{tons}{year}\right]$$

Eqn. 4.30

While as for the equipment yearly depreciation d_k, it was achieved with the suggested Double Declining Balance (DDB) method[20]:

$$d_{\text{k}}^{\text{DDB}} = \frac{2}{n_{\text{years}}} \cdot \left(FCI - \sum_{\text{j}}^{\text{k}-1} d_{\text{j}}^{\text{DDB}} \right)$$

Eqn. 4.31

Where the subscript k identifies the current year, n_{years} the assumed years allowed for equipment depreciation and *j* every jth year before the kth considered. Notice that after 5 working years this term by definition turns to 0.

With these data it is possible to compute the non – discounted cash flow for the kth year according to :

$$CF_{\text{k}} = (Rev - COM - d_{\text{k}}) \cdot (1 - t) + d_{\text{k}}$$

Eqn. 4.32

Where *t* represents the assumed tax rate and COM is the computed manufacturing cost. It has to be highlighted that such relation does not take into account inflation. Even if the profitability analysis and the useful economic indexes may be computed referring to the non

– discounted cash flow, for a more realistic result a discount rate *i* equal to 8% has been assumed for a more realistic result. One obtain:

$$CF_{\text{Discounted}_\text{k}} = \frac{(Rev - COM - d_\text{k}) \cdot (1 - t) + d_\text{k}}{1 + i\,\%}$$

Eqn. 4.33

At the end of the last working year both working capital and land cost are recovered and have to be added to the relative discounted cash flow.

All the required information are now collected and the profitability evaluation of the plant may be performed according to three possible criteria, each corresponding to an economic index:

- **Interest Rate Criterion**: the plant is evaluated depending on the non discounted rate at which money is made from a fixed capital investment. The representative economic index is the *ROROI* (Rate of Return on Investment):

$$ROROI\ [\frac{\%}{year}] = \frac{\sum_{\text{working period}} CF_\text{k}}{(k_{\text{end wp}} - k_{\text{end bp}}) \cdot (FCI - S)}$$

Eqn. 4.34

  Where $k_{\text{end wp}}$ and $k_{\text{end bp}}$ are the end of life year and the end of building phase year. S is the assumed salvage value. According to such criterion, higher is the *ROROI*, more profitable is the investment.

- **Cash criterion**: according to this criterion the plant profitability is evaluated looking at the discounted cumulative cash flow, NPV (Net Present Value), which is the sum of every yearly discounted cash flow:

$$NPV\ [M€] = \sum_{\text{k=0}}^{\text{k=k}_{\text{end wp}}} CF_{\text{Discounted}_\text{k}}$$

Eqn. 4.35

This is the most significant criterion since it points out the overall cash income from the investment. Of course, higher is the NPV, more profitable is the investment.

- **Time criterion**: it relies on the evaluation of the working years required to recover land cost, working capital and fixed capital investment, the PBP (pay back period). Shorter is the PBP, more profitable is the investment. Being *WC* the working capital, C_{land} the land cost and *k** the last year of negative cumulative cash flow (NPV) :

$$PBP = \left(k^* - k_{\text{end bp}}\right) + \frac{C_{\text{land}} + WC}{NPV_{\text{k}^*} - NPV_{\text{k}^*-1}}$$

Eqn. 4 36

The three mentioned criteria focus on different aspect of the investment under study. Depending on the one considered a certain plant arrangement could be more or less profitable, therefore all of them have been taken into account.

4.3 Methanol Reactor Modelling with Aspen EDR

Initially, process data known from the main plant have been used in EDR to model a Shell&Tube unit in the software "Design" mode. This step was useful to evaluate missing parameters necessary to run the analysis of the modelled exchanger in the "Simulation" mode which will provide the desired unit cost.

Among the input data it is possible to report:

- Tube length;
- Mass flow rate and pressure of both hot side and cold side fluid;
- Temperature and vapour fraction of inlet cold side water;
- The synthesis reaction heat release considered as the exchanger heat duty.

At least one between hot side inlet or outlet temperature was required. It has been chosen the crude outlet temperature, while syngas inlet temperature has been left free to vary depending on the result of the thermal balance, as shown in the example of

Figure 4.1. This was necessary since it is not possible to model a reacting fluid in Aspen EDR, and the real hot side temperature profile cannot be simulated. For the same reason, hot side stream composition has been assumed constant and equal to the product composition.

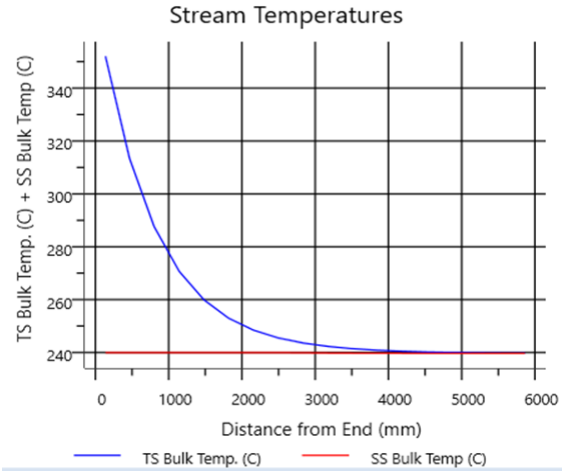

Figure 4.1: *Stream temperature profile along the axial direction.*

Notice that the number of tubes cannot be set in this mode. The software returns indeed the optimal number of tubes for the specified process. It can be instead modified in the "Simulation" mode.

	Assumptions
1.	Constant hot side reacting fluid composition
2.	Minimum fouling (fouling is not considered in the main simulation)
3.	New and smooth tube
4.	Single passage exchanger
5.	Hot fluid tube side/ Cold fluid shell side
6.	Material: carbon steel
7.	Negligible corrosion allowance
8.	Vertical disposition

Table 4.3: *Design step EDR assumptions*

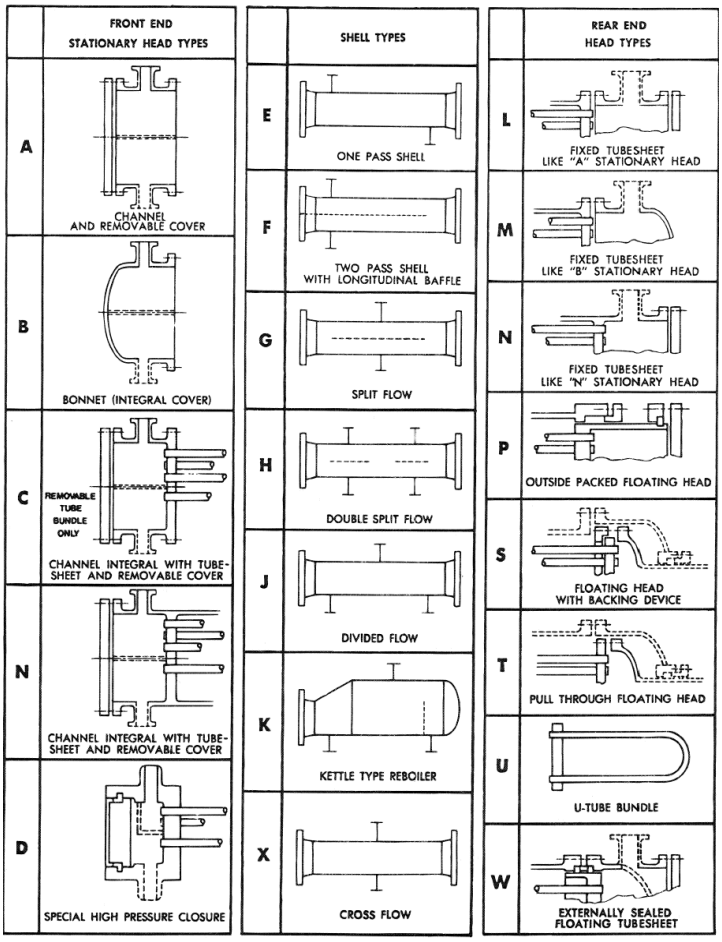

Figure 4.2:*TEMA available architectures for exchangers design.*

Table 4.3 reports the assumptions made to run the preliminary design calculations.

All other parameters or choices not strictly pertinent or necessary to run the design simulation have been kept to the default option. Among them it is possible to mention geometrical details of front end and rear end, tube patterns or nozzles geometry.

Results of the design calculation as the shell dimensions may be adopted to fulfil the fields required to run the software using the “Simulation” mode. In this mode it is possible to achieve a prediction of the unit total cost which takes into account the material used, the effect of pressure and the labour cost related to the installation of the component.

Among all the available TEMA (Tubular Exchanger Manufacturers' Association) architectures reported in

Figure ***4.2***, a front end B and a rear end M seemed to be the most suitable to represent the reactor under study since the other present features not coherent with the unit to model. Concerning the shell type, three arrangements have been initially taken into account with a preliminary cost analysis in function of the number of tubes: the cross flow X, the one pass shell E and the kettle reboiler K.

From Figure 4.3 it is evident that no differences in terms of cost may be appreciated between the BEM and BXM arrangement, while a significant gap respect to the BKM does exist. This is related to the usage of additional material for the kettle reboiler type shell.

A linear cost trend typical of modular technologies is coherent with the fact that once established the shell dimensions and the relative material usage, the total cost grows only depending on the number of implemented tubes.

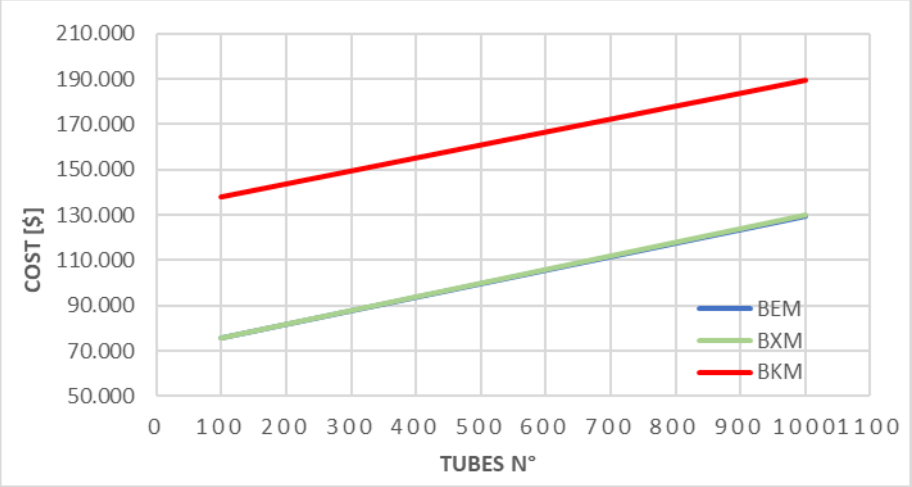

Figure 4.3: *TEMA architectures cost comparison.*

In the end, even if the Lurgi reactor produces steam, its configuration is better represented by simpler arrangements like the one pass or the cross flow shell which in this case are also cheaper under the economic perspective respect to a kettle reboiler type. The BEM architecture was definitely chosen to proceed with the analysis considering that typically

steam is drawn off below the upper tube sheet in Lurgi reactors [59], while with a cross flow shell it would be drawn on the same axis.

4.3.1 Methanol Reactor EDR Model Sensitivity Analysis and Cost Correlation Achievement

Before the computation of a suitable cost correlation as function of the useful heat exchange area, a sensitivity analysis on the BEM arrangement cost was pursued. The effect of several commercial diameters, tube length and operating pressure has been considered. Default values coincide with the one adopted in the main plant simulation:

- Tube diameter = 42 mm;
- Tube length = 6 m;
- Operating pressure = 93 bar;

Starting from the effect of different diameters, results reported in Figure 4.4 may be explained thinking that the useful heat exchange area is function of the adopted diameter as well as the number of tubes

$$\begin{cases} A_{\text{exc}} = \pi \cdot D_{\text{int}} \cdot Ln_{\text{tubes}} \\ D_{\text{int}} = D_{\text{ext}} - 2(th) \end{cases}$$

Eqn. 4.37

Where *D* represents the internal or external diameter, n_{tubes} the tubes number, *th* the thickness, and L the tube length. Therefore, for a certain value of heat exchange surface lower is *D*, higher will be the number of required tubes and consequently the cost value. That is why lines representing cost value of reactors with smaller diameters have the higher angular coefficient. Thus, a certain convenience in adopting larger tubes may be noticed.

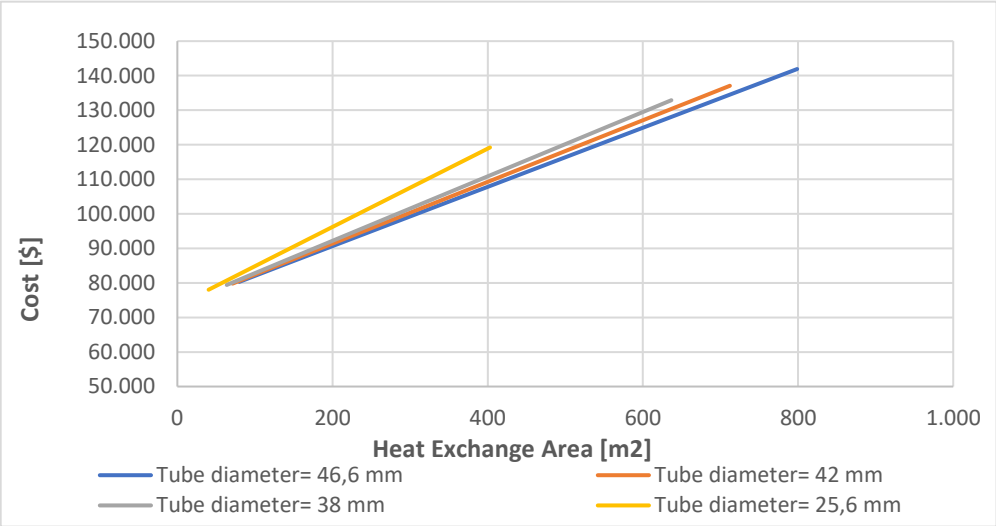

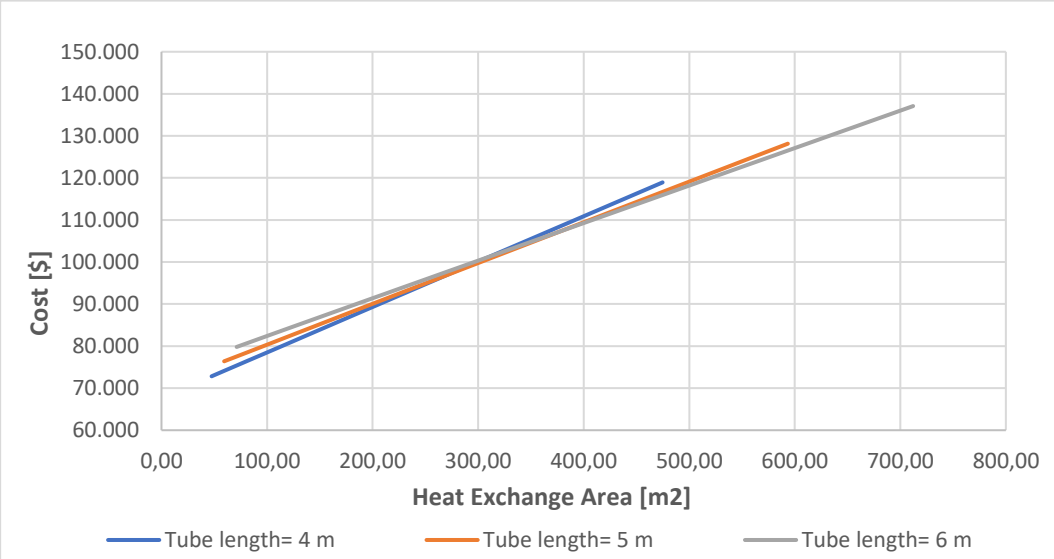

Figure 4.4: *Effect of different tube diameters on the reactor investment cost.*

As for the effect of tube length reported in Figure 4.5, it is evident that shorter tubes are cheaper for low values of heat exchange surface since less building material is used. Yet, the

Figure 4.5:*Efffect of different tube length values on the reactor investment cost.*

cost line associated with shorter tubes has a higher angular coefficient respect to the other cases, such that longer tubes turn to be the best option for greater sizes. The reason lies in the fact that even if the cost for a single longer tube is higher, less units will be required to achieve greater sizes.

The reactor under study is equipped with 500 tubes. Considering the default geometry and a tube thickness of 2.1 mm, according to Eqn. 4. the global heat exchange surface A_{exc} is about 356 m^2 . Considering this value in Figure 4.5 on the 6 m line, it is confirmed that the default geometry is an optimal solution under the economic perspective for the studied case.

As expected, from Eqn 4.37 it can be assessed that higher is the operating pressure higher will be the cost of the unit. The structure indeed has to be reinforced to allow operation under a more severe stress condition. The angular coefficient resultant from the linear regression keeps almost constant since the tubes geometry does not change and any value of heat exchange area is achieved with the same number of units.

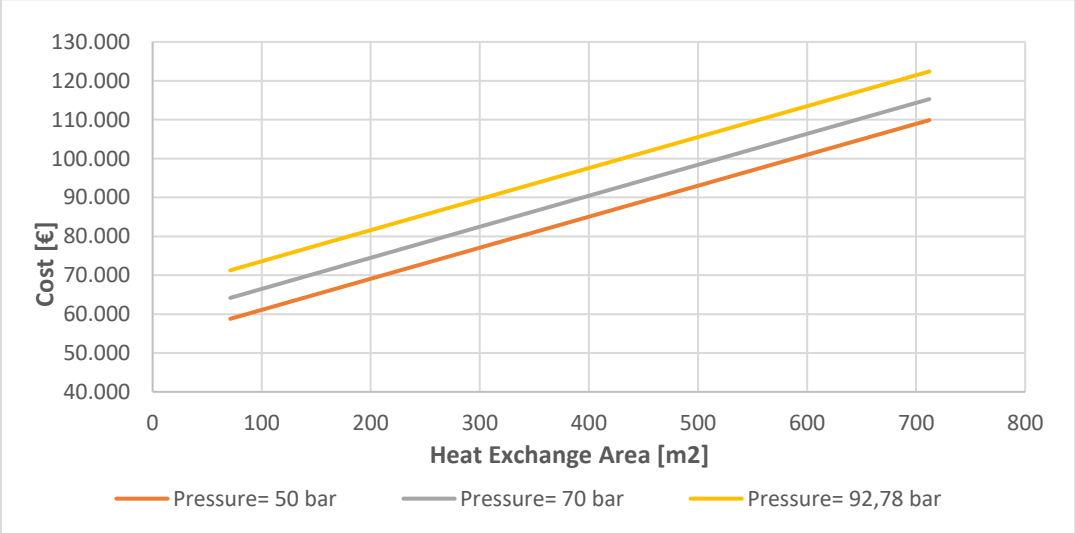

Figure 4.6:*Effect of different operating pressures on reactor investment cost.*

It has to be highlighted that costs reported in these graphs have been actualized at the year 2019 according to the procedure described in section 4.2.1. With the results of the linear

regression applied all the illustrated cases, it was possible to achieve a cost correlation in the form:

$$C_{\mathrm{tot}} = C_{\mathrm{o}} + m \cdot A_{\mathrm{exch}}$$

Eqn. 4.38

Where C_{tot} is the total cost of the unit including installation, pressure and material effect, C_{o} the initial cost for the minimum heat exchange surface, m the line angular coefficient and A_{exch} the actual heat exchange surface. Tables reporting source cost data and all the results of the linear regression are provided in Appendix. In Table 4.4 fitting parameters C_o and m are reported for each studied case with the respective validity range. Notice that for the default reactor geometry and operating pressure it has been achieved a further correlation with a wider validity range.

Pressure [bar]	Tube length [m]	Tube diameter [mm]	Co [$\$_{2019}$]	m [-]	Validity
93	6	42	73510	89.3	A = 0 - 800 m^2
70	6	42	65548	89.3	
50	6	42	63887	89.3	
93	5	42	70669	96.9	
93	4	42	67708	107.9	
93	6	46,6	73526	85.7	
93	6	38	73525	93.3	
93	6	25.6	73487	113.5	
93	6	42	68558	80.4	A = 3000 - 8000 m^2

Table 4.4: *fitting parameters for the Lurgi methanol reactor linear cost function and validity range.*

For sake of completeness, Figure 4.7 demonstrates how the linear interpolation well suit achieved cost data.

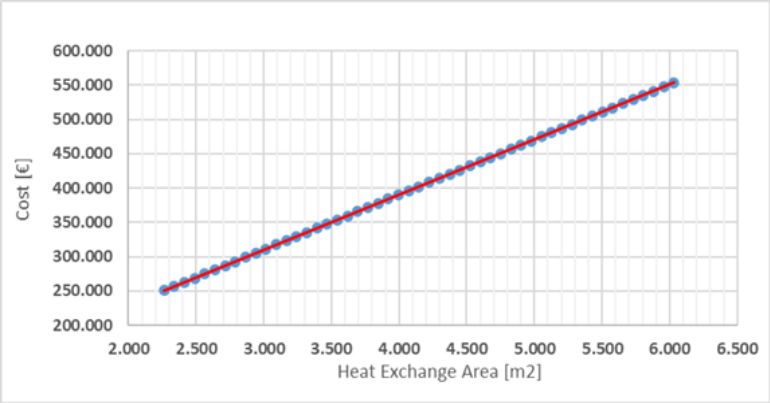

Figure 4.7: *linear interpolation of cost data for a synthesis reactor (tube length 6 m, tube diameter 42 mm, pressure 93 bar).*

As validation of the developed model, cost results have been compared with the cost of a real reactor for dimethyl ether production as reported in Table 4.5 [74]. The reactors have a quite similar geometry and are practically comparable under the economic perspective.

Cost [$]	tubes number [-]	Tubes length [m]	Tubes diameter [m]
DME reactor			
95000	315	6	0.038
Adopted Lurgi reactor			
91355	300	6	0.038

Table 4.5: *Cost validation by comparison with a real case.*

4.3.2 Technical Key Performance Indicators

In this section the main technical KPI according to which the plants performances have been evaluated are presented. To automate computation of all of them, proper calculators have been implemented.

Starting from the evaluation of the methanol synthesis rector performances, the main indicators considered where the reaction yield and the carbon conversion across the unit. The reaction yield is computed as the methanol molar flow produced in a reference control volume over the available convertible carbon molar flow at the inlet. Depending on the control volume boundaries, this parameter may refer to the total reaction yield, η_{tot}, or to the single stage yield η_{stage} (useful in the once through arrangement):

$$\begin{cases} \eta_{\mathrm{tot}} = \dfrac{\dot{n}_{\mathrm{CH_3OH}_{\mathrm{out}_{\mathrm{final\ sep}}}} - \dot{n}_{\mathrm{CH_3OH}_{\mathrm{in}_{\mathrm{Lurgi}}}}}{\dot{n}_{\mathrm{CO}_{\mathrm{in}_{\mathrm{Lurgi}}}} + \dot{n}_{\mathrm{CO_2}_{\mathrm{in}_{\mathrm{Lurgi}}}}} \\ \eta_{\mathrm{stage}} = \dfrac{\dot{n}_{\mathrm{CH_3OH}_{\mathrm{out}_{\mathrm{i^{th}stage}}}} - \dot{n}_{\mathrm{CH_3OH}_{\mathrm{in}_{\mathrm{i^{th}stage}}}}}{\dot{n}_{\mathrm{CO}_{\mathrm{in}_{\mathrm{i^{th}stage}}}} + \dot{n}_{\mathrm{CO_2}_{\mathrm{in}_{\mathrm{i^{th}stage}}}}} \end{cases}$$

Eqn. 4.39

$\dot{n}$ represents as usual the molar flow rate of the specified chemical species, the subscript *in* the Lurgi reactor inlet stream or the ith reaction stage one and the subscript *out* the outlet stream considered. Notice that to achieve a total reaction yield the produced crude methanol outlet stream (i.e. separated from unreacted syngas) has to be considered as outlet stream.

The same reasoning could be applied for the carbon conversion ε_C, that was evaluated both across the whole reactor and across each single stage in the once through case. This parameter represent how much carbon has been converted into methanol respect to the available convertible one at the control volume inlet

$$\begin{cases} \varepsilon_C = \dfrac{(\dot{n}_{\mathrm{CO}_{\mathrm{in}_{\mathrm{Lurgi}}}} + \dot{n}_{\mathrm{CO_2}_{\mathrm{in}_{\mathrm{Lurgi}}}}) - (\dot{n}_{\mathrm{CO}_{\mathrm{out}_{\mathrm{Lurgi}}}} + \dot{n}_{\mathrm{CO_2}_{\mathrm{out}_{\mathrm{Lurgi}}}})}{\dot{n}_{\mathrm{CO}_{\mathrm{in}_{\mathrm{Lurgi}}}} + \dot{n}_{\mathrm{CO_2}_{\mathrm{in}_{\mathrm{Lurgi}}}}} \\ \varepsilon_{C_{\mathrm{stage}}} = \dfrac{(\dot{n}_{\mathrm{CO}_{\mathrm{in}_{\mathrm{i^{th}stage}}}} + \dot{n}_{\mathrm{CO_2}_{\mathrm{in}_{\mathrm{i^{th}stage}}}}) - (\dot{n}_{\mathrm{CO}_{\mathrm{out}_{\mathrm{i^{th}stage}}}} + \dot{n}_{\mathrm{CO_2}_{\mathrm{out}_{\mathrm{i^{th}stage}}}})}{\dot{n}_{\mathrm{CO}_{\mathrm{in}_{\mathrm{i^{th}stage}}}} + \dot{n}_{\mathrm{CO_2}_{\mathrm{in}_{\mathrm{i^{th}stage}}}}} \end{cases}$$

Eqn. 4.40

A difference respect to the total yield is that the reaction total carbon conversion considers the reactor outlet carbon stream including potential unreacted syngas, while the total yield does not.

Reformer performances have been assessed according to two indicators, methane conversion and cold gas efficiency. The reformer methane conversion ε_{CH_4} quantifies how much methane respect to the fed amount has been converted into products on a molar basis:

$$\varepsilon_{\mathrm{CH_4}} = \frac{\dot{n}_{\mathrm{CH_4 in_{Reformer}}} - \dot{n}_{\mathrm{CH_4 out_{Reformer}}}}{\dot{n}_{\mathrm{CH_4 in_{Reformer}}}}$$

Eqn. 4.41

The reformer cold gas efficiency, CGE, tells how efficiently the inlet methane thermal power has been reallocated over the produced syngas stream, taking into account the required energy expenditure to sustain the reaction. This indicator may be defined as the ratio between the outlet syngas available thermal power respect to the overall inlet thermal power:

$$\eta_{\mathrm{CGE}} = \frac{\sum_{\mathrm{i=1}}^{\mathrm{nc_{outRef}}} (\dot{n}_{\mathrm{i}} \cdot LHV_{\mathrm{i}})}{\sum_{\mathrm{i=1}}^{\mathrm{nc_{in_{Ref}}}} (\dot{n}_{\mathrm{i}} \cdot LHV_{\mathrm{i}}) + \sum_{\mathrm{i=1}}^{\mathrm{nc_{biofuel}}} (\dot{n}_{\mathrm{i}} \cdot LHV_{\mathrm{i}}) + \sum_{\mathrm{i=1}}^{\mathrm{nc_{purge}}} (\dot{n}_{\mathrm{i}} \cdot LHV_{\mathrm{i}})}$$

Eqn. 4.42

In this relation LHV_{i} represents each species lower heating value expressed on molar basis and $\dot{n}_{\mathrm{i}}$ the relative molar flow rate, while nc the number of components present in the considered stream.

At last plant efficiency indicators have to be reported. The plant carbon efficiency, η_C takes into account how much of the carbon fed to the process has been converted into useful methanol product. Being *x* the molar fraction of the specified component

$$\eta_C = \frac{\dot{n}_{\mathrm{product}} \cdot x_{CH_3OH}}{\dot{n}_{\mathrm{fresh_{biogas}}} \cdot (x_{\mathrm{CH_4}} + x_{\mathrm{CO_2}})}$$

Eqn. 4.43

This equation is valid since according to the fresh biogas composition reported in Table 3.1 methane and carbon dioxide are the only species containing carbon. Since these are also the only present species, the denominator collapses in the full inlet biogas molar stream. When assuming purification performed in an external hub $\dot{n}_{\text{product}}$ refers to the produced outlet crude, while if the upgrading section is integrated, this terms refers to the purified methanol stream. It has to be specified that the theoretical maximum carbon efficiency obtainable in the process is not 100%. By reforming 1 mole of CH_4 the resulting syngas stoichiometric module as function of a variable amount of CO_2 results to be

$$\mathrm{M} = \frac{3 - zCO_2}{(CO + zCO_2)}$$

Eqn. 4.44

Thus, a module M equal to 2 may be obtained for zCO_2 equal to one third. This means that by processing an inlet biogas feed 60% CH_4 and 40 % CO_2 only an amount of carbon dioxide equal to one third of the available methane may be converted (i.e. 20 %). Half of the fed CO_2 cannot be anyway converted, dropping the maximum theoretical carbon efficiency from 100% to 80%. The only way to increase the maximum theoretical carbon efficiency is by addition of an external current of H_2, which can be for instance produced via electrolysis [14]. Even if electrolysers would enhance the methanol conversion, nowadays they are a quite expensive technology [19]. Their impact on the plant economics could be evaluated in a further development of this work.

Beside the carbon efficiency, another key indicator of the plant performances is the plant fuel efficiency. This latter considers the ratio between the produced methanol thermal power and the fresh inlet biogas thermal power. Information provided does not differ too much from carbon efficiency one, yet it is focused on the power flux associated with the streams.

$$\eta_{\text{fuel}} = \frac{\dot{n}_{\text{product}} \cdot x_{\text{CH}_3\text{OH}} \cdot LHV_{\text{CH}_3\text{OH}}}{\sum_{\text{i}=1}^{\text{nc}_{\text{inlet}_{\text{fuel}}}} \cdot (\dot{n}_{\text{i}} \cdot LHV_{\text{i}})}$$

Eqn. 21

Where refers to the produced outlet crude or to the upgraded methanol depending on the plant arrangement considered.

The mentioned KPI together with the economic indicators achieved by the profitability analysis will play a key role when comparing plants under study in the following chapter.

5. TECHNICAL RESULTS

5.1 TRADITIONAL PLANT ANALYSIS

Technical performances of the traditional arrangement adopting unreacted syngas recirculation are evaluated in this section. Initially the optimal location of the CO_2 separation section is established, then a sensitivity analysis varying the adopted recycle ratio has been reported. Even if higher synthesis reactor operating pressures favour methanol conversion, the effect of a reduced operating pressure have been considered in another sensitivity analysis. In a last section the impact of the methanol upgrading section integration on plant performances has been evaluated.

5.1.1 Base Case Optimal CO_2 separation location

In general terms, moving the CO_2 separation section after the reforming reaction, or not performing it at all, has a certain impact on several plant components. Starting from the reformer, it will process a CO_2 richer feed if the incoming biogas composition is not previously managed. As mentioned in section 3.4.1, a first consequence is that the excess of carbon dioxide supplied favours the RWGS reaction. The so produced additional water can take part in the SMR promoting methane conversion inside the unit as it is shown in Table 5.1.

Case	*Methane conversion* ε_{CH_4} [%]
Reformer Pre Separation	93.7
Reformer Post Separation	94.3
No Separation	94.3

Table 5.1: *Reformer methane conversion comparison.*

In Figure 5.1 one can notice that a greater amount of fresh biogas has to be burnt in the furnace to sustain the reaction and a bit lower reformer CGE is recorded when CO_2 is not

separated before the reforming reaction. CGE variation is almost negligible since when the fuel requirement increases, the inlet processed feed decreases.

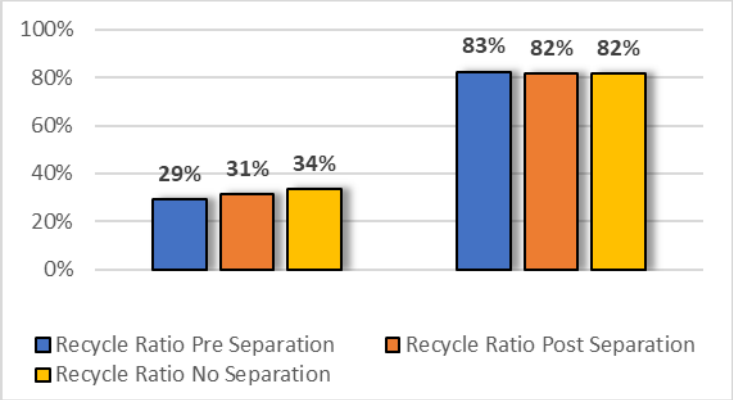

Figure 5.1: *fresh biogas burnt fraction (left side) and CGE comparison (right side).*

However, the alteration of the reformer behaviour has not a direct impact on the synthesis reactor performances. Indeed, whatever is the feed composition or flow rate, the task of the absorber operation is to achieve the desired syngas stoichiometric module at the synthesis reactor inlet. Looking at the CO_2 balance reported in Table 5.2, the amount carbon dioxide removed to meet the syngas module specification will be almost the same.

	Post Reformer CO_2 Separation	***Pre Reformer CO_2 Separation***
Separation inlet CO_2 [kmol/hr]	38.8	43.0
Separation outlet CO_2 [kmol/hr]	14.7	18.9
CO_2 removed [kmol/hr]	24.1	24.1
Separation Efficiency $\eta_{sep_{CO_2}}$ [-]	0.62	0.62

Table 5.2: *CO_2 balance across the separation section.*

Then, it is possible to state that the location of the separation section has no impact on the separation performances, which can be expressed in terms of separation efficiency:

$$\eta_{\mathrm{sep}_{\mathrm{CO_2}}} = \frac{\dot{n}_{\mathrm{in}} \cdot x_{\mathrm{CO_2in}} - \dot{n}_{\mathrm{out}} \cdot x_{\mathrm{CO_2out}}}{\dot{n}_{\mathrm{in}} \cdot x_{\mathrm{CO_2in}}}$$

Eqn. 5.122

Where the subscripts *in* and *out* represent respectively inlet and outlet boundaries of the separation section, $\dot{n}$ the molar flow rate of the fed biogas or syngas and x the relative CO_2 molar fraction. Of course, when separation is not performed all the carbon dioxide is fed to the reactor.

	Pre Reformer Separation	***Post Reformer Separation***	***No Separation***
RR [-]	5.9	4.6	1.2

Table 5.3: *RR values for the compared cases*

Table 5.3 highlights that by changing location of the separation section, the synthesis reactor will operate with a different recycle ratio. This values are obtained for a constant fraction of recycled unreacted syngas equal to 99% of the total separated stream. The remaining 1% is the purge stream fed to the reformer furnace. Higher is RR, higher will be the processed feed. This consideration is crucial when comparing reactor performances between the three cases. From Figure 5.2 and Figure 5.3 it seems that best performances are achieved when CO_2 is separated from reformed syngas both in terms of carbon conversion and synthesis reaction yield, 80% and 98.2% respectively. It has to be reminded that reactor yields are computed respect to the produced crude once the unreacted syngas has been separated, while carbon conversion is defined across the reactor.

On the other hand, the lowest yield and carbon conversion are recorded when separation is not performed. The main reason lies in the fact that in this case the synthesis reaction takes place with the greatest CO_2 excess and with a non-optimal stoichiometric module.

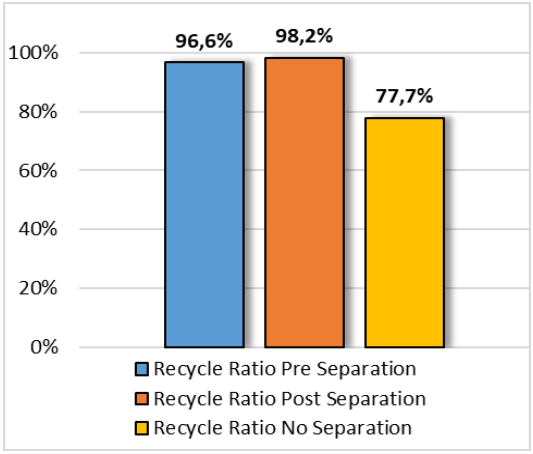

Figure 5.2: *synthesis reaction yield comparison.*

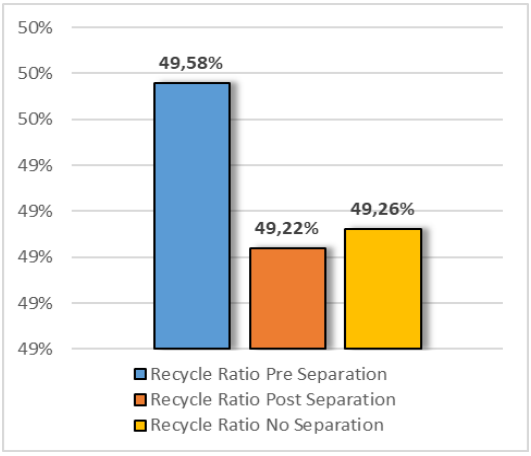

Figure 5.3: *carbon conversion comparison.*

Such penalization is somehow balanced by the lower RR: according to the definition of reaction yield and carbon conversion provided by Eqn. 4.40 and Eqn. 4.39, indeed, these parameters are influenced by the inlet carbon amount, present at the denominator. Therefore, higher is the RR, higher will be the fed carbon and lower the performance indicators.

For a more precise analysis Table 5.4 focuses on the amount of carbon actually converted in each case. It can be appreciated that despite the different reaction performances and flow rate processed, all the arrangements are able to convert almost the same amount of carbon, with a small convenience in the case of the reformer pre separation case.

	Pre Separation	***Post Separation***	***No Separation***
Methanol reactor inlet $CO + CO_2$ [kmol/hr]	108.6	91.6	137.6
Methanol reactor outlet $CO + CO_2$ [kmol/hr]	34.4	17.9	63.9
Carbon Conversion ε_C[-]	0.68	0.80	0.53
Converted carbon [-]	74.2	73.7	73.7

Table 5.4: *Carbon conversion comparison details.*

This fact is confirmed by the comparison between the overall process efficiencies reported in Figure 5.5 and Figure 5.4, which compare the produced methanol stream with the inlet biogas flow rate.

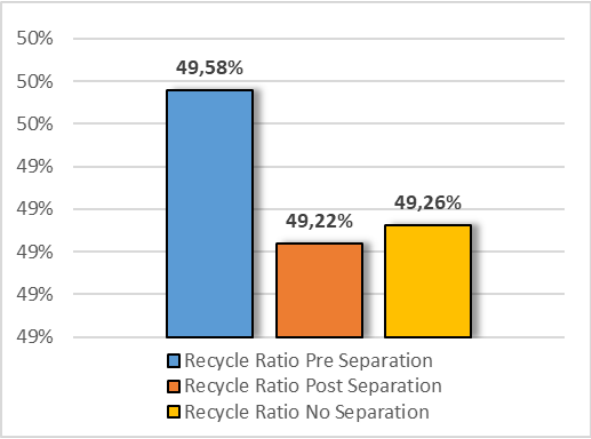

Figure 5.5: *carbon efficiency comparison.*

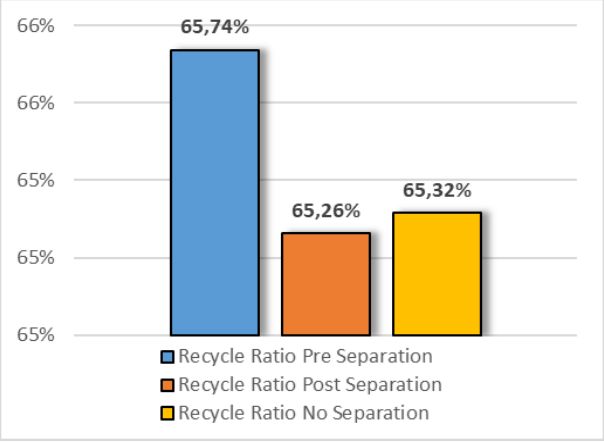

Figure 5.4: *fuel efficiency comparison.*

A rigorous definition for the carbon efficiency and the fuel efficiency is provided by Eqn. 4.43 and Eqn. 4.45. Even if for a small percentage, the greatest methanol production and consequently the highest process efficiencies are obtained when CO_2 separation is performed before the reforming reaction. Remarkable is the fact that also the arrangement without separation section has a carbon efficiency and a fuel efficiency at all comparable with other cases. To go deeper in the details, Sankey diagrams tracking the carbon path through the process are reported in Figure 5.6.

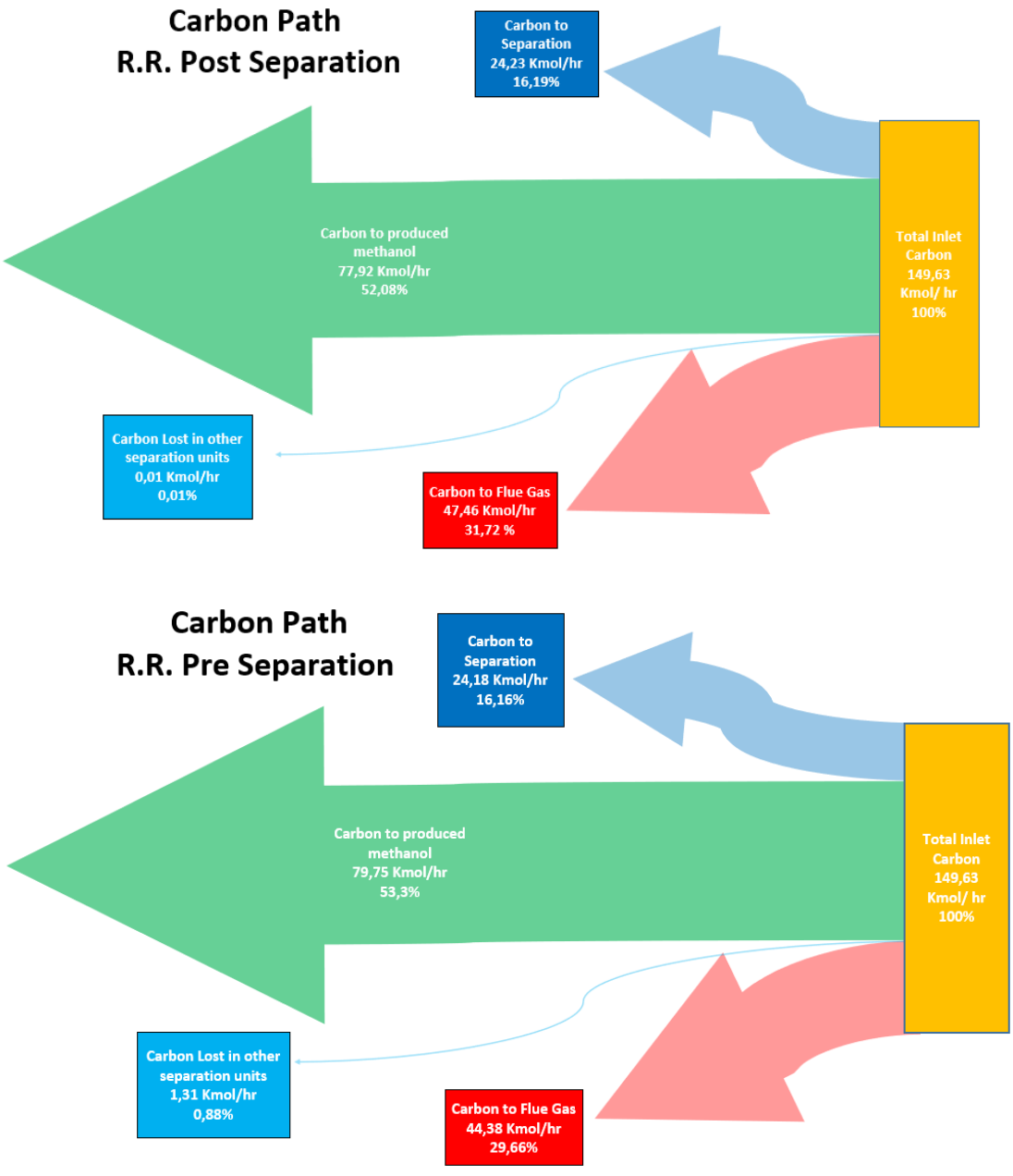

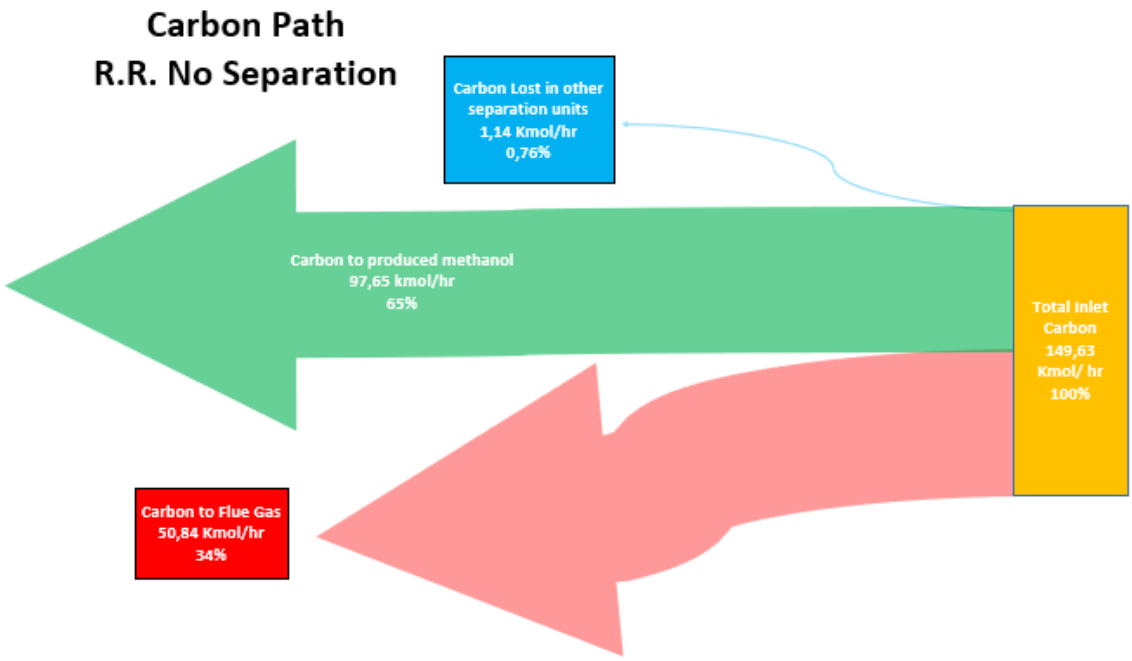

Figure 5.6:*Sankey diagrams tracking carbon path in the considered plant arrangements.*

The diagrams reported in Figure 5.6 represent the carbon balance applied to the whole plant. No significant differences may be appreciated between the cases adopting CO_2 separation. The most relevant consideration is that the carbon fraction "lost" in the reformer flue gases is greater in the arrangement performing separation on the produced syngas.

The cause is the higher reformer heat requirement, which is satisfied by a higher amount of fresh biogas and methanol reactor purge. This is the reason why despite the better synthesis reaction performances it has not the highest amount of methanol produced and the best plant performances.

As for the case without separation, the carbon amount allocated in the produced methanol stream could be misleading: it includes indeed a significant amount of carbon dioxide entrained in the product stream due to its affinity with methanol [63]. A greater amount of carbon is also accounted in the reformer flue gas stream, due to a CO_2 richer purge flux recycled to the furnace.

The item “carbon lost in other separation units” reports the carbon amount entrained both in water separated from the main stream and in condensation extracted from compressors. In any case such amount is less than one percent.

In the light of this considerations the optimal location for the CO_2 separation is upstream of reforming operation. The following technical analysis are pursued on this configuration.

5.1.2 Effect of the Recycle Ratio

A sensitivity analysis has been performed varying the Lurgi reactor RR to appreciate its effect on the performance indicators and on the overall plant behaviour. Recirculation of unreacted syngas is commonly adopted since it allows to enhance the overall methanol conversion, which in a single passage would be dramatically low, and the amount of useful product obtained.

The higher is the amount of recycled feed, the higher will be the total processed feed for a single passage. Considering the methanol molar fraction at the reactor outlet reported in Figure 5.7, a decreasing trend for higher RR is noticed as consequence of the greater dilution both for the real reaction and for the ideal equilibrium one. The actual methanol molar fraction obtained is always less than the equilibrium case, coherently with the fact that the highest conversion on a single passage is achieved in equilibrium conditions. It can also be observed that the RR has no effect on the distance from the equilibrium performances, which keeps almost constant for any amount of recycled feed.

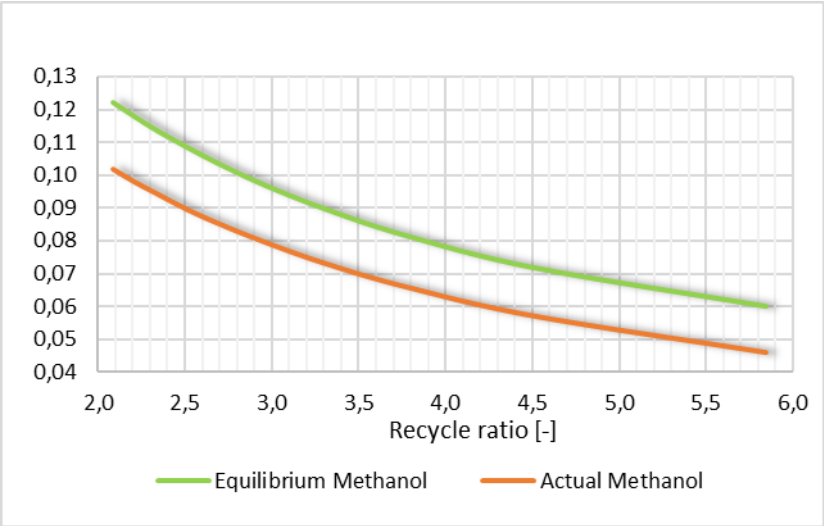

Figure 5.7: *reactor outlet methanol molar fraction and distance from equilibrium.*

Being aware of the fact that some traces of unconverted methane are present in the inlet syngas stream, the CH_4 concentration in function of the RR has been checked. Methane behaves indeed as an inert for the synthesis reaction, and its presence could be detrimental due to reduction of the partial pressure of the reactant species. Table 5.5 shows recorded methane concentration values.

Recycle Ratio	***Inert CH_4 [mol/mol]***
2.1	0.0230
2.2	0.0231
2.3	0.0232
2.5	0.0237
2.7	0.0239
2.9	0.0240
3.3	0.0246
3.8	0.0253
4.5	0.0260
5.8	0.0267

Table 5.5: *Inert methane concentration in the synthesis reactor feed.*

As expected, the methane molar fraction in the processed stream increases due to the higher amount of recycled feed. However, its value keeps always below 3% and the effect on the global performances is practically negligible respect to the benefits deriving from the adoption of recirculation.

The benefits of unreacted syngas recirculation may be recognized looking at the overall converted methanol, which increases as the RR does, although performances on the single passage are not affected by significant variations. This fact may be appreciated in

Figure ***5.8*** showing the increasing trend of the total reaction yield. It is able to reach 96.6% for a RR equal 5.8, with an increment about 7.5% respect to the case with minimum recirculation.

In Figure 5.9, instead, is a comparison between real and equilibrium reaction performances for the same reactor inlet feed is reported. It is remarkable that for any value of RR, the total yield achieved is significantly greater than the equilibrium one, which coincides with the best theoretical yield obtainable in a single passage.

As consequence of the total reaction yield increase, higher quantities of produced methanol are expected. Focusing on the pure methanol amount, which is the product actually sold on the market, Figure 5.10 shows an increase in the production rate about 3.35% (almost 200 tons more per year) in the considered range of RR, with the relative benefits under the economic point of view.

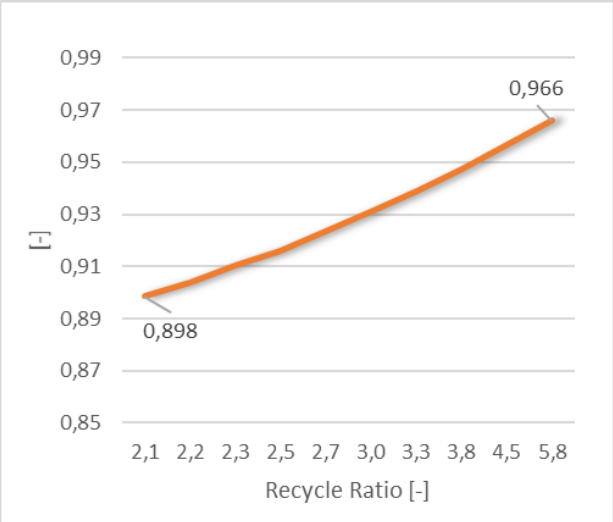

Figure 5.8: *Total reaction yield for different RR.*

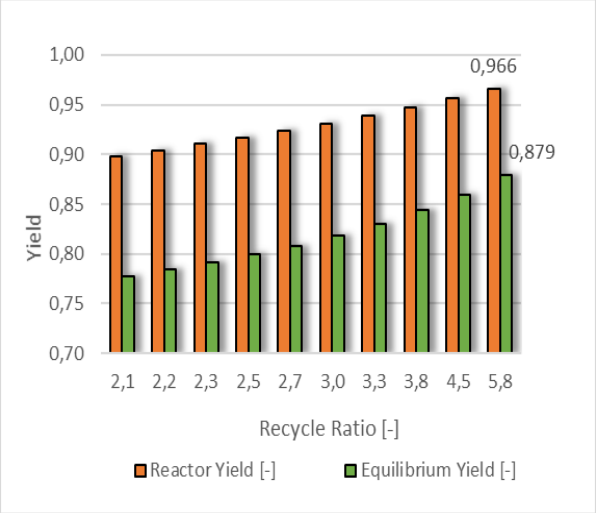

Figure 5.9: *comparison between reactor yield and equilibrium reactor yield for different RR.*

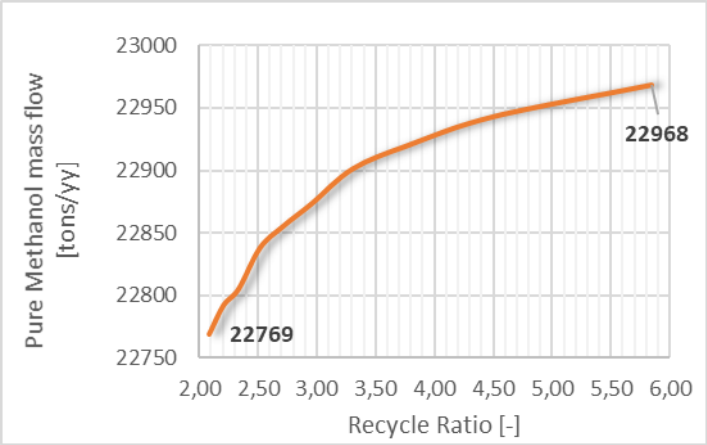

Figure 5.10: *yearly produced methanol mass flow rate in function of RR.*

Although the advantage of higher RR in terms of tons of useful product produced or reaction yield is noticeable, the increase in the overall plant efficiency is less evident. Table 5.6 shows that the increment of fuel efficiency and carbon efficiency is limited to almost 0.9% in both cases.

A further consideration concern the reformer operation and the biogas usage: the higher is the unreacted feed recirculated, the lower the purge fraction recycled to the reformer furnace will be. Thus, a higher fresh biogas fraction should be sent to the furnace as fuel, almost 19% more in the considered range of RR according to Table 5.6. It is reasonable that the reformer CGE keeps practically unaffected, since the additional biofuel input is balanced by less biogas to be reformed.

	Recycle Ratio										**Δ%**
RR	2.1	2.2	2.3	2.5	2.7	2.9	3.3	3.8	4.5	5.8	180
Biog. %	0.24	0.25	0.25	0.26	0.26	0.27	0.27	0.28	0.28	0.29	18.8
CGE	0.83	0.83	0.83	0.83	0.83	0.83	0.83	0.83	0.82	0.82	-0.4
η_{fuel}	0.65	0.65	0.65	0.65	0.65	0.65	0.66	0.66	0.66	0.66	0.9
η_C	0.49	0.49	0.49	0.49	0.49	0.49	0.49	0.49	0.50	0.50	0.9

Table 5.6: *Reformer biogas requirement and efficiencies indicators for several values of RR.*

In the considered model, the temperature profile of the reacting fluid inside the synthesis reactor is characterized by a certain peak before ending in a plateaux due to the action of thermal fluid. An example is provided in Figure 5.11.

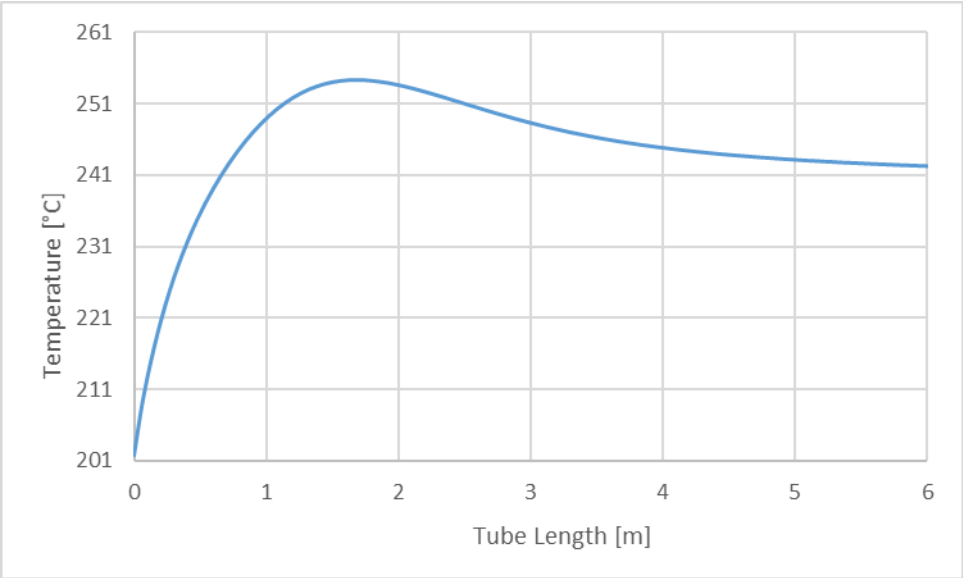

Figure 5.11: *methanol reactor temperature profile on the axial direction for a RR=5.8.*

It has been observed that by recirculating higher amounts of unreacted syngas the temperature peak is mitigated and the profile assumes a smoother trend. Recycled feed, indeed, behaves as an inert for the reaction, which takes place with almost the same conversion rate on the single passage. The lower is the reactor total inlet feed, the lower will be the peak temperature mitigation. An increase in the temperature peak about 25 °C in the range of RR from 2 to 3.5 may be appreciated in Figure 5.12.

An issue is the fact that for temperatures higher than 280 °C the validity range of the adopted reactor kinetic model is exceeded, therefore a certain amount of recirculation is mandatory for the reliability of the obtained results. Accordingly, a RR greater than 3 should be adopted.

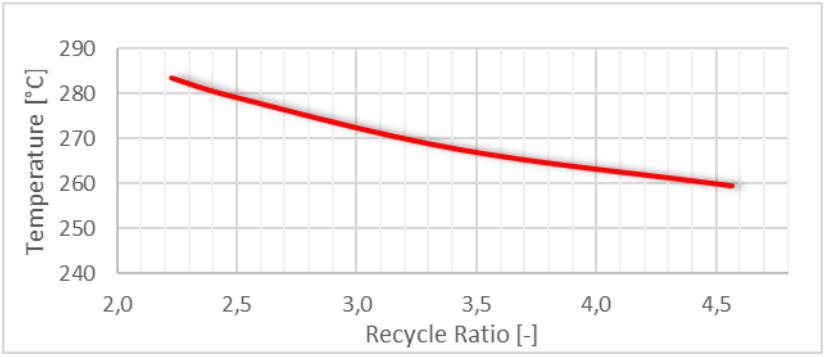

Figure 5.12: *reactor peak temperature for different values of RR.*

5.1.3 Effect of different reactor operating pressure

A further sensitivity analysis has been performed to evaluate the effect of different synthesis reactor operating pressures. In particular beside the 93 bar default case, values of 70 bar and 50 bar have considered for several operating recycle ratios.

It comes as no surprise that the highest reaction yield is achieved for higher operating pressures due to the synthesis reaction thermodynamics. This fact may be appreciated from the comparison between the single passage yields reported in Figure 5.13. Yet, in Figure 5.14 it can be noticed how differences in the global reaction yields are attenuated when higher recirculation is adopted. Indeed, for RR values around 6 a comparable yield is achieved for all the considered pressures.

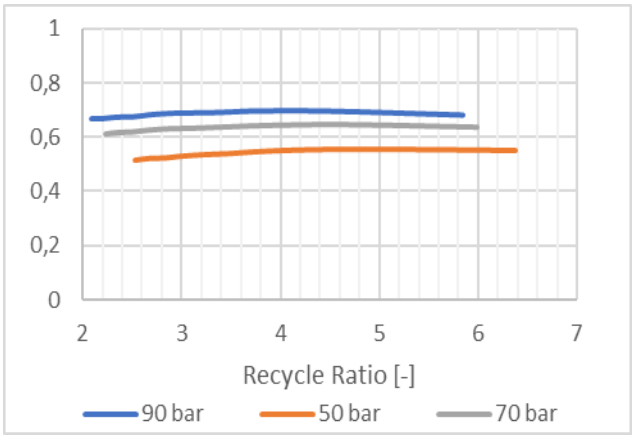

Figure 5.13: *single passage reaction yields for different reactor operating pressures.*

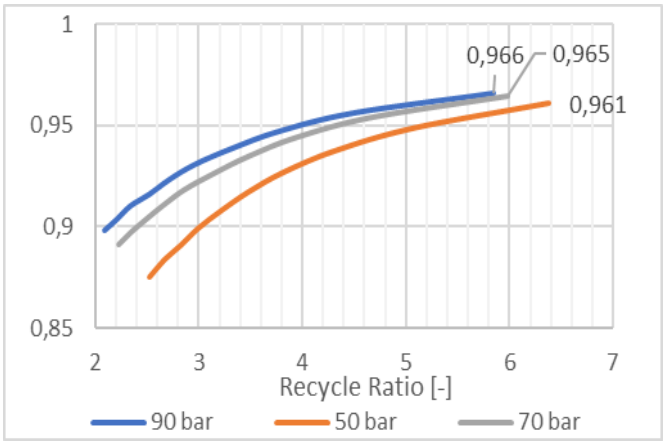

Figure 5.14: *total reaction yields for several reactor operating pressures.*

The reason may be found again in the fact that even if the conversion rate is dependent of thermodynamics, for higher RR more of the not converted carbon in a single passage will take part in the reaction.

Thus, when operating with low RR the penalization deriving from lower pressures is stronger and it results in a quite lower annual methanol production. On the other hand, recirculation is able to mitigate the thermodynamic effect. Additionally, the higher is the synthesis

pressure the more will be the amount of carbon dioxide entrained in the produced methanol stream due to its affinity with methanol. This fact implies a loss of useful reactant operating at higher pressures. A further factor influencing performances is the biogas consumption in the reformer furnace, which is lower when operating with lower synthesis pressures.

Biogas consumption trend for the considered pressure values is reported in Figure 5.15.

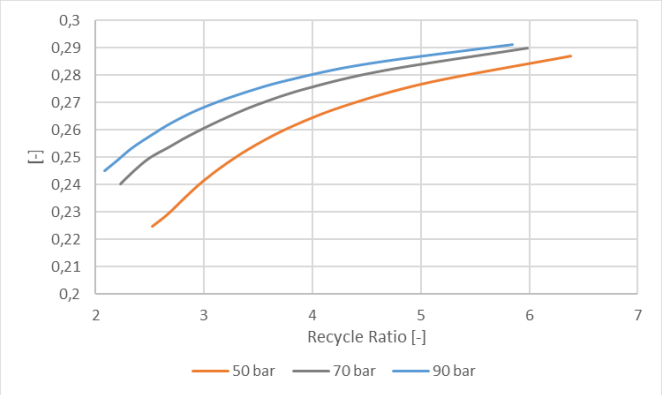

Figure 5.15: *biogas burnt fraction comparison for different synthesis pressures*

As result, over a certain value of RR the trade off between all these aspects leads to better performances for the low pressure operation. This trade off behaviour is reported in Figure 5.16, showing the methanol yearly production trend.

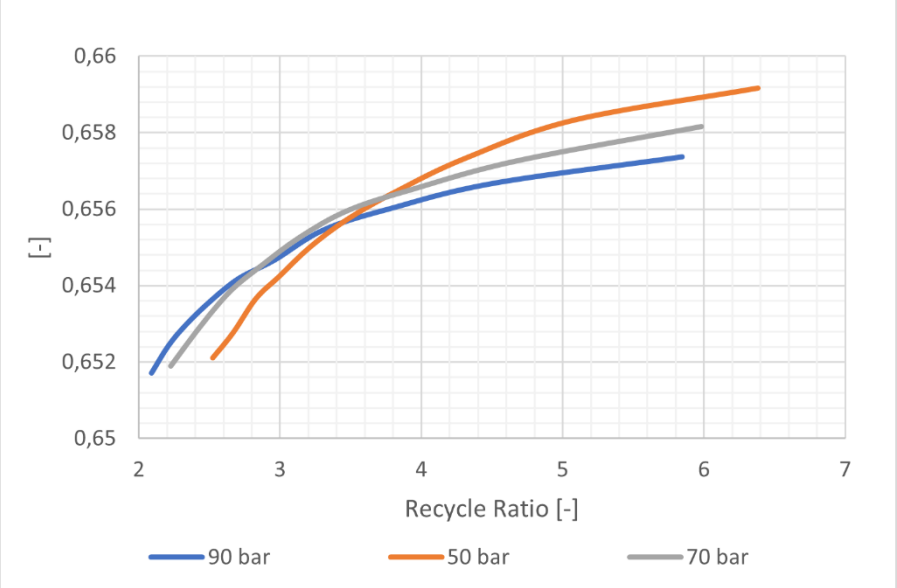

Figure 5.16: *methanol yearly production in tons for different reactor operating pressures.*

More precisely, the 70 bar curve overcomes the 90 bar one for RR greater than 3.1, while the 50 curve bar does so for RR greater than 3.5. For RR over 3.8 the greatest methanol production is achieved performing the synthesis reaction at 50 bar.

The same trade off behaviour could be observed for the overall carbon and fuel efficiencies, being them strictly dependent on the produced methanol flow. It has to be highlighted that this behaviour is crucial when evaluating plant profitability, since lower costs may be expected operating at more moderate pressures. Additional information about costs and plant consumptions are provided when discussing the economic results in the next chapter.

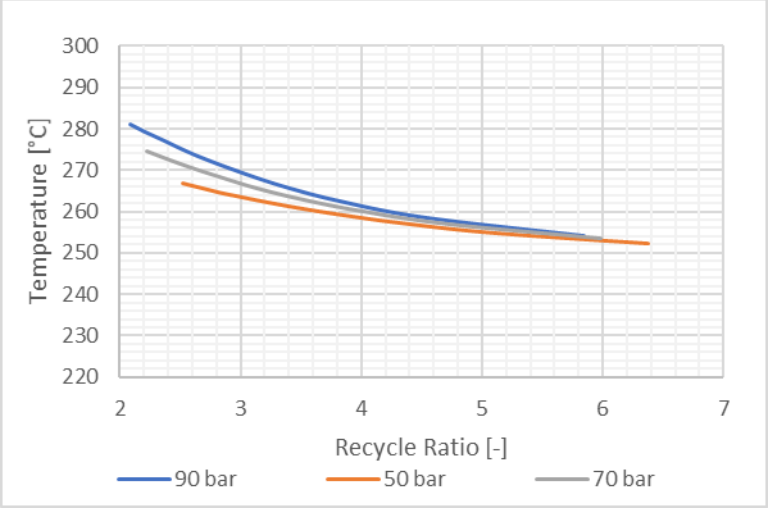

Figure 5.17: *methanol reactor peak temperature for different operating pressures.*

A further consideration deals again with the reaction thermodynamics: as the synthesis pressure decreases, also the relative reaction heat release will reduce because of the unfavoured conversion rate. This is helpful for the studied model since it is possible to achieve lower temperature peaks inside the reactor even when operating with lower RR. The issue is practically solved when operating the synthesis reaction at 50 bars.

5.1.4 Effect of the introduction of a methanol upgrading section

The integration of the methanol upgrading section in the traditional plant arrangement does not significantly affect the behaviour of the main components. The main difference affecting operation consists in the entity of the purge stream fed to the reformer furnace, which in this case accounts for the additional fraction extracted by the light end column top condenser.

	Global purge stream [kmol/hr]	***Methanol amount [kmol/hr]***	***Hydrogen amount [kmol/hr]***
With Purification	22.8	0.30	16.0
Without Purification	15.9	0.04	15.0

Table 5.7: *purge stream details comparison.*

Table 5.7 indeed reports an overall higher amount of purge when purification is adopted. It contains also more residual oxidable compounds, mainly hydrogen and methanol (CO

amount is practically negligible) which contribute to increase the stream LHV and the resultant thermal power contribution in the combustion process.

A reduction of fresh biogas consumption is expected with a consequent higher production rate due to the higher availability of raw material in the main process.

Parameter	***With Purification***	***Without Purification***
CGE	0.83	0.83
Biogas to the furnace [%]	0.25	0.29
η_{tot}	0.97	0.97
η_{eq}	0.88	0.88
η_{fuel}	0.68	0.66
η_C	0.56	0.50
Methanol yearly production [tons/year]	23998	22968

Table 5.8:*main performance indicators and yearly methanol production comparison.*

Results in Table 5.8 confirm that the main component operation is not affected: the reformer CGE keeps steady as well as the total reaction yield. Even if the yield is constant the higher amount of processed syngas brings to a slightly higher methanol production, which in this case is a pure AA methanol stream. The increase in methanol production is about 4.5% respect to the baseline and it allows to obtain coherently higher carbon and fuel efficiency respect to the inlet processed biogas.

In terms of plant performances it is possible to state that the adoption of the purification section is beneficial. The impact on plant energy consumptions and costs remains to be evaluated.

5.2 ONCE THROUGH ARRANGEMENT ANALYSIS

In this section the technical analysis performed on the once through arrangement are reported. A first sensitivity analysis concerns the synthesis reactor outlet stream cooling: several values of target temperatures have been simulated to assess the better design. It follows the determination of the optimal CO_2 separation location, as it has been done for

the traditional arrangement. In the end, a discussion about the temperature profiles in the synthesis reactor is reported.

5.2.1 Determination of the optimal cooling target temperature

In the once through arrangement each stage outlet stream exits the reactor at high temperature, almost 240 °C. A proper cooling is needed to ensure separation of unreacted syngas from produced crude. Aiming to establish the optimal target temperature, a range between 20 and 90 °C has been considered. The analysis consider the default arrangement performing CO_2 separation before the reforming reaction. The main result of the simulations have been reported in Table 5.9.

Parameter	***Target 20°C***	***Target 30°C***	***Target 40°C***	***Target 50°C***	***Target 60°C***	***Target 70°C***	***Target 80°C***	***Target 90°C***
Reformer CGE [%]	82.5	82.6	82.9	83.0	83.1	83.2	83.4	83.6
Biofuel to the furnace [%]	14.5	14.0	11.4	10.7	10.1	9.5	5.4	2.5
η_{fuel} [%]	64.7	64.7	64.5	64.3	63.9	63.5	62.9	62.1
η_C [%]	48.8	48.8	48.7	48.6	48.4	47.8	47.4	45.6
$\eta_{\text{equilibrium}}$[%]	67.0	65.9	66.9	66.9	66.9	65.6	66.9	67.0
$\eta_{1^{\text{st}}_{\text{stage}}}$[%]	62.3	61.8	62.1	62.2	62.1	62.0	62.0	62.0
$\eta_{2^{\text{nd}}_{\text{stage}}}$[%]	48.5	46.7	45.6	44.4	42.99	40.0	40.0	38.4
$\eta_{3^{\text{rd}}_{\text{stage}}}$[%]	48.2	45.5	43.6	41.5	39.3	35.9	34.7	32.3
$\eta_{4^{\text{th}}_{\text{stage}}}$[%]	62.6	58.4	54.8	51.1	47.2	41.8	39.3	35.2
η_{tot}[%]	78.9	77.9	77.8	76.9	75.4	72.5	71.1	68.3
Methanol lost in final separation [Kmol/hr]	0.74	1.4	2.5	3.6	5.0	6.9	9.2	11.7
Produced Methanol [tons/year]	26197	26151	26039	25959	25861	25790	25483	25178
Pure Methanol [tons/year]	22608	22591	22520	22453	22338	22200	21979	21726

Table 5.9: *simulation results for several values of crude cooling target temperature.*

In general terms the lower is the temperature of the separators inlet streams, the higher is the expected crude liquid fraction obtained from the unit. As consequence, flow rate and composition of the separated gaseous stream varies, affecting performances of the following reaction stage.

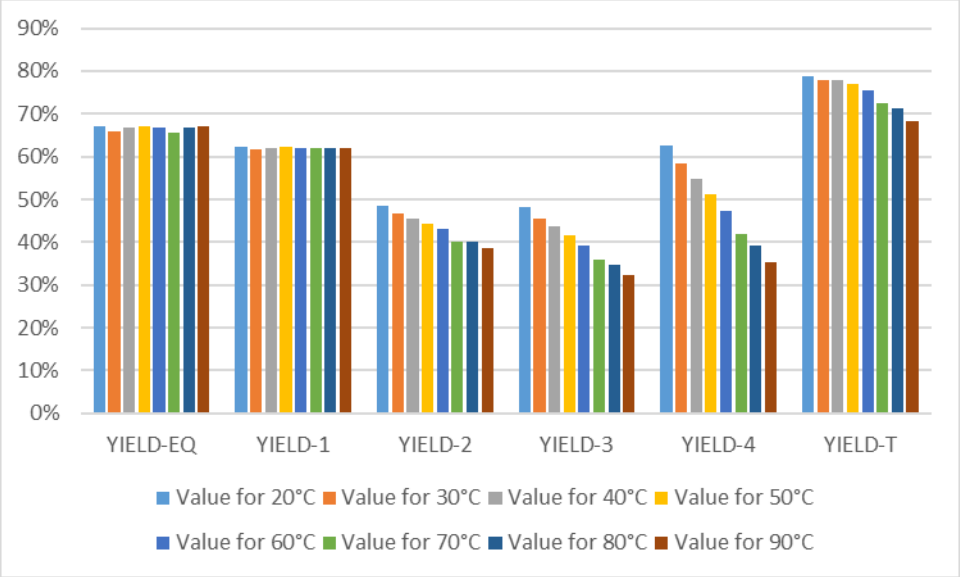

Figure 5.18: *reaction yields comparison for different values of cooling target temperature.*

Looking in particular at the reaction yields, the comparison reported in Figure 5.18 shows how lower cooling target temperatures favour the operation of each reaction stage. Inert heavier components, such as reacted methanol or water are obtained in higher amounts, leaving a higher concentration of reactant species in the reacting stream.

The first reaction stage is not affected by the cooling target temperature, since it is fed with a high temperature syngas stream. Its yield keeps almost constant.

Total reaction yields are in any case higher that the equilibrium reaction yield. This fact confirms that by adopting a multistage once through reactor it is possible to achieve conversion rates greater respect to the equilibrium condition, just like adopting recirculation

Focusing on the last separator it is possible to observe the fraction of methanol lost in the overhead purge recycled to the reformer furnace. Higher is the feed temperature, lower will be the global condensed methanol at the outlet. In the considered temperature range the methanol amount in the separator overheads is increased about 15 times, from nearly 0.7 to 11.76 kmol/hr. The higher purge flow rate affects the reformer heat requirement. Referring to Table 5.9 it is possible to observe a sharp decrease in the reformer furnace fresh biogas requirement down to 2.51% for a cooling target temperature of 90°C. Even if in this

condition more biogas is converted into syngas, the methanol synthesis reaction takes place under less favourable conditions and a lot of produced methanol would be lost. It is remarked that the reformer CGE keeps almost unaffected since even if the biogas usage is reduced, the required heat stream is compensated by the purge flux.

As consequence of the improved performances per stage and of the greater liquid product extraction, the yearly methanol production is quite increased when lower cooling target temperatures are achieved. More precisely an increment both in the pure methanol flow rate and in the total product flow rate (including impurities) about 4% is recorded. Figure 5.19, Figure 5.20 and Figure 5.21 provide a graphical representation of the produced mass flow trend and of the overall plant efficiencies strictly dependent on it.

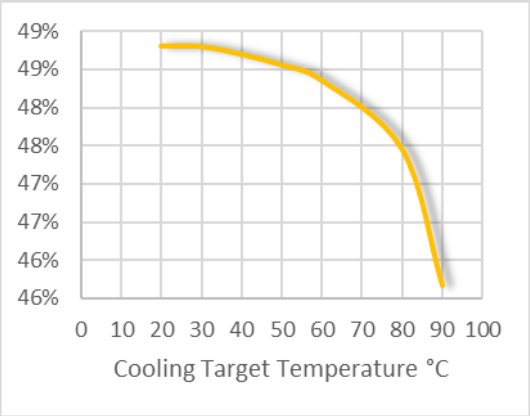

Figure 5.19: *carbon efficiency trend for different cooling target temperature.*

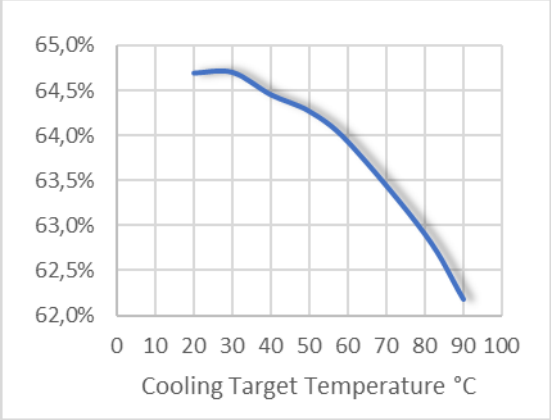

Figure 5.20: *fuel efficiency trend for different cooling target temperature*

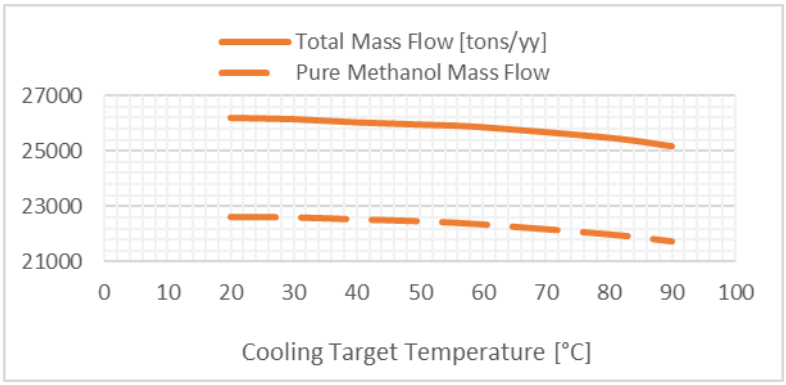

Figure 5.21: *yearly methanol production trend for different cooling target temperature.*

In the light of these considerations, the optimal cooling target temperature ensuring the best performances is equal to 20 °C. However, adopting such value the higher evaporation rate in the last separator decreases the liquid outlet product temperature down to 10 °C. This temperature is out of the suggested temperature interval for methanol storage, whose lower limit is about 15°C [62].

In conclusion, even if the optimal temperature value resulted 20 °C, it was chosen as design specification the value of 30°C, which allows a suitable methanol storage temperature. Produced methanol outlet temperature variation for the considered cooling target range is reported in Figure 5.22.

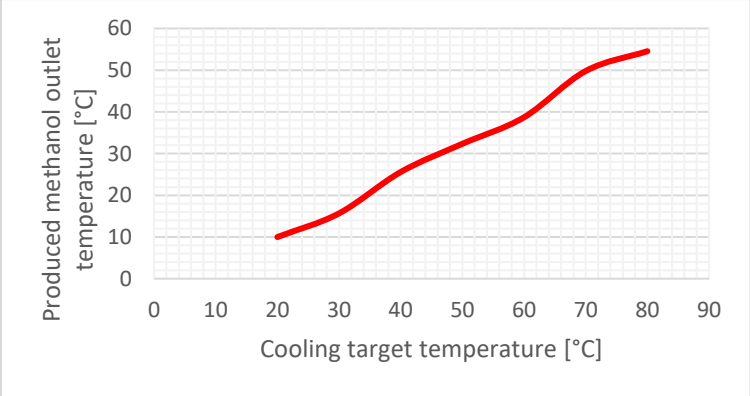

Figure 5.22: *produced methanol outlet temperature for different cooling target temperatures.*

5.2.2 Optimal CO_2 separation location in the once through configuration

The optimal CO_2 separation location has been determined also for the once through configuration. As in the previous plant arrangement, varying the position of the separation section has a certain impact both on the reformer and on the synthesis reactor.

Starting from the latter, if the CO_2 separation is performed, wherever it is located, a syngas stoichiometric module equal to 2.1 is achieved at the first stage reactor inlet. However, the value of M at the inlet of the following stages strictly depends on the previous stages performances. Therefore each individual stage operation affects the downstream process. This is a crucial difference respect to the case adopting recirculation, where for every value of RR the conversion rate on the single passage keeps almost unchanged.

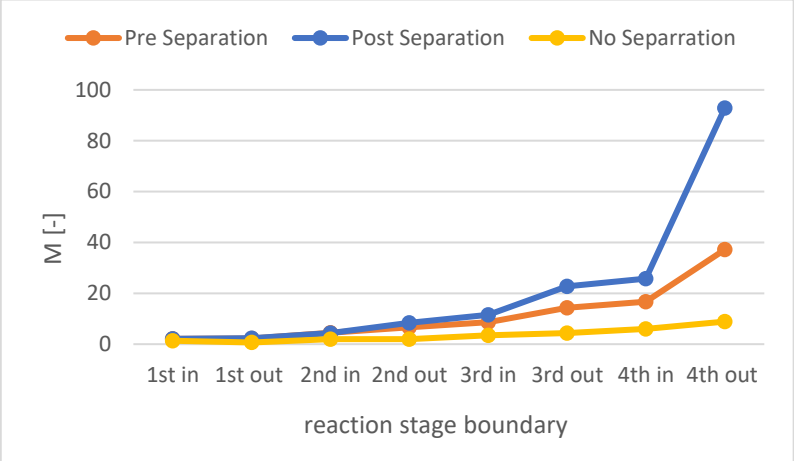

Figure 5.23: *syngas module M evolution inside the synthesis reactor.*

From the syngas module evolution reported in Figure 5.23 it is possible to observe that differences between the considered cases become wider as the reaction proceeds. In general M increases due to the conversion of the available carbon, which is progressively reduced. If CO_2 separation is not performed this effect is strongly mitigated and M keeps at low values, according to Eqn.2.3.

In the other cases the growth is much sharper: the more carbon is converted, the more M rises, suggesting best reaction performances for the case adopting separation after the

reforming reaction. This fact is confirmed by results reported in Table 5.10, showing a comparison in terms of global reaction performances and stage performances.

In all the studied cases the greatest methanol amount will be converted in the first stage, being it the one fed with the highest flow rate in optimal conditions. Methanol production progressively decreases in all the following stages due to the reduction in the inlet feed and in the available CO_2 amount. The lack of CO_2 is both related to its consumption during the synthesis reaction and to the entrainment in the separated product stream due to its affinity with methanol. Focusing on the latter, the global amount of CO_2 lost during methanol separation is reported in Figure 5.24.

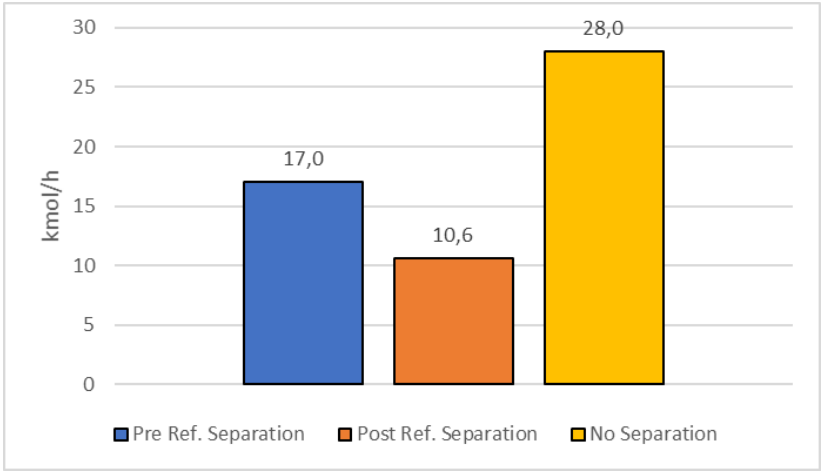

Figure 5.24: *entrained CO_2 in the produced methanol stream.*

As consequence, even if in the first two stages the limiting reactant is hydrogen, the maximum theoretical methanol that can be obtained in the third and fourth stages is limited by the carbon availability. Because of this fact a considerable amount of residual unconverted hydrogen is present in the fourth stage outlet stream.

Coherently with the reduction in methanol conversion, also stage yields are reduced as the reaction proceeds. An exception may be noticed for the fourth stage, which shows an improved yield. This improvement is only apparent, since it is related to the reduction of available carbon at the denominator of Eqn. 4.40 and Eqn. 4.39. Methanol conversion in

this stage is minimum and despite the improved performances it would be useless adopting more than four stages.

		Post Separation	*Pre Separation*	*No Separation*
Produced MeOH [kmol/h]	Stage 1	61.1	57.9	55.56
	Stage 2	10.2	9.9	12.43
	Stage 3	2.3	4.0	3.59
	Stage 4	1.3	2.5	2.07
Single stage yield η_{stage}[%]	Stage 1	69.5	61.8	52.6
	Stage 2	63.9	46.7	44.5
	Stage 3	53.6	45.5	35.9
	Stage 4	73.1	58.4	42.0
Total reaction yield η_{tot}[%]		84.8	77.9	69.0
Equilibrium reaction yield η_{eq}[%]		74.8	65.9	56.8
Fuel efficiency η_{fuel}[%]		65.3	64.7	64.7
Carbon Efficiency η_C[%]		50.1	49.7	49.2

Table 5.10: *reaction performances and overall plant efficiencies comparison.*

To enter deeper in the details Table 5.10, Table 5.11 and Table 5.12 provide more precise information about the entity of the converted streams and the maximum theoretical methanol conversion per stage

No Separation	***1st in***	***1st out***	***2nd in***	***2nd out***	***3rd in***	***3rd out***	***4th in***	***4th out***
CO_2 [kmol/hr]	40.04	38.19	17.02	13.7	8.29	5.67	4.22	2.47
CO [kmol/hr]	65.63	11.92	10.91	1.79	1.71	0.73	0.71	0.39
CO_2+CO [kmol/hr]	105.67	50.12	27.93	15.49	9.99	6.41	4.93	2.86
CH_3OH [kmol/hr]	0	55.56	0.27	12.7	0.12	3.71	0.07	2.14
H_2 [kmol/hr]	184.65	71.69	71.69	43.51	43.51	33.72	33.72	27.83
Limiting reactants	**H_2**		**H_2**		**$CO+CO_2$**		**$CO+CO_2$**	
Theoretical Maximum Methanol [kmol/hr]	83.43		27.53		9.99		4.93	
Converted Methanol/Theoretical maximum [-]	0.67		0.45		0.36		0.42	

Table 5.11: *synthesis reaction details for the arrangement without separation.*

Post Separation	***1st in***	***1st out***	***2nd in***	***2nd out***	***3rd in***	***3rd out***	***4th in***	***4th out***
CO_2 [kmol/hr]	16.9	16.1	7.1	4.7	3.3	1.6	1.4	0.33
CO [kmol/hr]	70.0	9.8	8.9	1.1	1.1	0.44	0.44	0.14

CO_2+CO [kmol/hr]	86.9	25.9	16.1	5.9	4.4	2.0	1.8	0.47
CH_3OH [kmol/hr]	0.00	61.1	0.27	10.5	0.14	2.5	0.09	1.4
H_2 [kmol/hr]	199.8	76.9	76.9	54.1	54.1	47.6	47.7	43.9
Limiting reactants	**H_2**		**H_2**		**$CO+CO_2$**		**$CO+CO_2$**	
Theoretical Maximum Methanol [kmol/hr]	86.9		16.1		4.4		1.8	
Converted Methanol/Theoretical maximum [-]	0.7		0.64		0.54		0.74	

Table 5.12: *synthesis reaction details for the arrangement with post reformer separation...*

Pre Separation	***1st in***	***1st out***	***2nd in***	***2nd out***	***3rd in***	***3rd out***	***4th in***	***4th out***
CO_2 [kmol/hr]	32.3	28.5	14.5	9.7	7.3	3.9	3.3	1.3
CO [kmol/hr]	61.6	7.3	6.8	1.7	1.7	0.90	0.89	0.44
CO_2+CO [kmol/hr]	93.8	35.8	21.3	11.4	8.9	4.9	4.2	1.8
CH_3OH [kmol/hr]	0.00	57.9	0.35	10.3	0.19	4.2	0.1	2.6
H_2 [kmol/hr]	229.3	109.6	109.6	84.9	84.9	73.5	73.5	66.5
Limiting reactants	**H_2**		**H_2**		**$CO+CO_2$**		**$CO+CO_2$**	
Theoretical Maximum Methanol [kmol/hr]	93.8		21.3		8.9		4.2	
Converted Methanol/Theoretical maximum [-]	0.62		0.47		0.45		0.58	

Table 5.13: *synthesis reaction details for the arrangement with pre reformer separation.*

Residual hydrogen abundance in the last stages outlet stream may be noticed independently of the CO_2 separation. Being hydrogen more volatile than other species, a significant amount will be recycled to the reformer furnace, enhancing the purge stream LHV. It is reminded that since CO amount is negligible, the purge flux LHV depends mainly on the amount of H_2 and methanol.

Focusing on the reformer performances reported in Table 5.14 the methane conversion is improved due to the carbon dioxide excess in the processed stream, with a consequent higher heat requirement. Anyway, H_2 abundance in the purge stream is quite useful in reducing fresh biogas consumption, which is significantly lower respect to the values reported in Figure 5.1 for the traditional arrangement.

	Pre Separation	***Post Separation***	***No Separation***
ε_{CH_4}	94.6	95.1	95.0
Reformer CGE [%]	82.6	82.1	80.5
Biofuel to the furnace [%]	14.1	20.8	26.4
H_2 in the purge stream [kmol/hr]	66.5	43.9	27.8
CH_3OH in the purge stream [kmol/hr]	1.4	1.2	0.66

Table 5.14: *main performance indicators and burnable species in the purge flux for different CO_2 separation section locations.*

On the other hand the higher amount higher purge amounts will reduce the quantity of methanol in the product stream, penalizing performances. If separation is not performed, this effect counteracts the worst reaction performances, allowing this plant configuration to reach overall plant efficiencies at all comparable with the case adopting CO_2 separation before the reforming reaction. This latter is able to process more fuel, but it has the greater methanol loss in the purge stream.

In conclusion, both due to the higher reaction performances and to a reduced methanol loss, the arrangement able to produce more final product is the one performing separation after the reformer. Coherently, the best overall plant efficiencies have been computed for this case, as reported in Table 5.10**.**

The overall plant carbon balance has been performed also for this analysis and it is reported in the Sankey diagrams in Figure 5.25. Noticeable is that the highest amount of carbon in the flue gas is recorded if separation is not performed: this amount is mostly related to the higher biogas usage, at CO_2 richer purge stream. Also the highest carbon amount in the product stream is recorded for this case, but it is still related to the CO_2 presence, since the higher methanol production is achieved adopting CO_2 separation after the reforming reaction. In any case the amount of carbon entrained in separated water is less than a percentage point.

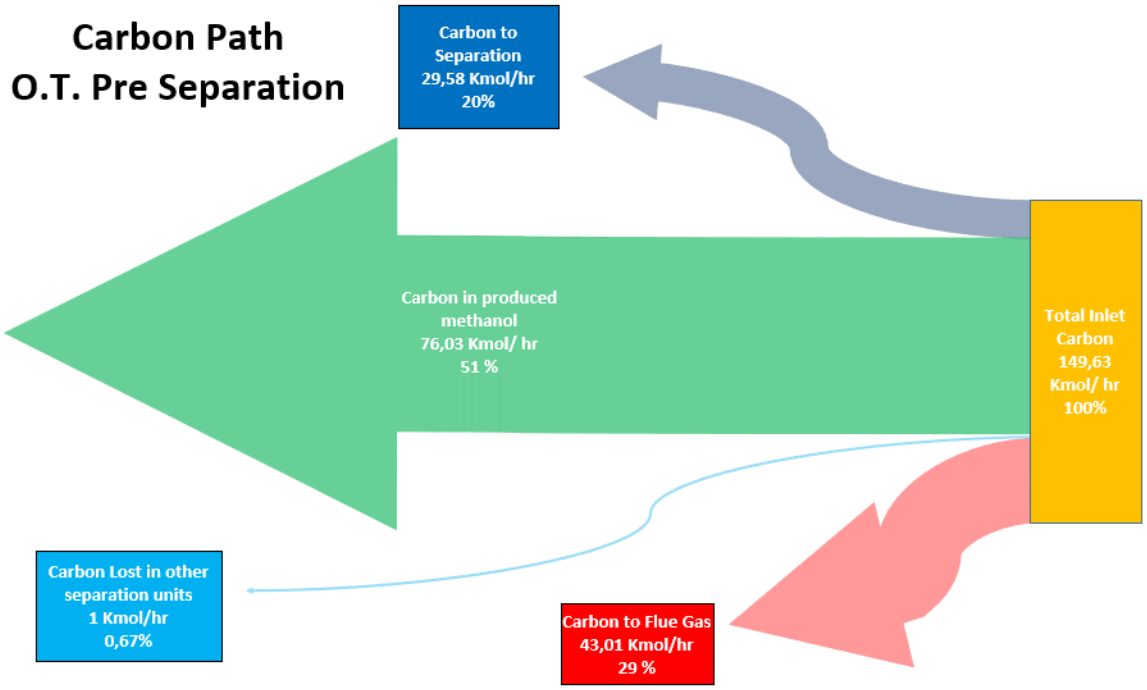
Carbon Path
O.T. Pre Separation
Carbon to Separation 29,58 Kmol/hr 20%
Carbon in produced methanol 76,03 Kmol/ hr 51 %
Total Inlet Carbon 149,63 Kmol/ hr 100%
Carbon Lost in other separation units 1 Kmol/hr 0,67%
Carbon to Flue Gas 43,01 Kmol/hr 29 %

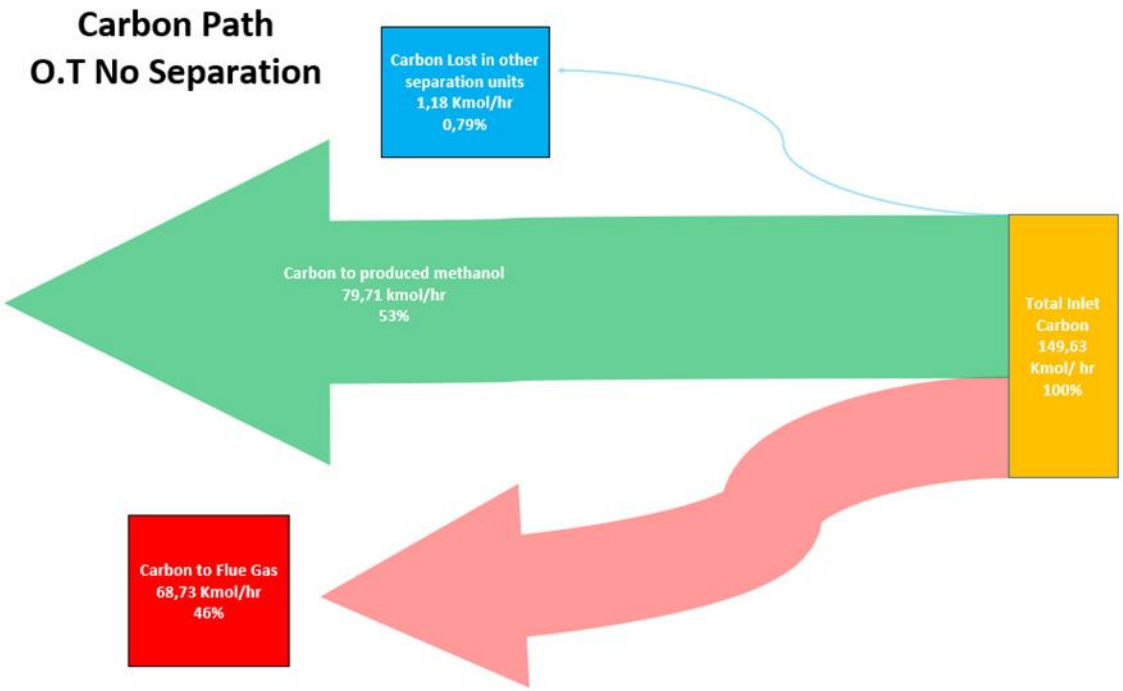
Carbon Path
O.T No Separation
Carbon Lost in other separation units 1,18 Kmol/hr 0,79%
Carbon to produced methanol 79,71 kmol/hr 53%
Total Inlet Carbon 149,63 Kmol/ hr 100%
Carbon to Flue Gas 68,73 Kmol/hr 46%

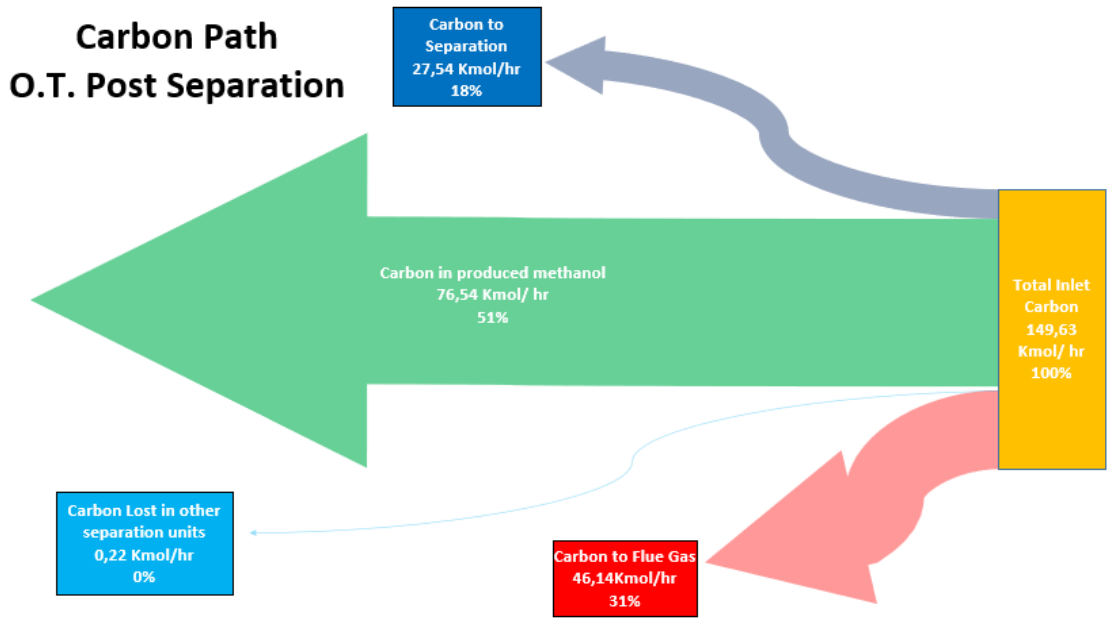

Figure 5.25: *Sankey diagrams tracking carbon path in the considered plant arrangements.*

5.2.3 About the possibility to reduce the catalyst usage

When studying conversion rates across each reaction stage it has been observed that, except for the first stage, methanol conversion is not immediate inside the catalysed tubes. This is because the feed temperature requires to reach a suitable temperature before the conversion starts.

Dealing with the first stage, syngas is fed at high temperature and the conversion is almost immediate. While concerning the others, the inlet feed temperature is about 30 °C, too low to let the synthesis reaction start.

Looking at the methanol concentration profiles along the catalysed tubes reported in Figure 5.27, Figure 5.26, and Figure 5.28 it is possible to observe that at least for a length about 25 cm the feed will not react. Thus, such portion could not be loaded with useful catalyst, reducing the catalyst loading and the and the maintenance cost related to its replacement.

The potential catalyst loading and cost saving estimation is reported in Table 5.15.

Only about 1.3% of the fixed investment related to the catalyst purchase can be avoided, while concerning the replacement cost a saving about 2.2% of the initial estimated cost is reached.

Catalyst free length [m]	***Actual Catalyst Usage [Kg/yy]***	***Actual Catalyst Replacement Cost [$/yy]***	***Potential Catalyst Saving [Kg/yy]***	***Potential Catalyst Saving [$/yy]***	***Actual Catalyst FCI [$]***	***Potential Catalyst FCI Saving[$]***
0	426.9	5550.2	0	0	11038.3	0
0.25	213.5	2775.1	8.9	115.6	1839.7	76.6
0.25	149.4	1942.6	6.2	80.9	2136.4	89.0
0.25	106.7	1387.5	4.4	57.8	1226.5	51.1
Fixed investment saving [%]			1.3			
Replacement cost saving [%]			2.2			

Table 5.15: *catalyst usage and cost saving estimations.*

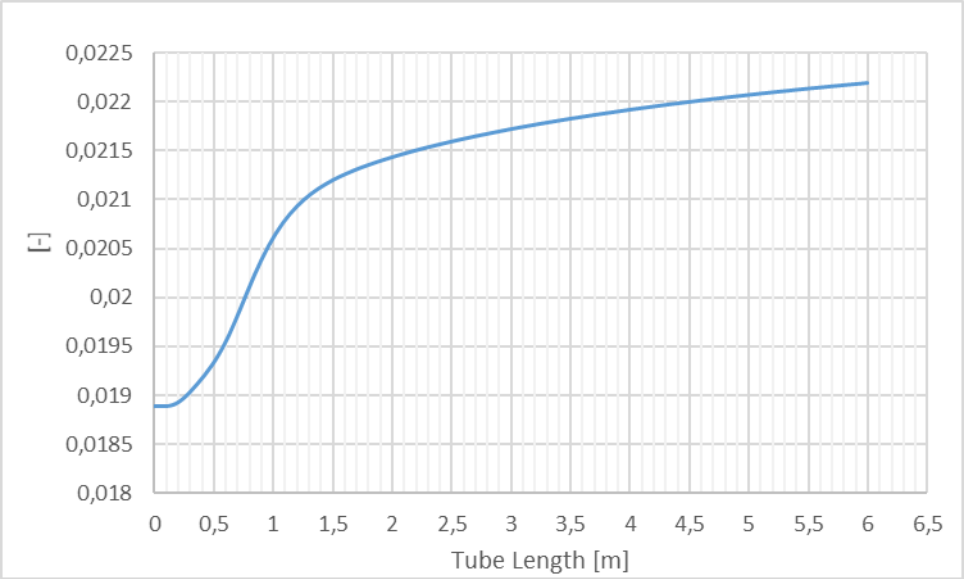

Figure 5.27 : *methanol concentration profile in the second reaction stage.*

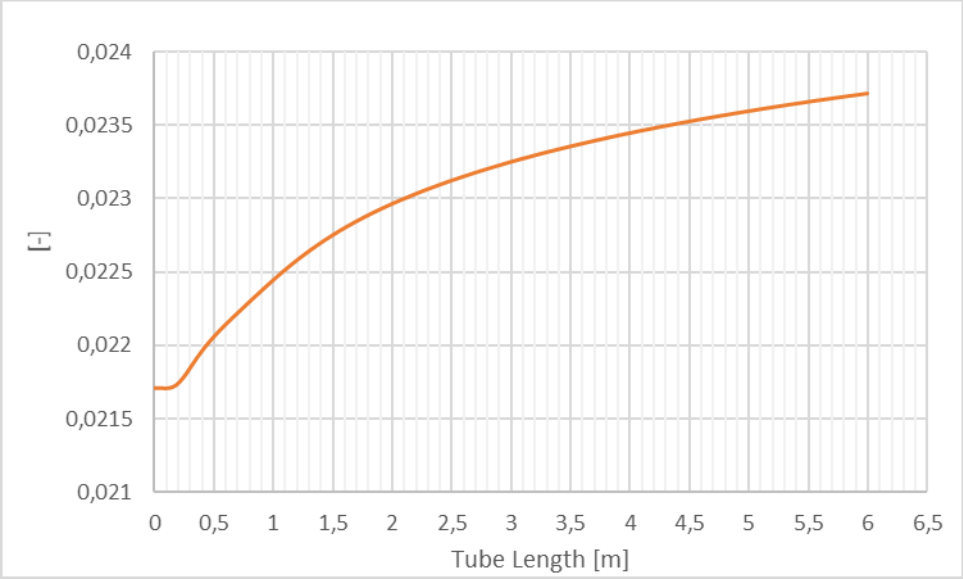

Figure 5.26: *methanol concentration profile in the fourth reaction stage.*

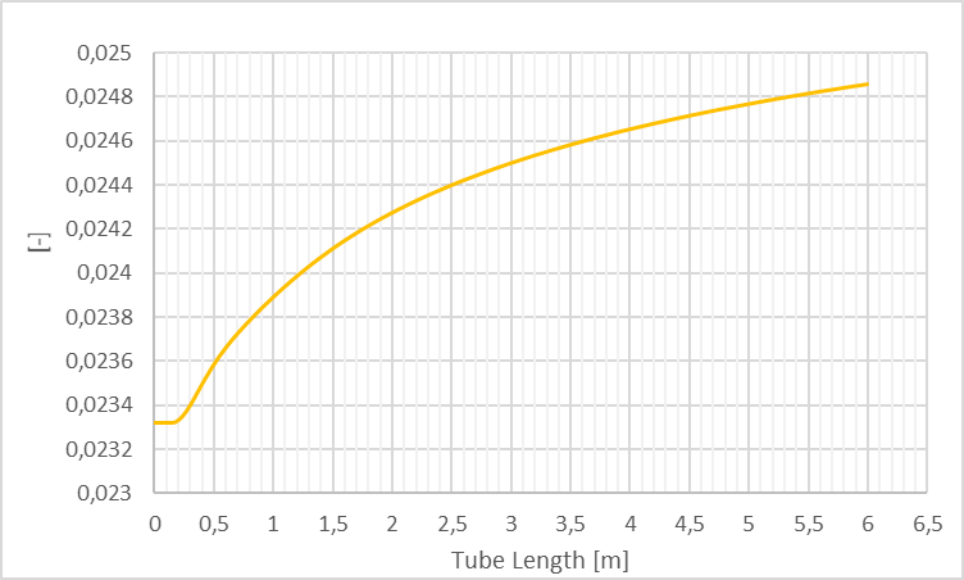

Figure 5.28: *methanol concentration profile in the third reaction stage.*

5.2.4 Effect of the once through configuration on the reactor temperature profile

When adopting the once through configuration the reactor total inlet feed is strongly reduced, due to the absence of the recycled stream contribution. It has been shown how adopting recirculation the conversion rate keeps almost unaffected; thus the excess stream behaves as a thermal inert mitigating the temperature profile inside the reactor. Such effect comes less since the fraction of inert inlet stream is quite limited.

Focusing on the once through configuration adopting reformer downstream separation, it has been investigated the temperature profile in each reaction stage. This configuration has been chosen since it is the one with the best technical performances. Figure 5.25 Figure 5.29, Figure 5.30, Figure 5.31 and Figure 5.32 show the temperature profile results. It is evident that before reaching the reaction temperature, the first stage reacting fluid has a temperature peak about 320 °C, quite far from the validity range of the implemented kinetic model (280°C). It would be also detrimental for the catalyst resistance during operation. This

phenomenon interests only the first stage since the greatest part of the conversion takes place there, with a consequent much more intense reaction heat release to be handled.

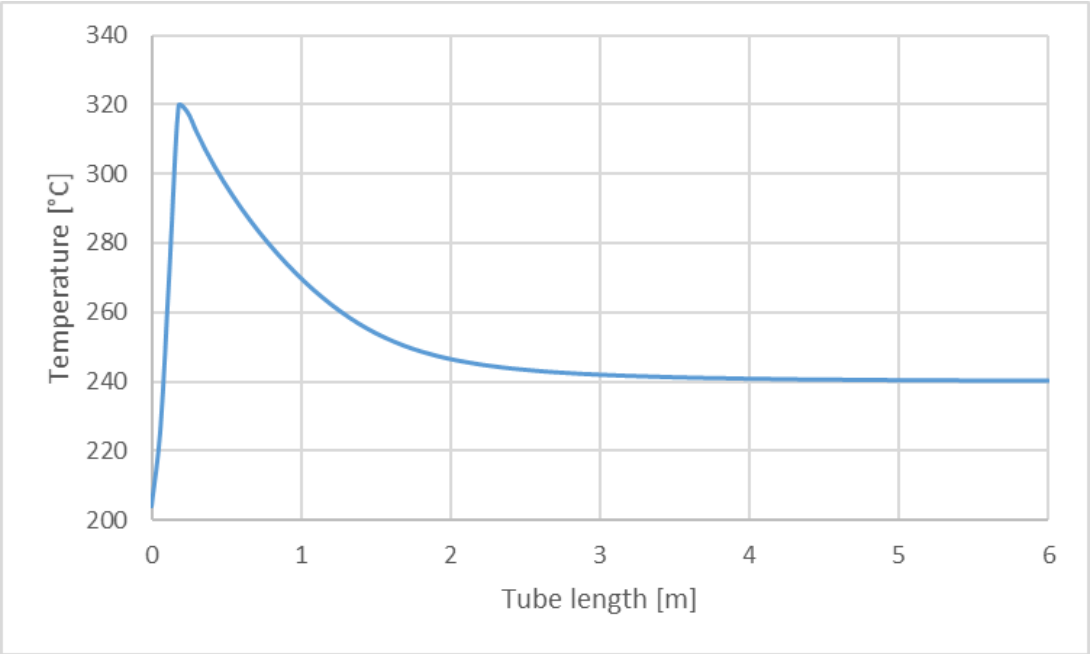

Figure 5.29: *first reaction stage temperature profile.*

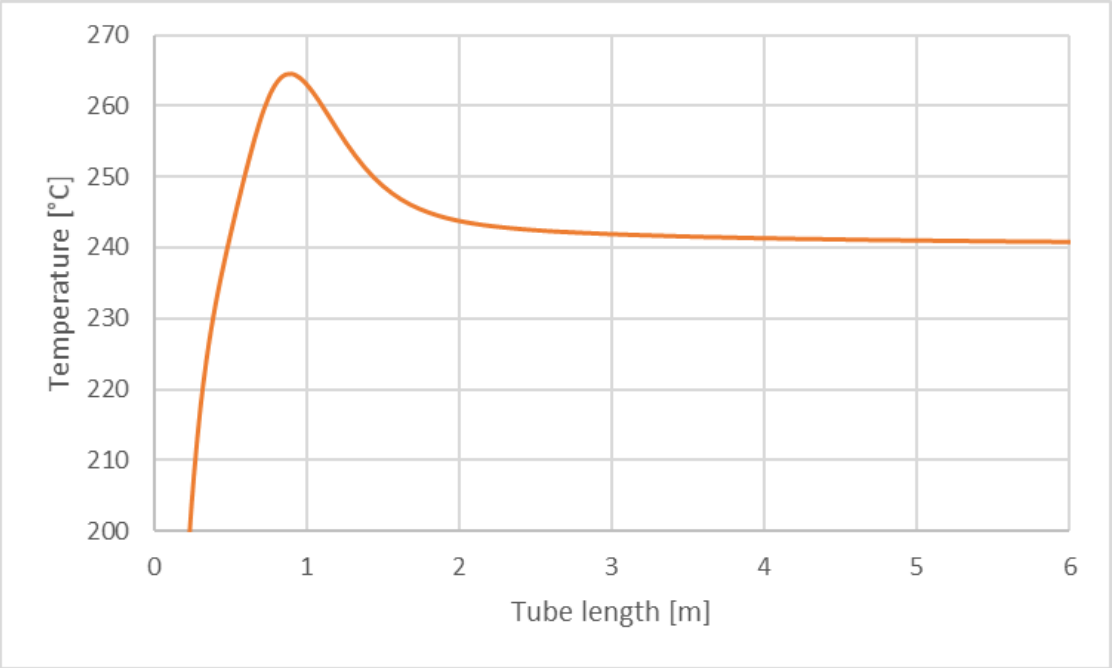

Figure 5.30: *second reaction stage temperature profile.*

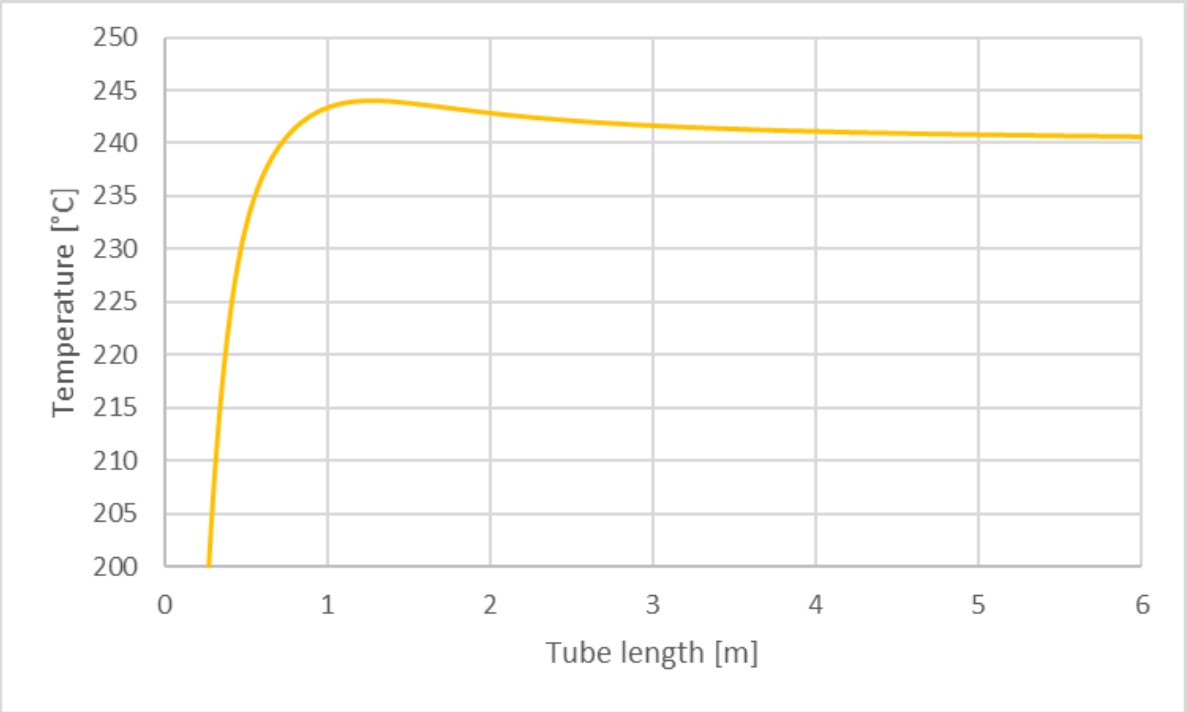

Figure 5.31: *third reaction stage temperature profile.*

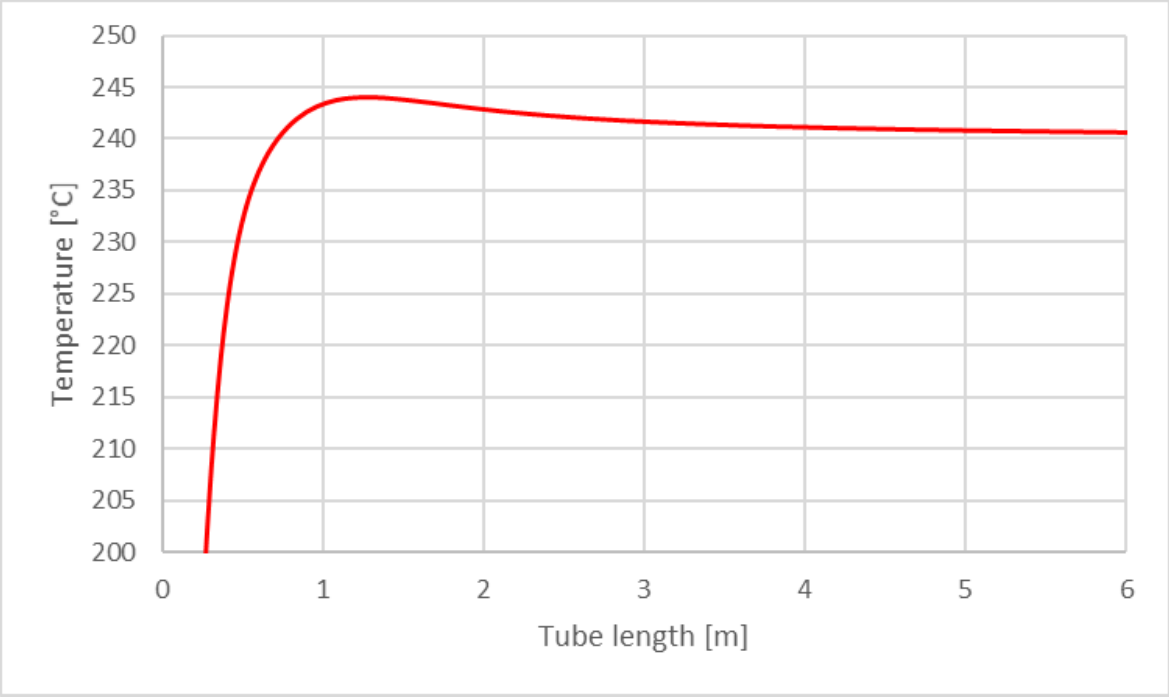

Figure 5.32: *fourth reaction stage temperature profile.*

Aiming to mitigate the temperature peak, the effect of a possible enhancement of the synthesis reaction heat exchange coefficient, U, has been investigated in a sensitivity analysis. When the Lurgi reactor was designed, it has been set to 600 W/m^{2}K [80, 81]. A range of U from 500 to 1200 W/m^{2}K has been considered to perform the simulations.

Of course, the higher is the heat exchange coefficient, the more is the thermal power that the thermal fluid can extract. As result the temperature increase of the reacting fluid will be mitigated. Beside the effect of U improvements, also the effect of a reduced tube diameter has been considered. Lower diameters would enhance the overall surface to volume ratio, with a consequent higher heat exchange. A definition of the surface to volume ratio is provided by

$$SV = \frac{A_{\text{exch}}}{V_{\text{reac}}}$$

Eqn. 5.2

Where A_{exch} and V_{reac} could be expressed according to Eqn. 4. and Eqn. respectively.

As result, by passing from 500 to 1200 W/m^{2}K a temperature decrease only about 16 °C has been recorded. Adopting a reduced diameter equal to 25 mm an overall temperature difference about 23 °C has been so. The comparison between the 2 cases is reported in Figure 5.33.

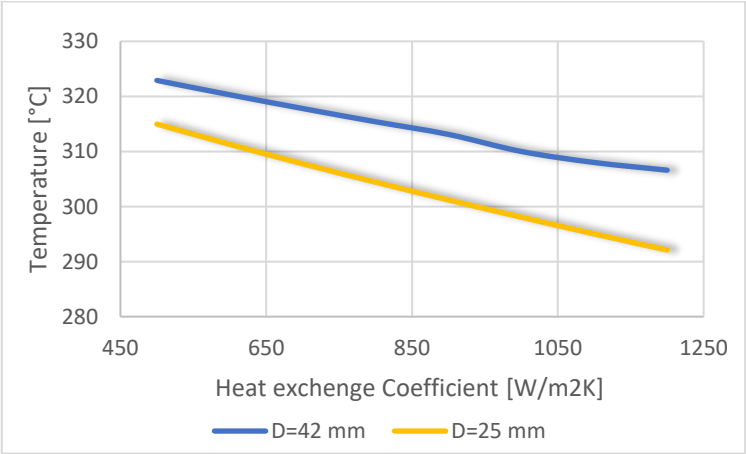

Figure 5.33: *reactor peak temperature decrease for two different diameters.*

It is confirmed a certain advantage in adopting reduced diameters, yet the temperature peak still remains to high, near 290 °C.

5.3 OPTIMAL CASES TECHNICAL COMPARISON

In this section a comparison between the traditional arrangement adopting recirculation and the one adopting a once through reactor is reported. In such comparison, the optimal designs per each case have been taken into account. More precisely the case with recirculation has a RR equal to 5.84 and adopts CO_2 separation before the reforming reaction. The once through arrangement, instead, separate carbon dioxide from the produced syngas stream. A synthesis operating pressure of 93 bar is considered for both, as well as the same reacting geometry and inlet biogas stream.

Both the configurations aim to enhance the overall reaction yield and methanol production, one by recirculating unreacted syngas at the reactor inlet, the other processing it in further reaction stages. This main operating difference has a first direct consequence on the syngas module evolution, which has already been introduced in the previous section.

Figure 5.35 and Figure 5.34 show the evolution of the stoichiometric module across the reactor. Even if for both the initial value is equal to 2.1, in the case with recirculation it immediately rise up to 15 due to the mixing with the recycled stream. The reaction will then proceed always in the same conditions. In the case with the multistage reactor, the module evolution is initially flatter and its growth depends on each individual stage performances.

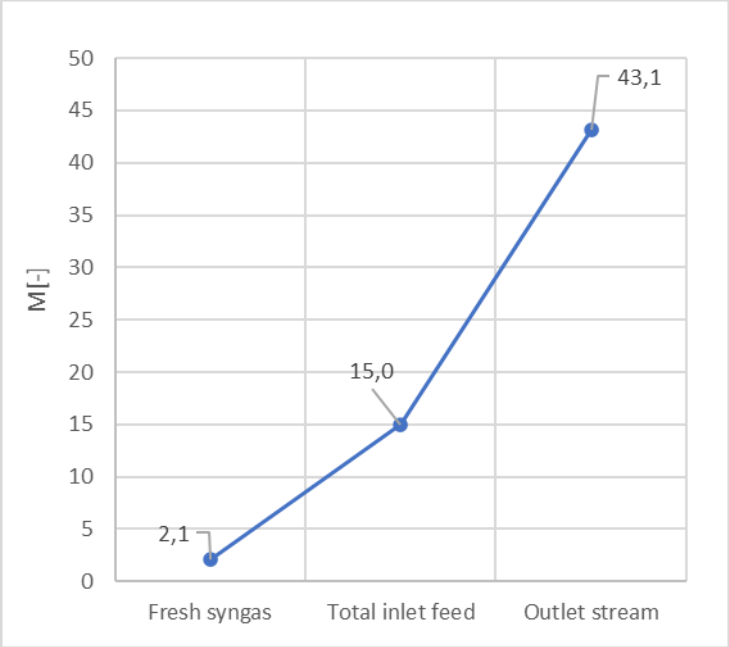

Figure 5.35: *traditional reactor syngas module evolution*

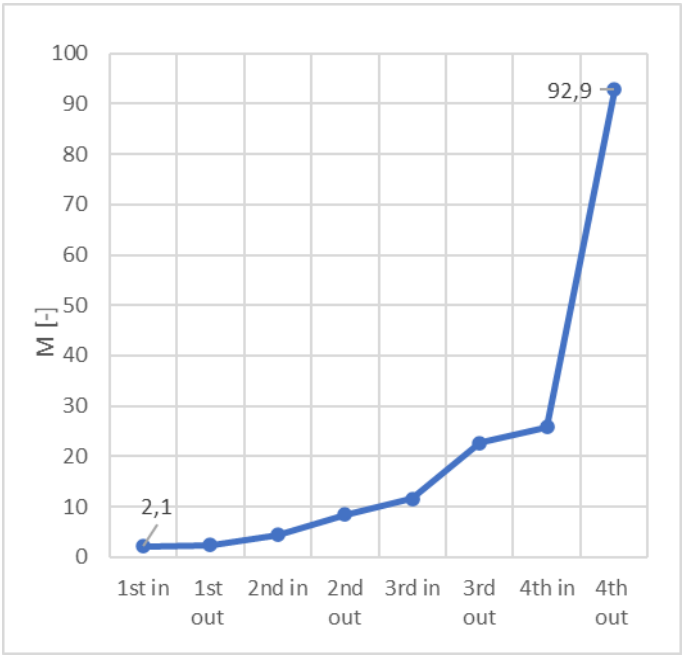

Figure 5.34: *once through reactor syngas module evolution*

These will therefore affect the following operation. In the end a quite elevate value of M is obtained due to the lack of carbon in the last stages respect to the overall processed feed.

It is possible to observe that the overall operation in this latter case is less stable respect to the adoption of recirculation, since it depends also on the cooling process and on the separation process performed between each stage. In any case, it has been shown how the overall yield and methanol production have been successfully enhanced, whatever the arrangement is.

Table 5.16 provides a comparison in terms of main plant performances. Concerning biofuel consumption, it is noticeable that the once through arrangement has the lower biofuel requirement, although the CO_2 separation downstream the reforming reaction rises the reformer heat requirement. The lower consumption is related to a recycled purge stream richer in oxidable compounds.

Parameter	*Once Through*	*Recirculation*
CGE [%]	82.1	82.5
Biofuel to the furnace [%]	20.8	29.1
ε_{CH_4} [%]	95.1	93.7
$\eta_{Sep_{CO_2}}$ [%]	62.1	62.0
η_{tot} [%]	84.8	96.6
η_{fuel} [%]	65.4	65.7
η_C [%]	50.1	52.0
Methanol yearly production [tons/year]	24793.5	28695.3

Table 5.16: *optimal cases main performance indicators comparison.*

As for the CO_2 separation, its performances keep almost unchanged in terms of efficiency, whatever is the separation location or the reactor configuration considered.

As for the reaction yield, only the total yield has been reported for a meaningful comparison. Here a net difference about 12% is noticed, which is related to the more favourable and stable operating condition achieved in the traditional configuration. Such difference is not so consistent when looking at the overall plant efficiencies, since only a minimal variation is recorded. The reason lies in the higher available fresh biogas in the once through arrangement, which counteracts the loss in reaction yield.

Anyway, even small differences in the global efficiencies values bring to important changes in the methanol yearly production. A variation of 1.9 percentage points in the carbon efficiency (or 0.38 considering the fuel efficiency, which actually provides almost the same information) implies an increment about 16% of methanol annual production, corresponding to 3902 tons per year.

Such kind of variations may have a significant impact on the yearly revenues of the plant, but for more precise considerations also costs should be taken into account.

6. ECONOMIC RESULTS

In the previous chapter the plant arrangements ensuring best performances both for the traditional process and for the once through case have been identified. However, in order to assess the more profitable design solution for the studied small scale plant, all the modelled arrangements have been compared in an economic analysis. Investment costs, manufacturing costs and profitability indicators have been commented. Focusing on the traditional arrangement, the impact of the different operating pressures on economic indexes, as well as the impact of the methanol upgrading section integration has been also evaluated.

6.1 Economic comparison between the modelled arrangements

When evaluating plant economics, the design able to produce more product not necessarily correspond to the most profitable, since also costs should be taken into account. That is why all the modelled plant variations have been included in this analysis. For sake of simplicity the plant configurations are often referred with the names reported in Table 6.1, which provides a first analysis on the fixed investment costs related to the purchase of all the equipment.

Plant Configuration	***FCI [M€]***	***Biogas compression [M€]***	***CO_2 removal [M€]***	***Syngas production [M€]***	***Syngas compression [M€]***	***CH_3OH production [M€]***	***Steam production [M€]***	***Cooling system [M€]***
Once Through Pre Separation	10.8	0.74	0.76	4.3	1.9	0.54	1.8	0.11
Once Through Post Separation	10.2	0.74	0.76	4.3	1.9	0.54	1.8	0.11
Once Through No Separation	9.6	0.72	-	3.7	2.2	0.65	1.8	0.11
Traditional Pre Separation	10.5	0.70	0.61	4.00	1.97	1.4	1.7	0.11
Traditional Post Separation	10.5	0.68	0.80	3.9	1.8	1.4	1.8	0.11
Traditional No Separation	9.3	0.68	-	3.8	2.0	1.01	1.8	0.11

Table 6.1: *fixed investment costs comparison .*

The greatest differences in terms of global FCI may be noticed for the cases without separation section. These are the cheapest arrangements, since the whole investment related to the absorber, the stripper and all the auxiliary units like exchangers or the regenerated amines pump is saved. Such investment saving is about 1 million of euros respect the other plants, both when recirculation and once through reactors are adopted.

Being the other plant arrangements quite similar, significant variations of the FCI are not recorded. To better enter in the details, the fixed investment has been partitioned in various cost components depending on the purpose in the plant. For a more immediate understanding, a graphical representation is provided by Figure 6.3, Figure 6., Figure 6.1, Figure 6., Figure 6.2, Figure 6.3.

It is noticeable that the methanol production island has a greater weight in traditional arrangements with respect to the once through cases. In general a once through multistage reactor is expected to cost more than a simple Lurgi reactor, due to the more complex design. However, if recirculation is adopted, a further compressor is necessary to manage the recycled stream pressure up to the synthesis one. The cost of the recirculation compressor and its driver is much greater than the costs related to the additional exchangers and separators needed in the once through case. Thus, even if the multistage reactor alone is more expensive respect to the simple Lurgi reactor, the higher costs for the methanol production island are recorded in the traditional case.

Almost half of the global expenditure is related to syngas production, since the FTR cost is the greatest investment to account for in the plant. Being the one with the lower biogas processed due to the higher fuel consumption, the traditional post separation case has the lower syngas production and compression costs. It is reminded that often the processed flow rate is directly involved in the cost functions as reference capacity. In some cases, even if not directly involved, it may affect the reference capacity. This occurs for the heat exchangers, whose reference capacity is the heat duty.

Compression costs are related to the purchase of the compressors and their drivers; they are the second higher investment to sustain. Coherently with the CO_2 excess in the main stream, syngas compression costs are slightly higher when separation is not performed, due to the higher flow rate to be processed in the multi stage compressor. Other sections account almost for the same investment and have at all a comparable weight in the global FCI.

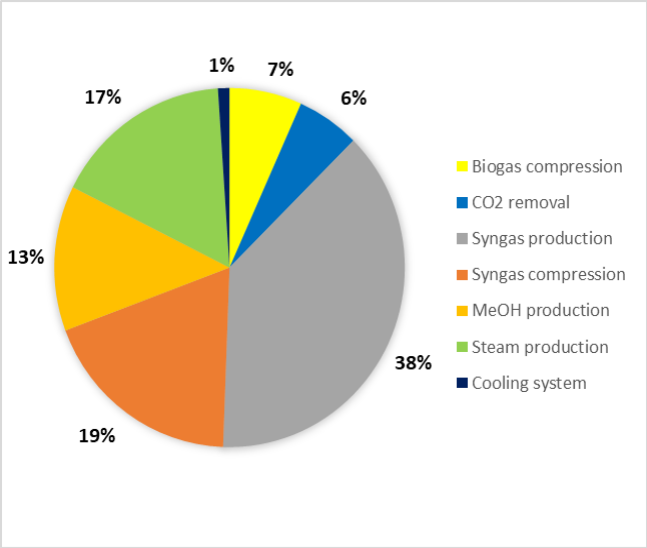

Figure 6.1: *traditonal – post separation FCI partition.*

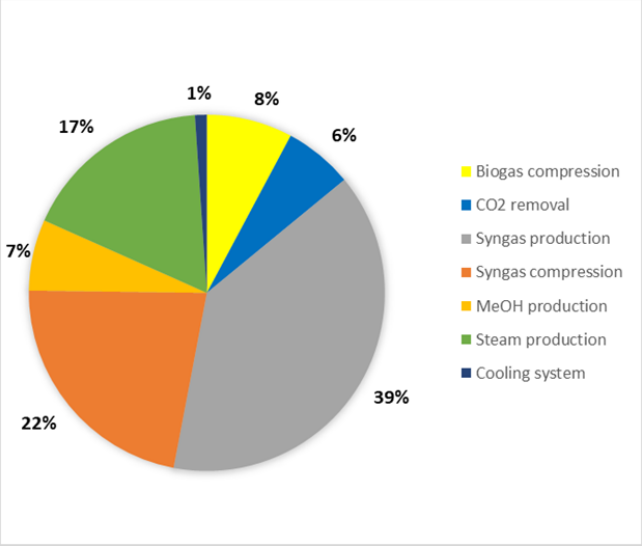

Figure 6.1: *traditional – pre separation FCI partition.*

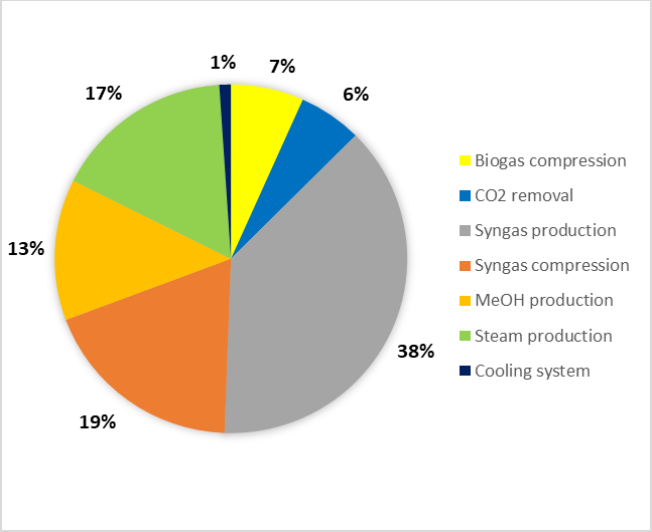

Figure 6.3: *once through – post separation FCI partition.*

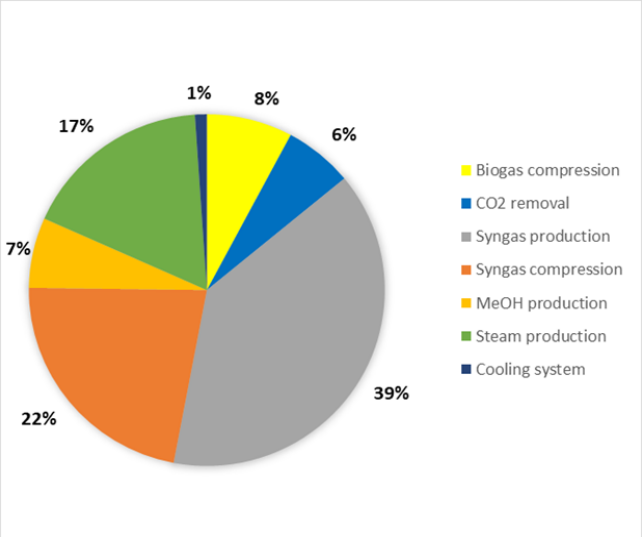

Figure 6.4 : *once through – pre separation FCI partition.*

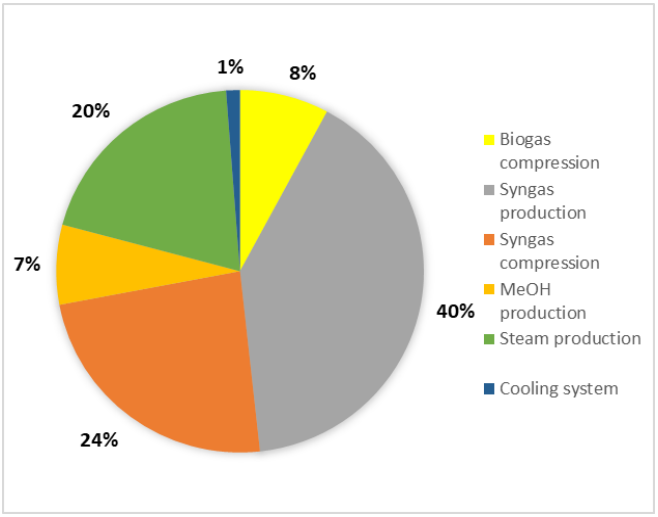

Figure 6.2: *once through – no separation.FCI partition.*

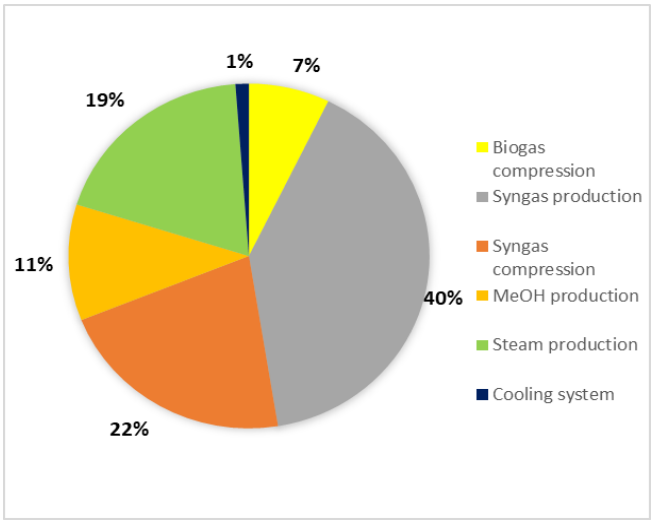

Figure 6.3: *traditional – no separation. FCI partition.*

As far as the operating costs are concerned, a summary of the main results is reported in Table 6.2.

Plant Configuration	***Cut[k€/yy]***	***Col[k€/yy]***	***Crm[k€/yy]***	***COMd[k€/year]***
Once Through Pre Separation	1050	1109.1	13.2	6292.3
Once Through Post Separation	890.0	1109.1	13.2	5989.7
Once Through No Separation	947.4	985.9	12.8	5599.0
Traditional Pre Separation	932.1	986.0	13.1	5746.6
Traditional Post Separation	839.9	986.0	13.1	5633.0
Traditional No Separation	854.6	924.2	12.8	5270.5

Table 6.2: *cost of manufacturing and its components comparison.*

The greatest expenditure for this kind of costs is for the operating labour. In general terms once through configurations have more heat exchangers and separators, such that more operators are required to run the plant, with a consequent higher global salary to pay. When

CO_2 separation is not performed, less cost of operating labour have to be afforded, since all the related equipment is absent.

Beside the operating labour, also the utility costs account for a great share of the overall COM. These consist in the cost for utility water provisioning and electricity. Considering that in any case the cost of utility water is about 4% of the total utility cost, more attention has been dedicated to the plant electric consumption.

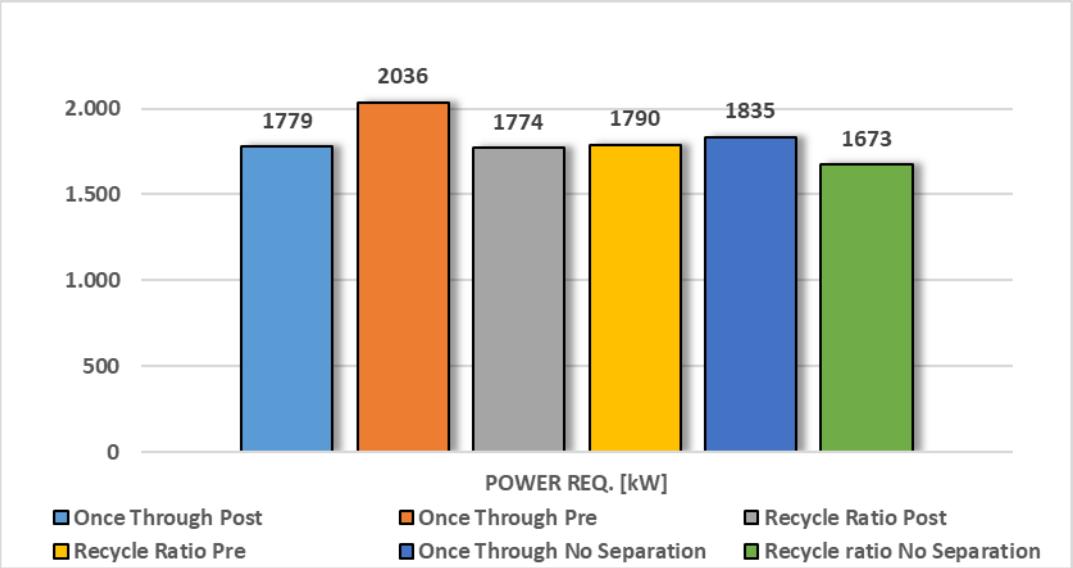

Figure 6.4: *plant electric power requirement comparison.*

Among the components requiring electricity it is possible to include blowers, pumps and compressors. Compressors consumption is the greatest share, more than 90% of the total requirement. Concerning the once through configuration, the plant consuming more is the one separating CO_2 from raw biogas, due to the highest circulating flow rate among all the plants. It has to be highlighted that when performing CO_2 separation at least one between raw biogas compressor and syngas compressor avoids processing the excess CO_2, with a consequent advantage in electric consumption. If separation is not adopted this benefit comes less. That is why despite the lower circulating flow rate the once through no separation case requires more electricity respect the post separation one.

Traditional arrangements have a generally lower circulating flow rate, yet they account for an additional compressor, the one devoted to syngas recirculation. A certain convenience

may be noticed when separation is not adopted, mainly due to a reduction in the recirculation compressor consumption: it processes a lower flow rate respect to the other cases according to the lower operating RR. This fact counteracts the additional power requirement due to the compression of excess CO_2.

Concerning the raw material cost its contribution is much lower respect to the other terms, but still not negligible. Lowest values are recorded again when separation is not performed, since there is no need to purchase amines.

Looking at the overall cost of manufacturing, the lowest COM are achieved again for the arrangement without separation section, thanks most of all to the reduction in required operators. The highest cost of manufacturing is recorded for the once through pre separation case, both due to higher electric consumption and to the higher number of operators required to run the plant.

Such considerations about COM and FCI are useful for a better understanding of the profitability analysis results. Accordingly, a summary of the yearly pure methanol production per each configuration is also reported in Table 6.3.

	Once Through Pre Separation	***Once Through Post Separation***	***Once Through No Separation***	***Traditional Pre Separation***	***Traditional Post Separation***	***Traditional No Separation***
Pure Methanol [tons/year]	22608	22836	22596	22968	21906	22821

Table 6.3: *summary of pure methanol yearly production.*

Figure 6.5 provides a graphical comparison of each plant PBP and ROROI, which respectively tell information about the time required to recover land and working capital costs and about the yearly return on the investment. Beside FCI and COM, both depend on the yearly income related to methanol retail on the market.

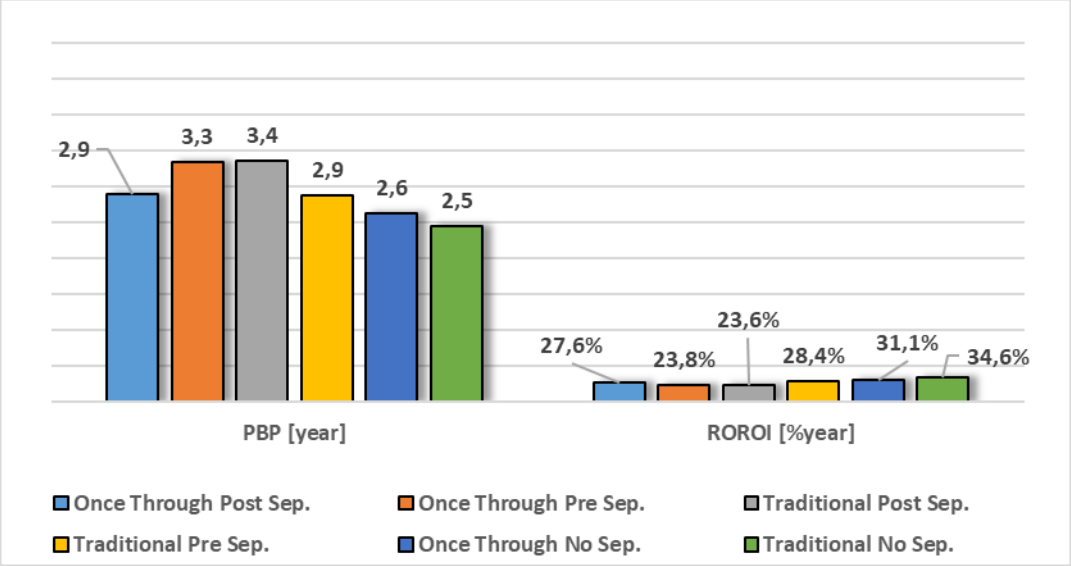

Figure 6.5: *PBP and ROROI comparison.*

The longest payback time as well as the lowest yearly return on investment are achieved for the once through pre separation and the traditional post separation cases for different reasons. The first has to sustain the highest fixed and operating costs, while the second is penalized by a lower pure methanol production and consequently lower yearly incomes.

It has been demonstrated that best performances in terms of methanol production are achieved for the once through post separation and the traditional pre separation cases. Thus, a higher income from methanol retail is expected. Despite the once through arrangement is cheaper in terms of fixed investment costs, the slightly lower methanol production and the higher COM make the traditional one more profitable, both according to the time criterion and the interest rate criterion. The difference in PBP is minimum, since almost 3 years are anyway required, yet from higher ROROI values more consistent cash flows are expected.

The best economic results have been recorded when CO_2 is not performed. The absence of the CO_2 separation section penalizes the synthesis reaction performances but allows a significant cost saving, especially considering the small scale of the plant under study. With such production rates it is more convenient to avoid the investment for additional equipment and the related operating costs, resulting in higher yearly cash flows. It can be noticed that

the highest ROROI, about 35%, is achieved for the traditional arrangement, coherently with the greater methanol production respect the once through case. This latter is anyway able to reach ROROI values over 30%. In terms of PBP more than 2 years are required in any case to recover land and working capital costs.

All these facts are coherent with the trend of the discounted cumulative cash flow (or NPV) reported. This is the profitability index that better quantifies the earning from the investment since it provides an estimation of the global cash flow obtained during the plant life time. A comparison of each case NPV along the life time of 25 years is reported in Figure 6.6, while Figure 6.8 and Figure 6.7 show a comparison focused on the specific configuration. In general the NPV curve is characterized by a minimum negative peak during the plant building phase, then it starts to rise depending on the yearly incomes.

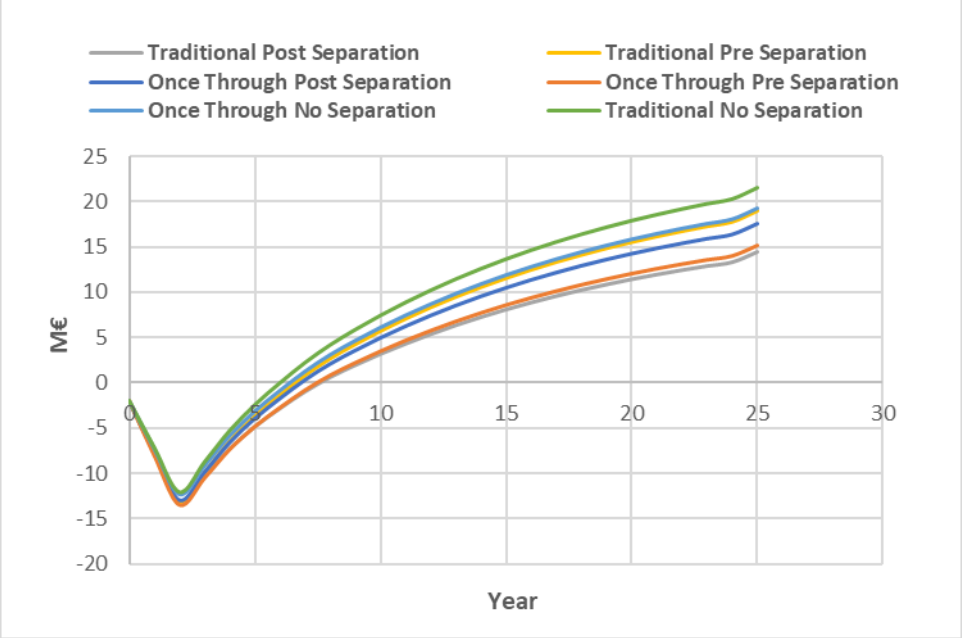

Figure 6.6: *discounted cash flow comparison between all the considered cases.*

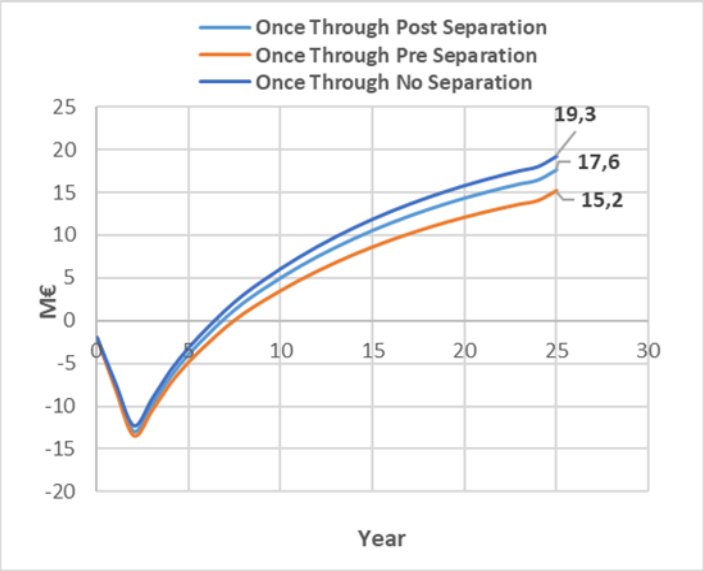

Figure 6.8: *discounted cumulative cash flow comparison – once through arrangement.*

Figure 6.7: *discounted cumulative cash flow comparison – traditional arrangement.*

Looking at the final NPV result, it is possible to state that the optimal plant configuration for the studied process is the one avoiding CO_2 separation and producing methanol with a traditional synthesis reactor. It is able to achieve a NPV equal to 21.6 M€. The absence of the separation section brings to similar results also with a multi stage once through Lurgi reactor, 19.3 M€. The once through no separation case is indeed confirmed to be the best solution for such plant variation.

Considerable and comparable NPV are achieved also performing CO_2 separation. In the traditional case the better solution is to perform it before the reforming reaction, while in the once through variation it is better after. The CO_2 location optimization allows to earn about 2 – 3 M€ more depending on the specific case.

6.2 Economic Impact of different operating pressures

Results of the technical analysis reported in section 5.1.3 showed that lower synthesis pressures are less favourable under a thermodynamic point of view. In spite of this fact, a yearly methanol production comparable at all with the high pressure operation could be obtained adopting high values of recycle ratio. This fact is crucial since it implies that almost the same revenues are achievable with lower fixed and operating costs. In this section the effect of different synthesis reaction operating pressures on plant economics has been assessed. For this purpose, the traditional arrangement adopting CO_2 separation before the reforming reaction has been assumed as base case.

As for the fixed investment, the operating pressure influences the overall FCI mainly due to two facts. At first, higher is the operating pressure of a certain component, higher will be the related pressure factor F_p , which is a multiplicator for the overall unit cost. Moreover, higher is the syngas compressor target pressure, higher will be its power requirement, which is used as capacity reference in the unit fixed cost correlation. The same is valid for the recirculation compressor. Because of these reasons, in Table 6.4 it is evident that lower is the synthesis pressure lower is the resultant FCI.

	90 bar	***70 bar***	***50 bar***
FCI [M€]	10.5	10.4	10.2
COM [k€]	5746.6	5636.4	5549.1

Table 6.4: *FCI and COM comparison for different synthesis reaction pressures.*

The cost of manufacturing is also reduced, mainly due to the reduction in the plant electric consumption. Raw material usage and number of operators are not affected by different operating pressures, such that their cost contribution keeps unchanged. Focusing on the plant electric power requirement, Table 6.5 confirms the utility cost reduction is related to the lower compression duty. Blowers and pumps operation is almost not affected by the synthesis reaction operating pressure change. A decrease in the synthesis pressure of 40 bar allows a cost saving about 200 k€/year on the manufacturing cost, a considerable amount.

Powered Units	***90 bar***		***70 bar***		***50 bar***	
	Power [kW]	%	Power [kW]	%	Power [kW]	%
Blowers	112.3	6.2	111.6	6.7	111.5	7.2
Pumps	44.9	2.5	43.5	2.6	42.2	2.7
Compressors	1647.5	91.3	1508.9	90.7	1392.0	90.1
TOTAL	1804.7	100.0	1664.0	100.0	1545.7	100.0

Table 6.5: *plant electric power consumptions for different synthesis reaction pressures.*

Such cost reduction has a positive effect also on plant profitability since, as anticipated, a similar methanol production is achieved in the three considered cases.

Table 6.6 and Figure 6.9 show that optimal results are achieved for the operating pressure of 50 bar, which ensures the greatest cost saving and the greatest methanol production thanks to the higher amount of recirculated unreacted feed.

	90 bar	***70 bar***	***50 bar***
PBP [year]	2.9	2.7	2.6
ROROI [%year]	28.4	29.3	30.5
Methanol yearly production [tons/year]	22968	22992	23030

Table 6.6: *profitability indicators and methanol yearly production comparison for different synthesis reaction pressures.*

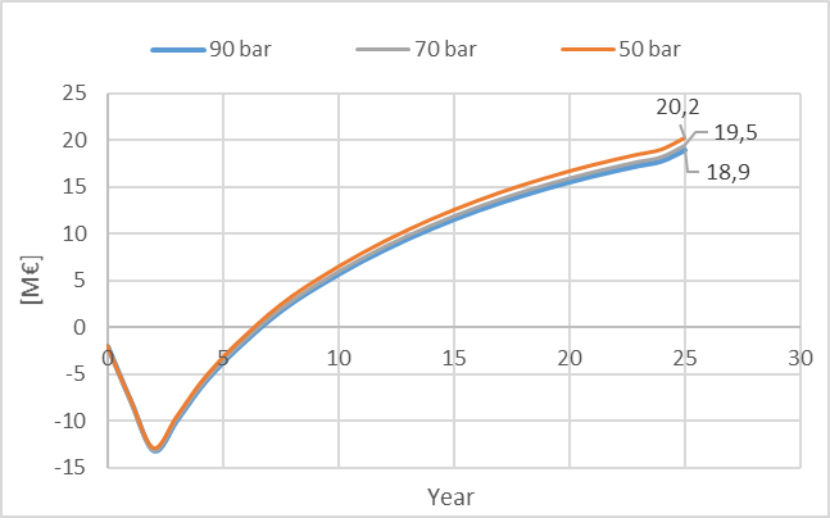

Figure 6.9: *discounted cumulative cash flow comparison for different synthesis reaction pressures.*

6.3 Economic Impact of methanol upgrading section integration

It has been demonstrated that the integration of a methanol upgrading section in the traditional plant arrangement is beneficial in terms of methanol production, even if it does not affect the reaction performances. This was related to the higher availability of fresh biogas in the main process. In this section it is detailed the impact on plant economics deriving from the integration of such additional components. To better appreciate differences, all the results have been compared with the baseline case.

Plant Configuration	***FCI [M€]***	***Biogas compression [M€]***	***CO_2 removal [M€]***	***Syngas production [M€]***	***Syngas compression [M€]***	***CH_3OH production [M€]***	***CH_3OH Purification [M€]***	***Steam production [M€]***	***Cooling system [M€]***
Without Purification	10.5	0.71	0.61	4.00	1.9	1.38	-	1.7	0.11
With Purification	12.3	0.73	0.62	4.2	2.0	1.4	1.5	1.8	0.11

Table 6.7: *fixed investment cost comparison.*

Table 6.7 provides a comparison in terms of fixed investment cost. Respect to the base case, an increase of FCI about 1.75 M€ it is recorded. It is mainly related to the purchase of the additional components, exchangers and distillation columns. Their cost has been estimated to be 1.46 M€. The remaining increase in the investment cost is related to the higher main stream flow rate circulating in the process. Due to the greater size of the components, higher costs are recorded almost in every section of the plant.

It is remarkable that the purification section fixed investment share is comparable with the methanol production island one. Figure 6.10 provides a graphical representation of the new FCI partition. Respect to the baseline, all the shares are simply redistributed as consequence of the introduction of the purification section, since the cost increase affect all the equipment.

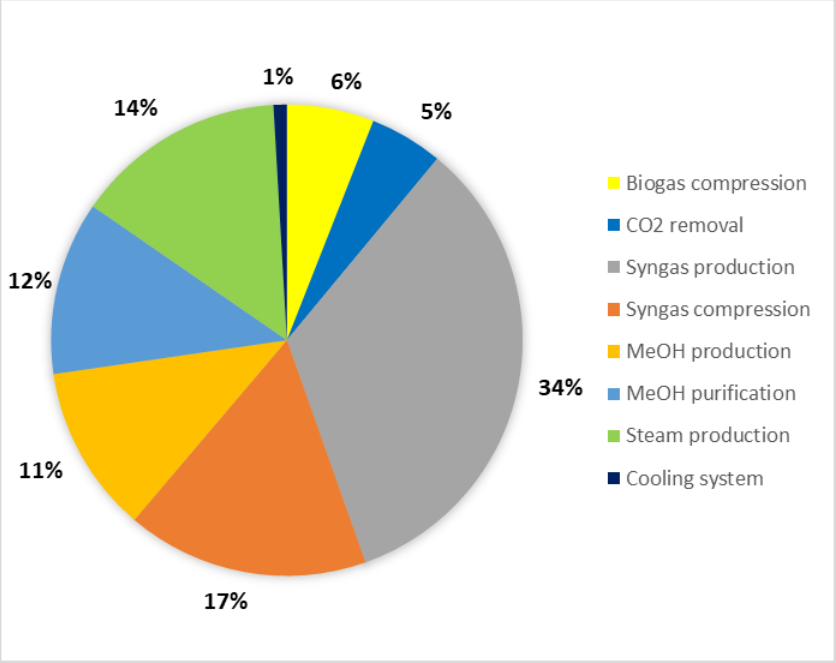

Figure 6.10: *FCI partition adopting a methanol upgrading section.*

As far as the operating costs are concerned, Table 6.8 shows that although more units are involved the operating labour cost keeps steady. This because there is no need for further operators. No significant variations concern the raw material cost, which gives a small contribution to the overall COM, anyway.

Plant Configuration	***Cut[k€/yy]***	***Col[k€/yy]***	***Crm[k€/yy]***	***COM[k€/year]***
Baseline	932.1	986.0	13.1	5746.6
Methanol upgrading integration	1018.1	986.0	13.2	6168.1

Table 6.8: *cost of manufacturing and its components comparison.*

The increase in the COM is mainly related to the higher FCI and utility costs. As in the previous case utility water contribution is almost negligible respect to the electricity cost contribution, about 6% of the total utility cost. Focusing on the electric consumption, Table 6.9 shows that almost 90% of the global power requirement is related to the compressors

operation. A higher consumption is recorded also for pumps and blowers due to the higher processed biogas flow rate.

Powered Units	***Baseline***		***Methanol upgrading integration***	
	Power [kW]	%	Power [kW]	%
Blowers	112.3	6.2	114.4	6.0
Pumps	44.9	2.5	49.9	2.6
Compressors	1647.5	91.3	1731.5	91.3
TOTAL	1804.7	100.0	1895.8	100.0

Table 6.9: *plant electric consumption details*

When evaluating plant profitability, the additional costs deriving from the integration of the purification section are balanced by the higher revenues related to the yearly methanol production (almost 1030 tons/year more are sold on the market). Anyway, for this specific small scale plant and its production rates, the benefits on the production efficiency are not enough respect to the cost increase. Even if the revenues are higher, the higher operating costs decreases the yearly cash flow during the plant working phase. Figure 6.11 indeed shows that the payback period is more than 3 years, while the rate of return on investment is penalized about 4 percentage points.

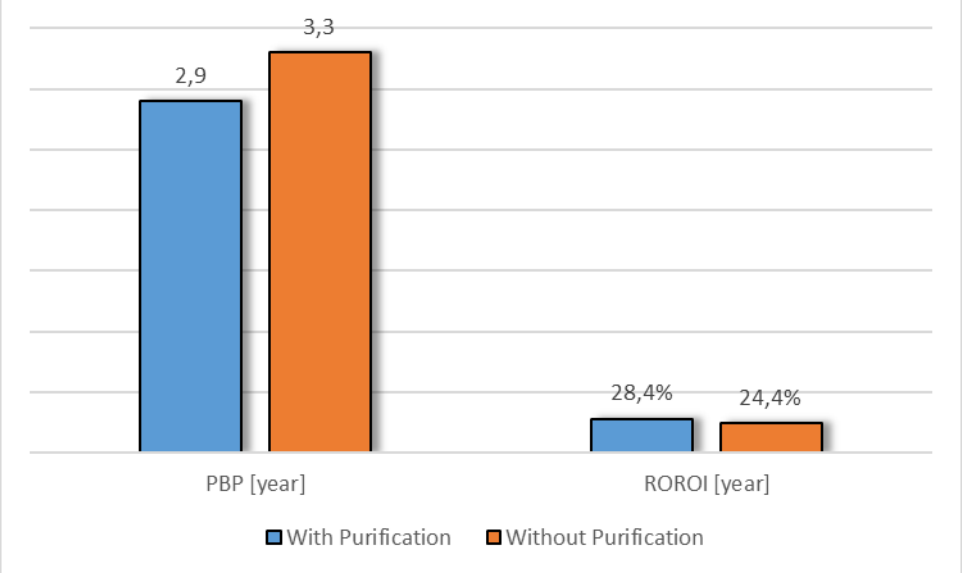

Figure 6.11: *PBP and ROROI comparison.*

Looking at the NPV trend along the whole plant lifetime in Figure 6.12 it is also evident a more negative peak, related to the higher investment cost.

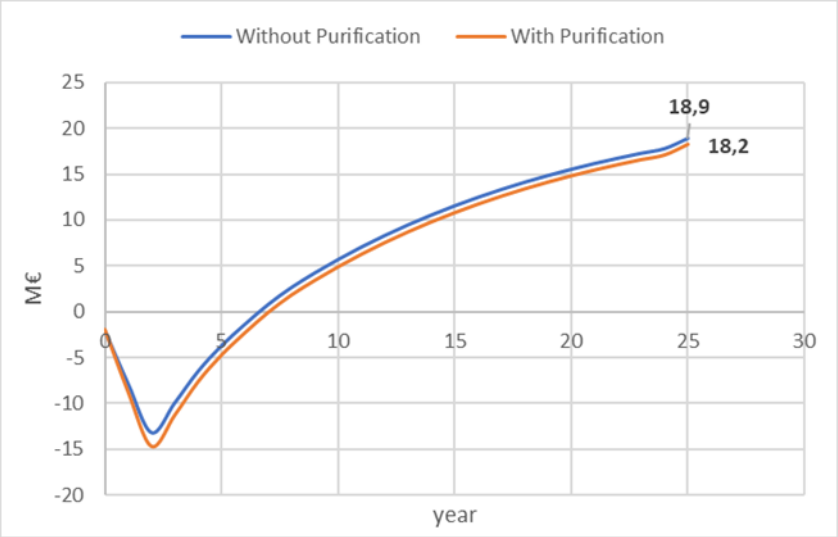

Figure 6.12: *discounted cash flow comparison.*

In the end, by integrating the purification section in the plant an overall NPV of 18.25 M€ is achieved, with a loss about 700 k€ respect to the base case. Results are practically comparable and the investment is confirmed to be quite profitable. Therefore, despite a certain economic loss it is still a valid solution for the considered case, considering that in this case there is no need of the external purification hub.

7. CONCLUSIONS

The present thesis work aimed to analyse performance and profitability of a small scale methanol production plant. An optimal plant design has been found both adopting a traditional synthesis reactor with unreacted feed recirculation and a once through multistage reactor. The main results are reported below:

- In the traditional arrangement the best synthesis reaction performances are obtained through CO_2 separation from the produced syngas. In particular a yield of 98% and a carbon conversion equal to 80% have been recorded, with an overall fuel efficiency of 65%. However, due to the lower fuel consumption and the higher fraction of processed syngas, the optimal location of the CO_2 separation section resulted to be upstream of the reforming reaction. In this case despite the lower reaction yield and carbon conversion (96% and 68% respectively) the highest methanol production rate and plant fuel efficiency are achieved. Respectively, 22968 tons/year and 66%. Sensitivity analysis showed that RR values about 6 favours the overall performances and allow to reach analogous production rates also for lower synthesis operating pressures.

- When a once through reactor is adopted a consistent amount of residual H_2 is recycled to the reformer as purge, mitigating the biofuel consumption. As result the optimal location of the CO_2 separation section resulted to be downstream the reforming reaction due to the favoured reaction operation. A sensitivity analysis highlighted that by performing a severe cooling of each reaction stage outlet stream down to 30°C it is possible to enhance the overall reactor and plant performances. In the optimal design a fuel efficiency of 65.4% and a global reaction yield of 85% are recorded, with a methanol yearly production about 22836 tons/year.

- Independently of the reactor configuration, the absence of a CO_2 separation section is detrimental for the synthesis reaction because of the inlet syngas stoichiometric

module different from the optimal value of 2.1. Reaction yields drop down to 70% but production levels over 22000 tons/year are still achieved.

- Globally, plant performances are comparable both adopting a once through and a traditional reactor, with a small convenience for this latter case.

- Results of the profitability analysis depend on fixed and operating costs, especially for the small plant size considered. All the studied plant arrangements are quite remunerative in a life time of 25 years with NPV values ranging from 15 to 21 M€. Land and working capital costs are recovered in 2 – 3 years with a yearly return on investment in the between 24 and 35%. Best economic results are recorded when the CO_2 separation is not performed due to the lower investment and manufacturing costs. The most profitable plant design is the one adopting a traditional reactor without syngas composition adjustment.

- The integration of a methanol purification section at the end of the traditional process does not affect reaction performances but reduces fuel consumption due to the additional purge stream recycled to the reformer furnace. This allows to process more inlet biogas and to boost plant productivity with a fuel efficiency of 2 percentage points greater (68%). This compensate the additional fixed and operating costs, resulting in an overall NPV about 18 M€.

FURTHER DEVELOPMENTS

- Evaluate the effect of Mathias modification of the RKS EoS on reactor performances.
- Enhance the once through reactor design by feeding part of the inlet syngas stream to all the reaction stages.
- Evaluate the integration in the plant of electrolysers providing additional H_2 for the synthesis reaction.
- Evaluate the integration of a methanol upgrading section in the once through arrangement.

- Evaluate the introduction of steam turbines to exploit the excess generated steam instead for power generation.
- Assess the effect of different tube lengths and diameters on reactor performances.
- Reduce tubes catalyst loading in the once through arrangement and evaluate the effect on the first stage temperature peak.

List of Symbols

$(CH_3)_3COCH_3$	*Methyl-tertiary-butyl-ether*
A_{exch} [m^2]	*Heat exchange area*
Al_2O_3	*Aluminium oxide*
A	*Reference Capacity*
C	*Carbon*
$C_{catalyst}$ [$/year]	*Catalyst cost*
$C_{cooling\ water}$ [$/year]	*Cooling water cost*
$C_{fresh\ water}$ [$/year]	*Fresh water cost*
C_{BM} [$]	*Bare module cost*
C_{elec} [$/kWh]	*Electricity cost*
CF [€/year]	*Cash Flow*
C_{GR} [$/year]	*Grassroots cost*
CH_3COOH	*Acetic Acid*
CH_3OH	*Methanol*
CH_4	*Methane*
C_{land} [M€]	*Land cost*
C_{MDEA} [$/year]	*Methyl-di-ethanol-amine cost*
CO	*Carbon Monoxide*
Co	*Cobalt*
CO_2	*Carbon Dioxide*
$CO3^-$	*Carbonate ion*
Col [$/year]	*Operating labour cost*
C_p^o[$]	*Purchase cost in base condition*
Cr_2O_3	*Chromium oxide*
C_{rm} [$/year]	*Raw material cost*
C_{TM} [$]	*Total module cost*
C_{ul} [$/year]	*Utility cost*
Df [-]	*Distillate to feed ratio*
d_k^{DDB}	*Yearly depreciation – Double Declining Balance Method*
D	*Diameter*
ε_C [-]	*Carbon conversion*
ε_{CH_4} [-]	*Methane conversion*
η_C [-]	*Carbon efficiency*
η_{CGE}[-]	*Cold gas efficiency*
η_{fuel}[-]	*Fuel efficiency*
η_{eq} [-]	*Equilibrium reaction yield*

$\eta_{Sep_{CO_2}}$ [-]	*Separation efficiency*
η_{Stage}[-]	*Reaction yield per stage*
η_{tot}[-]	*Total reaction yield*
F_{BM} [-]	*Bare module factor*
F_m [-]	*Material factor*
F_p [-]	*Pressure factor*
F_q [-]	*Quantity factor*
F_t [-]	*Superheating factor*
H_2	*Hydrogen*
H_2O	*Water*
H_2S	*Sulfuric acid*
HCO_3	*Hydrogen Carbonate*
I	*CEPCI*
K_p	*Chemical Equilibrium Constant*
M [-]	*syngas stoichiometric module*
Ni	*Nickel*
N_{ol}	*Rounded n° of operators*
O_2	*Oxygen*
Op_{lab}	*N° of operators*
P	*Total Pressure*
pi	*Partial pressure of the i-th species*
R [kJ/molK]	*Universal gas constant*
Rev [€/year]	*Yearly Revenues*
Rh	*Rhodium*
Rr	*Reflux ratio*
Ru	*Ruthenium*
SF [-]	*Stream Factor*
St	*Steam*
T	*Temperature*
$t_{replacement}$ [year]	*Catalyst replacement time*
V_o [m^3/kmol]	*Gas molar specific volume at normal conditions*
V_{reac} [m^3]	*Methanol reactor volume*
ω	*Pitzer acentric factor*
x_i	*Molar fraction of the i-th species*
ZnO	*Zinc oxide*
ΔH [kJ/kg]	*Enthalpy Variation*

Appendix

Aspen Unit Operation	*Inlet Stream(s)*	*Outlet Stream(s)*	*Heat Flux*
SPLITIN	BG1	BGCOMB - BG2	
BGMIX	BG2 - BGREC	BG3	
COMPR1	BG3	BG4 - COND	
ABSORBER	BG4	BG5 - LIQ1	
HEATM	LIQ1	LIQ2	
COOLER	REC3	REC4	
STRIPPER	LIQ2	VENT1 - REC1	
PUMP	REC1	REC2	
REBH	REB1 - LIQWAT2	REB2 - LIQWAT1	
REBF	REB2	REB3 - REB4	
HXBIO	BG5 - WS5	BG6 - WS6	
HXREF1	BG6 - WS2	BG7 - WS3	
MIX4	BG7 - WAT	BG8	
HXREF2	BG8 - WS1	BG9 - WS2	
REF	BG9	WS1	QLOSS - QREF
HXT2	WS3	WS5	QSYN2
HREC	WS6 - LIQWAT1	WS7 - LIQWAT2	
HXSYN2	WS7 - LIQWAT3	WS8 - LIQWAT4	
HBIOG1	LIQWAT4	LIQWAT3	
WATSEP1	WS8 - WATOUT1	DS1 - FW1	
COMPR3	DS1	DS2 - WATOUT1	
MIX2	DS2 - TG4	SM	
WATSEP2	FW1	BGREC - FW2A	
SEPID	FW2A	OUT - FW2	
DUPL	SM	SMR - SMID	
REQUIL	SMID	SYCR1V	
LURGI	SMR	SYCR1	QREAC1
HXMEOH1	SYCR1 - TG3	SYCR2 - TG4	
HXSEP3	SYCR2 - LIQWAT6	SYCR3 - LIQWAT5	
HXSEP4	SYCR3	SYCR4	
HBIOG2	LIQWAT5	LIQWAT6	
SEP3	SYCR4	TG1 - MEOHPROD	

SPLIT2	TG1	TG2 - PURGE1	
COMPR4	TG2	TG3	
BLOWER3	BGCOMB	BGCOMB2	
COMB	BGCOMB2 - PURGE1 - AIR 4	FG1	QRES - QREF
HXAIR2	FG1 - AIR3	FG2 - AIR4	
HXT1	FG2	FG5	QFG1
HXAIR1	FG5 - AIR2	FG6 - AIR3	
BLOWER1	AIR1	AIR2	
BLOWER2	FG6	FG7	
SC HIERARCHY	FW2	WAT	QREAC1 - QFG1 - QSYN1

Table A.1: *Table of base case Aspen flowsheet streams and unit operations*

Aspen Unit Operation	***Inlet Stream(s)***	***Outlet Stream(s)***	***Heat Flux***
SPLITIN	BG1	BGCOMB - BG2	
BGMIX	BG2 - BGREC	BG3	
COMPR1	BG3	BG4 - COND	
ABSORBER	BG4	BG5 - LIQ1	
HEATM	LIQ1	LIQ2	
COOLER	REC3	REC4	
STRIPPER	LIQ2	VENT1 - REC1	
PUMP	REC1	REC2	
REBH	REB1 - LIQWAT2	REB2 - LIQWAT1	
REBF	REB2	REB3 - REB4	
HXBIO	BG5 - WS5	BG6 - WS6	
HXREF1	BG6 - WS2	BG7 - WS3	
MIX4	BG7 - WAT	BG8	
HXREF2	BG8 - WS1	BG9 - WS2	
REF	BG9	WS1	QLOSS - QREF
HXT2	WS3	WS5	QSYN2

HREC	WS6 - LIQWAT1	WS7 - LIQWAT2	
HXSYN2	WS7 - LIQWAT3	WS8 - LIQWAT4	
HBIOG1	LIQWAT4	LIQWAT3	
WATSEP1	WS8 - WATOUT1	DS1 - FW1	
COMPR3	DS1	DS2 - WATOUT1	
WATSEP2	FW1	BGREC - FW2A	
SEPID	FW2A	OUT - FW2	
DUPL	SM	SMR - SMID	
REQUIL	SMID	SYCR1V	
LURGI	SMR	SYCR1	
HXSYCR1	SYCR1 - DS2	SYCR2 - DS3	
HXSEP3	SYCR2 - LIQWAT6	SYCR3 - LIQWAT5	
HXSEP4	SYCR3	SYCR4	
HBIOG2	LIQWAT5	LIQWAT6	
SEP3	SYCR4	SYCR5 - MEOH1	
LURGI2	SYCR5	SYCR6	QREAC2
HXSYCR2	SYCR6 - LIQWAT8	SYCR7 - LIQWAT7	
HBIOG3	LIQWAT7	LIQWAT8	
LRHX1	SYCR7	SYCR8	
SEP4	SYCR8	SYCR9 - MEOH2	
LURGI3	SYCR9	SYCR10	QREAC3
HXSYCR3	SYCR10 - LIQWAT10	SYCR11 - LIQWAT9	
HBIOG4	LIQWAT9	LIQWAT10	
LRHX2	SYCR11	SYCR12	
SEP5	SYCR12	SYCR13 - MEOH3	
LURGI4	SYCR13	MEOH4	QREAC4
HXSYCR4	MEOH4 - LIQWAT12	MEOH5 - LIQWAT11	
HBIOG5	LIQWAT11	LIQWAT12	
LRHX3	MEOH5	MEOH6	
SEP6	MEOH7	MEOHPRDO - PURGE1	
HUBMIX	MEOH6 - MEOH2 - MEOH3 - MEOH1	MEOH7	
HEATMIX	-	-	QREAC1 - QREAC2 - QREAC 3- QREAC4 - QTOT
BLOWER3	BGCOMB	BGCOMB2	
COMB	BGCOMB2 - PURGE1 - AIR 4	FG1	
HXAIR2	FG1 - AIR3	FG2 - AIR4	
HXT1	FG2	FG5	QRES - QREF
HXAIR1	FG5 - AIR2	FG6 - AIR3	
BLOWER1	AIR1	AIR2	QFG1

BLOWER2	FG6	FG7

Table A.2: *Table of Once Through Aspen flowsheet streams and unit operations*

Aspen Unit Operation	*Inlet Stream(s)*	*Outlet Stream(s)*	*Heat Flux*
MIX3	FW2 - FRESHWAT	19	
PUMP2	19	21	
HXF	21	22	QFG5 - QFG6
FLASH	20 - 22	23 - 24	
PUMP1	24	1	
SPLIT1	1	1 - 3	
ECO1	2	4	QSYN2 - QSYN3
ECO2	3	5	QFG4 - QFG5
MIX1	4 - 5 - 14	6	
SPLIT 2	6	7 - 8 - 9	
EVA1	7	10	QSYN1 - QSYN2
EVA2	8	11	QREAC1 - QREAC2
EVA3	9	12	QFG3 - QFG4
MIX2	10 - 11 - 12	13	
DRUM	13	14 - 15	
HXC3	15	16	QFG1 - QFG2
SPLIT3	16	17 - 18	
COND2	18	20	

Table A.3: S*ummary of streams and unit operations implemented in the heat recovery section Aspen flowsheet*

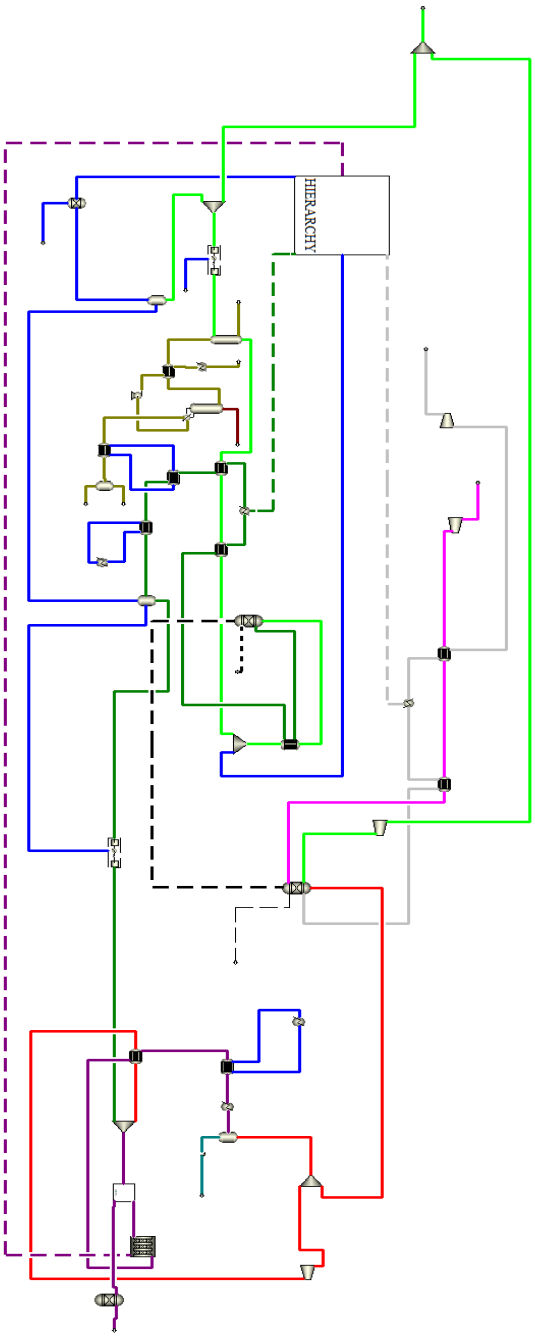

Figure A.0.1: *Traditional configuration Aspen flowsheet*

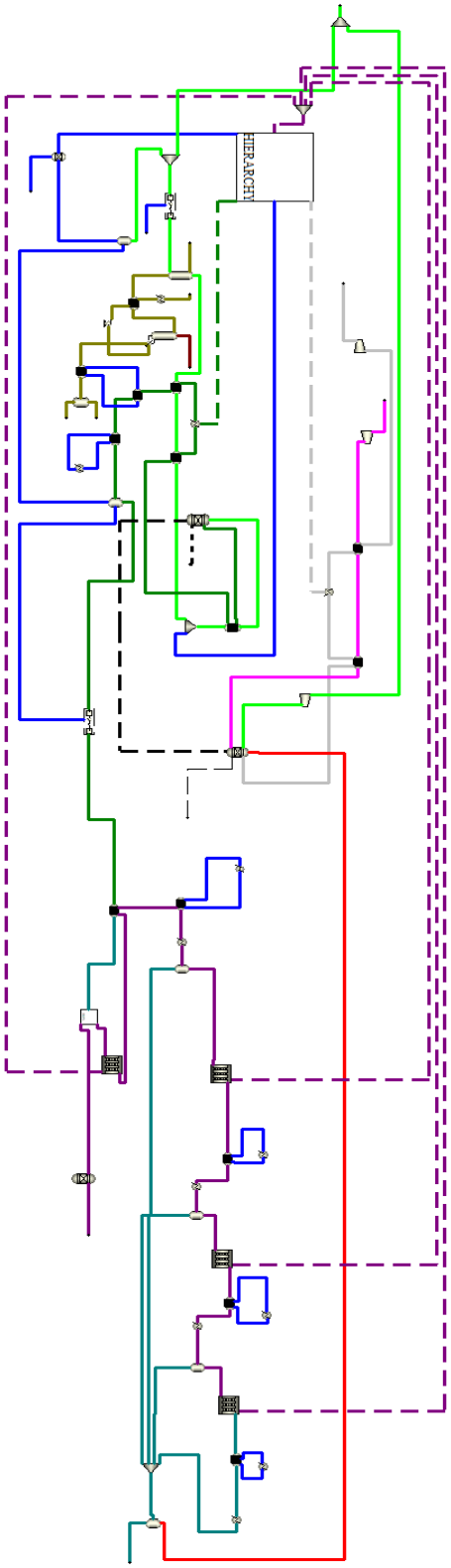

Figure A.0.2: *Once Through configuration Aspen flowsheet*

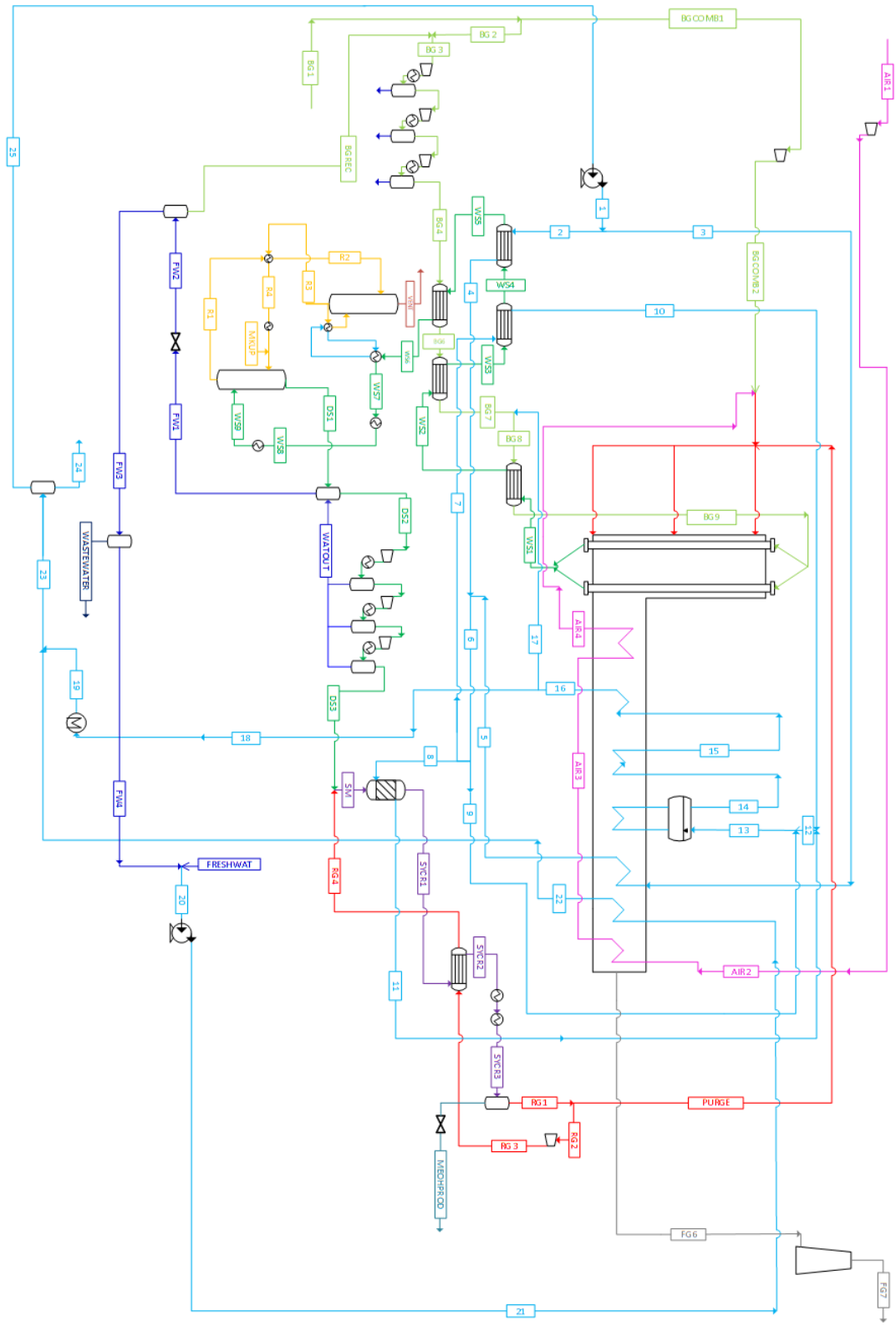

Figure A.0.3: *Traditional plant scheme adopting post reformer CO_2 separation*

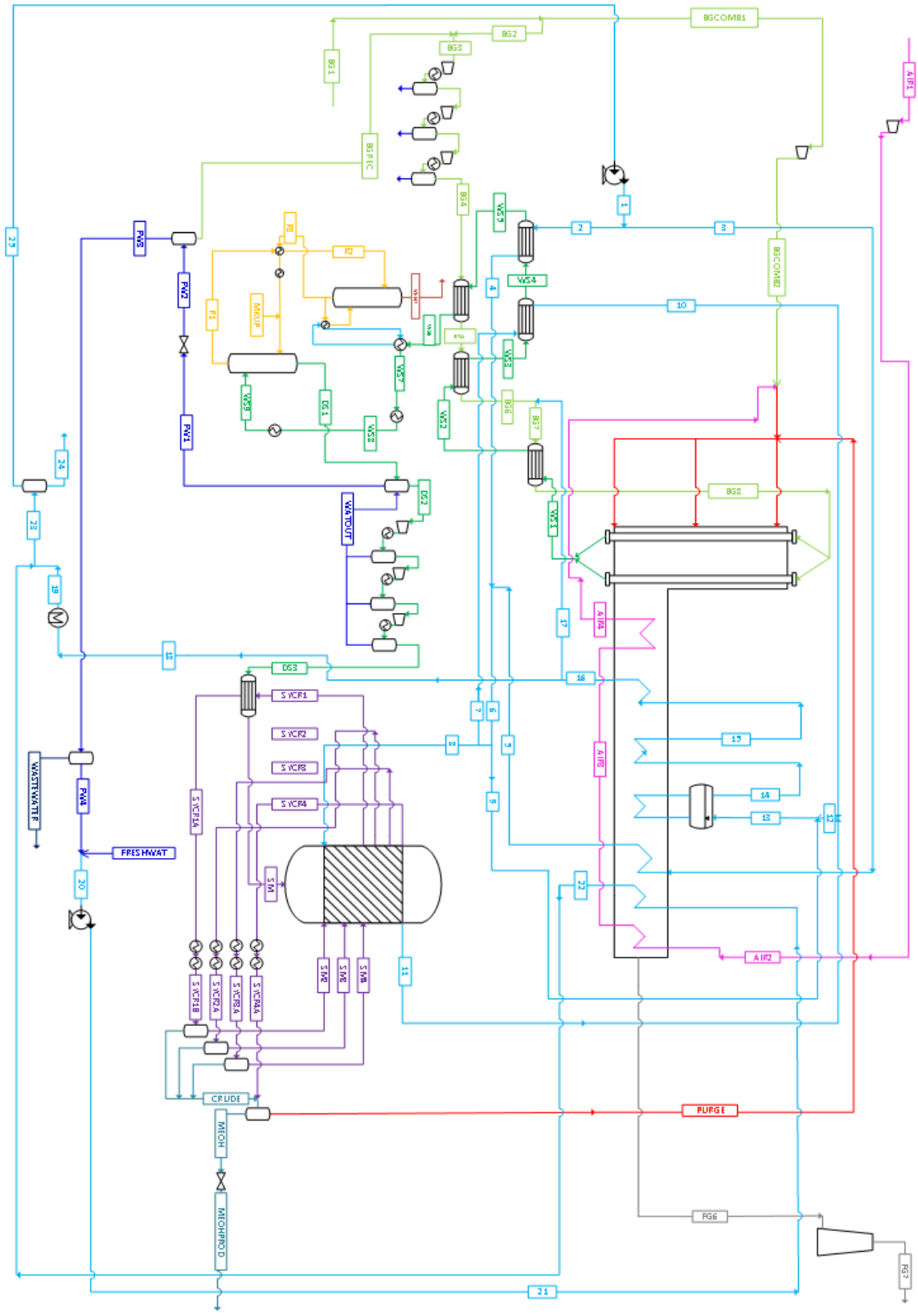

Figure A.0.4: *Once Through plant scheme adopting post reformer CO_2 separation*

Desing Variable = Tube Diameter						
Tube length [m]	6					
Tube Diameter [mm]	**46,6**			**42**		
Pressure [bar]	92,78					
n°Tubes	**Cost [$] 2019**	**Cost [$] 2015**	**Area [m2]**	**Cost [$] 2019**	**Cost [$] 2015**	**Area [m2]**
100	80.313,88	76.242,00	79,88	79.800,87	75.755,00	71,21
150	83.762,74	79.516,00	119,83	83.027,46	78.818,00	106,82
200	87.202,11	82.781,00	159,77	86.224,55	81.853,00	142,43
250	90.636,22	86.041,00	199,71	89.416,37	84.883,00	178,03
300	94.066,11	89.297,00	239,65	92.605,04	87.910,00	213,64
350	97.493,90	92.551,00	279,60	95.790,54	90.934,00	249,25
400	100.918,53	95.802,00	319,54	98.972,88	93.955,00	284,85
450	104.342,10	99.052,00	359,48	102.154,17	96.975,00	320,46
500	107.763,57	102.300,00	399,42	105.334,41	99.994,00	356,07
550	111.182,93	105.546,00	439,36	108.512,54	103.011,00	391,67
600	114.602,29	108.792,00	479,31	111.689,62	106.027,00	427,28
650	118.019,54	112.036,00	519,25	114.865,64	109.042,00	462,89
700	121.436,80	115.280,00	559,19	118.041,66	112.057,00	498,50
750	124.853,00	118.523,00	599,13	121.215,58	115.070,00	534,10
800	128.268,14	121.765,00	639,08	124.389,50	118.083,00	569,71
850	131.683,29	125.007,00	679,02	127.563,41	121.096,00	605,32
900	135.096,33	128.247,00	718,96	130.736,28	124.108,00	640,92
950	138.510,42	131.488,00	758,90	133.908,08	127.119,00	676,53
1000	141.923,46	134.728,00	798,84	137.079,89	130.130,00	712,14

Desing Variable = Tube Diameter					
6					
38			**25,6**		
92,78					
Cost [$] 2019	**Cost [$] 2015**	**Area [m2]**	**Cost [$] 2019**	**Cost [$] 2015**	**Area [m2]**
79.415,32	75.389,00	63,67	78.031,15	74.075,00	40,30
82.410,16	78.232,00	95,51	80.327,57	76.255,00	60,45
85.396,57	81.067,00	127,35	82.629,27	78.440,00	80,60
88.377,71	83.897,00	159,18	84.925,70	80.620,00	100,75
91.355,70	86.724,00	191,02	87.221,07	82.799,00	120,90
94.331,57	89.549,00	222,86	89.513,29	84.975,00	141,05
97.305,34	92.372,00	254,70	91.803,39	87.149,00	161,20
100.275,95	95.192,00	286,53	94.092,45	89.322,00	181,35
103.246,56	98.012,00	318,37	96.380,45	91.494,00	201,50
106.215,06	100.830,00	350,21	98.667,40	93.665,00	221,65
109.182,51	103.647,00	382,04	100.953,29	95.835,00	241,80
112.149,96	106.464,00	413,88	103.238,13	98.004,00	261,95

115.115,30	109.279,00	445,72	105.522,97	100.173,00	282,10
118.080,64	112.094,00	477,55	107.806,76	102.341,00	302,25
121.044,93	114.908,00	509,39	110.090,55	104.509,00	322,40
124.009,22	117.722,00	541,23	112.373,28	106.676,00	342,55
126.972,45	120.535,00	573,06	114.656,01	108.843,00	362,70
129.935,69	123.348,00	604,90	116.937,69	111.009,00	382,85
132.897,87	126.160,00	636,74	119.219,37	113.175,00	403,00

Table A.4: *EDR reactor cost sensitivity analysis: tube diameter*

Desing Variable = Pressure				
Tube length [m]	6			
Tube Diameter [mm]	42			
Pressure [bar]	**40**		**50**	
Area [m2]	**Cost [€] 2019**	**Cost [$] 2015**	**Cost [€] 2019**	**Cost [$] 2015**
71,21362227	56.398,68	59.964,00	58.788,59	62.505,00
106,8204334	59.233,47	62.978,00	61.628,09	65.524,00
142,4272445	62.088,02	66.013,00	64.482,64	68.559,00
178,0340557	64.937,86	69.043,00	67.332,48	71.589,00
213,6408668	67.783,94	72.069,00	70.179,50	74.616,00
249,247678	70.628,14	75.093,00	73.023,70	77.640,00
284,8544891	73.470,46	78.115,00	75.865,08	80.661,00
320,4613002	76.310,90	81.135,00	78.705,52	83.681,00
356,0681114	79.149,45	84.153,00	81.545,01	86.700,00
391,6749225	81.988,01	87.171,00	84.382,63	89.717,00
427,2817336	84.824,68	90.187,00	87.219,30	92.733,00
462,8885448	87.660,42	93.202,00	90.055,98	95.749,00
498,4953559	90.495,21	96.216,00	92.890,77	98.763,00
534,102167	93.330,01	99.230,00	95.725,57	101.777,00
569,7089782	96.163,86	102.243,00	98.559,42	104.790,00
605,3157893	98.997,71	105.256,00	101.392,34	107.802,00
640,9226004	101.829,69	108.267,00	104.225,25	110.814,00
676,5294116	104.662,60	111.279,00	107.057,22	113.825,00
712,1362227	107.493,63	114.289,00	109.889,19	116.836,00

Desing Variable = Pressure
6
42

70		92,78341	
Cost [€] 2019	**Cost [$] 2015**	**Cost [€] 2019**	**Cost [$] 2015**
64.160,03	68.216,00	71.250,78	75.755,00
67.017,40	71.254,00	74.131,66	78.818,00
69.871,94	74.289,00	76.986,20	81.853,00
72.721,79	77.319,00	79.836,05	84.883,00
75.567,87	80.345,00	82.683,07	87.910,00
78.412,07	83.369,00	85.527,27	90.934,00
81.254,39	86.391,00	88.368,65	93.955,00
84.094,82	89.411,00	91.209,08	96.975,00
86.933,38	92.429,00	94.048,58	99.994,00
89.771,94	95.447,00	96.886,20	103.011,00
92.608,61	98.463,00	99.722,87	106.027,00
95.444,35	101.478,00	102.558,61	109.042,00
98.279,14	104.492,00	105.394,34	112.057,00
101.113,93	107.506,00	108.228,20	115.070,00
103.947,79	110.519,00	111.062,05	118.083,00
106.781,64	113.532,00	113.895,90	121.096,00
109.613,62	116.543,00	116.728,82	124.108,00
112.446,53	119.555,00	119.560,79	127.119,00
115.277,56	122.565,00	122.392,76	130.130,00

Table A.5: *EDR reactor cost sensitivity analysis: operating pressure*

Linear regression			
92,78 bar			
Coefficiente angolare	89,31	73.510,44	**Intercetta**
s1,s2,..,sn	0,03	12,86	**sb**
R^2	1,00	24,99	**Errore Standard**
F	9.232.875,14	17,00	**gdl**
sqreg	5.764.242.689,03	10.613,39	**sqres**
70 bar			
Coefficiente angolare	89,30	65.548,28	**Intercetta**
s1,s2,..,sn	0,02	10,79	**sb**
R^2	1,00	20,96	**Errore Standard**
F	13.112.721,12	17,00	**gdl**
sqreg	5.762.675.048,97	7.471,03	**sqres**
65,00			
Coefficiente angolare	89,29	63.887,74	**Intercetta**
s1,s2,..,sn	0,02	10,28	**sb**
R^2	1,00	19,97	**Errore Standard**

F	14.450.445,76	17,00	**gdl**
sqreg	5.762.159.248,21	6.778,80	**sqres**
50 bar			
Coefficiente angolare	89,29	59.516,88	**Intercetta**
s1,s2,..,sn	0,02	9,61	**sb**
R^2	1,00	18,67	**Errore Standard**
F	16.529.887,18	17,00	**gdl**
sqreg	5.761.663.565,35	5.925,53	**sqres**
40 bar			
Coefficiente angolare	89,29	56.836,00	**Intercetta**
s1,s2,..,sn	0,02	9,30	**sb**
R^2	1,00	18,06	**Errore Standard**
F	17.664.350,26	17,00	**gdl**
sqreg	5.761.228.185,83	5.544,55	**sqres**

Table A.6: *Linear regression results: operating pressure*

Linear regression			
46,6 mm			
Coefficiente angolare	85,66	73.526,33	**Intercetta**
s1,s2,..,sn	0,02	11,73	**sb**
R^2	1,00	22,78	**Errore Standard**
F	12.857.354,37	17,00	**gdl**
sqreg	6.672.452.388,31	8.822,32	**sqres**
42 mm			
Coefficiente angolare	89,31	73.510,44	**Intercetta**
s1,s2,..,sn	0,03	12,86	**sb**
R^2	1,00	24,99	**Errore Standard**
F	9.232.875,14	17,00	**gdl**
sqreg	5.764.242.689,03	10.613,39	**sqres**
38 mm			
Coefficiente angolare	93,29	73.525,26	**Intercetta**
s1,s2,..,sn	0,03	10,61	**sb**
R^2	1,00	20,62	**Errore Standard**
F	11.823.249,92	17,00	**gdl**
sqreg	5.028.052.745,99	7.229,56	**sqres**
25,6 mm			
Coefficiente angolare	113,53	73.487,34	**Intercetta**
s1,s2,..,sn	0,03	7,89	**sb**
R^2	1,00	15,32	**Errore Standard**

F	12.709.622,86	17,00	**gdl**
sqreg	2.983.148.676,04	3.990,17	**sqres**

Table A.7:*Linear regression results: tube diameter*

Desing variable = tube Length												
Tube length [m]	4			5			6					
Tube Diameter [mm]	42											
Pressure [bar]	92,78341											
n°Tubes	Cost [$] 2019	Cost [$] 2015	Area [m2]	Cost [$] 2019	Cost [$] 2015	Area [m2]	Cost [$] 2019	Cost [$] 2020	Area [m2]			
100	72.825,21	69.133,00	47,48	76.386,78	72.514,00	59,34	79.800,87	75.755,00	71,21362227			
150	75.389,20	71.567,00	71,21	79.262,58	75.244,00	89,02	83.027,46	78.818,00	106,8204334			
200	77.944,77	73.993,00	94,95	82.155,24	77.990,00	118,69	86.224,55	81.853,00	142,4272445			
250	80.502,44	76.421,00	118,69	85.042,63	80.731,00	148,36	89.416,37	84.883,00	178,0340557			
300	83.074,86	78.863,00	142,43	87.926,86	83.469,00	178,03	92.605,04	87.910,00	213,6408668			
350	85.645,18	81.303,00	166,17	90.807,92	86.204,00	207,71	95.790,54	90.934,00	249,247678			
400	88.212,33	83.740,00	189,90	93.685,83	88.936,00	237,38	98.972,88	93.955,00	284,8544891			
450	90.777,38	86.175,00	213,64	96.562,69	91.667,00	267,05	102.154,17	96.975,00	320,4613002			
500	93.341,37	88.609,00	237,38	99.438,49	94.397,00	296,72	105.334,41	99.994,00	356,0681114			
550	95.904,31	91.042,00	261,12	102.312,19	97.125,00	326,40	108.512,54	103.011,00	391,6749225			
600	98.465,14	93.473,00	284,85	105.184,83	99.852,00	356,07	111.689,62	106.027,00	427,2817336			
650	101.025,98	95.904,00	308,59	108.056,42	102.578,00	385,74	114.865,64	109.042,00	462,8885448			
700	103.585,76	98.334,00	332,33	110.928,00	105.304,00	415,41	118.041,66	112.057,00	498,4953559			
750	106.144,48	100.763,00	356,07	113.797,49	108.028,00	445,09	121.215,58	115.070,00	534,102167			
800	108.702,15	103.191,00	379,81	116.666,97	110.752,00	474,76	124.389,50	118.083,00	569,7089782			
850	111.259,83	105.619,00	403,54	119.536,45	113.476,00	504,43	127.563,41	121.096,00	605,3157893			
900	113.816,45	108.046,00	427,28	122.403,82	116.198,00	534,10	130.736,28	124.108,00	640,9226004			
950	116.373,07	110.473,00	451,02	125.272,25	118.921,00	563,77	133.908,08	127.119,00	676,5294116			
1000	118.928,63	112.899,00	474,76	128.138,57	121.642,00	593,45	137.079,89	130.130,00	712,1362227			

Table A.8: *EDR reactor cost sensitivity analysis: tube length*

Linear regression			
4 m			
Coefficiente angolare	107,93	67.708,78	**Intercetta**
s1,s2,..,sn	0,02	5,74	**sb**
R^2	1,00	11,15	**Errore Standard**
F	30.087.779,19	17,00	**gdl**
sqreg	3.741.302.758,83	2.113,89	**sqres**
5 m			
Coefficiente angolare	96,89	70.669,57	**Intercetta**
s1,s2,..,sn	0,03	9,65	**sb**
R^2	1,00	18,74	**Errore Standard**
F	13.414.210,39	17,00	**gdl**
sqreg	4.710.921.395,99	5.970,21	**sqres**
6 m			
Coefficiente angolare	89,31	73.510,44	**Intercetta**
s1,s2,..,sn	0,03	12,86	**sb**
R^2	1,00	24,99	**Errore Standard**
F	9.232.875,14	17,00	**gdl**
sqreg	5.764.242.689,03	10.613,39	**sqres**

Table A.9: *Linear regression results: tube length*

Tube length [m]	6		
Tube External Diameter [mm]	42		
Pressure [bar]	93		
N° Of Tubes	**Area [m2]**	**Cost [€] 2019**	**Cost [$] 2015**
3000	2.261,95	250.382,75	257.025,00
3100	2.337,34	256.449,80	263.253,00
3200	2.412,74	262.515,88	269.480,00
3300	2.488,14	268.581,95	275.707,00
3400	2.563,54	274.648,03	281.934,00
3500	2.638,94	280.713,13	288.160,00
3600	2.714,34	286.779,21	294.387,00
3700	2.789,73	292.844,31	300.613,00
3800	2.865,13	298.908,44	306.838,00
3900	2.940,53	304.973,54	313.064,00
4000	3.015,93	311.037,67	319.289,00
4100	3.091,33	317.101,80	325.514,00
4200	3.166,73	323.165,93	331.739,00
4300	3.242,12	329.230,06	337.964,00
4400	3.317,52	335.293,21	344.188,00
4500	3.392,92	341.356,36	350.412,00

4600	3.468,32	347.419,52	356.636,00
4700	3.543,72	353.482,67	362.860,00
4800	3.619,11	359.545,83	369.084,00
4900	3.694,51	365.608,01	375.307,00
5000	3.769,91	371.670,19	381.530,00
5100	3.845,31	377.733,34	387.754,00
5200	3.920,71	383.795,52	393.977,00
5300	3.996,11	389.856,73	400.199,00
5400	4.071,50	395.918,91	406.422,00
5500	4.146,90	401.981,09	412.645,00
5600	4.222,30	408.042,29	418.867,00
5700	4.297,70	414.103,50	425.089,00
5800	4.373,10	420.165,68	431.312,00
5900	4.448,50	426.226,88	437.534,00
6000	4.523,89	432.288,09	443.756,00
6100	4.599,29	438.348,32	449.977,00
6200	4.674,69	444.409,53	456.199,00
6300	4.750,09	450.470,73	462.421,00
6400	4.825,49	456.530,97	468.642,00
6500	4.900,88	462.591,20	474.863,00
6600	4.976,28	468.652,40	481.085,00
6700	5.051,68	474.712,64	487.306,00
6800	5.127,08	480.772,87	493.527,00
6900	5.202,48	486.833,10	499.748,00
7000	5.277,88	492.892,36	505.968,00
7100	5.353,27	498.952,59	512.189,00
7200	5.428,67	505.012,82	518.410,00
7300	5.504,07	511.072,08	524.630,00
7400	5.579,47	517.132,31	530.851,00
7500	5.654,87	523.191,57	537.071,00
7600	5.730,27	529.250,83	543.291,00
7700	5.805,66	535.311,06	549.512,00
7800	5.881,06	541.370,31	555.732,00
7900	5.956,46	547.429,57	561.952,00
8000	6.031,86	553.488,83	568.172,00

Table A.10: *Default arrangement cost values for a wider validity range*

Linear Regression			
92,78 bar			
Coefficiente angolare	80,40	68.558,30	**Intercetta**
s1,s2,..,sn	0,00	7,73	**sb**

R^2	1,00	14,28	**Errore Standard**
F	1.992.074.205,18	49,00	**gdl**
sqreg	406.057.130.793,31	9.987,98	**sqres**

Table A.0.11:*Linear regression results applied on Table A0.10*

Calculator	***Task***	***Arrangement***
C-AEXCMD	Heat exchange surface calculation	Once Through/Recirculation
C-ACOOL	Heat exchange surface calculation	Once Through/Recirculation
C-AHXSE4	Heat exchange surface calculation	Once Through/Recirculation
C-CARBE	Carbon Efficiency calculation	Once Through/Recirculation
C-CONVME	Reformer Methane Conversion calculation	Once Through/Recirculation
C-CGEFT	Reformer Cold Gas Efficiency calculation	Once Through/Recirculation
C-CO2	Separation Efficiency calculation	Once Through/Recirculation
C-CONVC	Carbon Conversion calculation	Once Through/Recirculation
C-ECONOM	Economic analysis calculations	Once Through/Recirculation
C-GHSV	Synthesis reactor GHSV calculation	Once Through/Recirculation
C-HXSEP3	Heat exchange surface calculation	Once Through/Recirculation
C-RECY	Recycle Ratio calculation	Once Through/Recirculation
C-MDEA	Fresh make up MDEA calculation	Once Through/Recirculation
C-MR	Syngas module M calculation	Once Through/Recirculation
C-POWTOT	Global Power requirement calculation	Once Through/Recirculation
C-PPUMP	Steam cycle main pump outlet pressure calculation	Once Through/Recirculation
C-QLOSS	Reformer Heat Loss calculation	Once Through/Recirculation
C-SC	Steam to Methane ratio calculation	Once Through/Recirculation
C-THXRE1	Outlet cold side fluid temperature calculation	Once Through/Recirculation

C-TQ	T-Q diagrams parameters calculation	Once Through/Recirculation
C-VOLABS	Absorber volume calculation	Once Through/Recirculation
C-VOLSEP	Separator volume calculation	Once Through/Recirculation
C-VOLSTR	Stripper volume calculation	Once Through/Recirculation
C-VOLWS1	Separator volume calculation	Once Through/Recirculation
C-VOLWS2	Separator volume calculation	Once Through/Recirculation
C-YIELDT	Global reaction yield calculation	Once Through/Recirculation
C-YIELDV	Equilibrium reaction yield calculation	Once Through/Recirculation
C-FUELEF	Plant Fuel Efficiency calculation	Once Through/Recirculation
C-HXSYC4	Heat exchange surface calculation	Once Through
C-LRHX1	Heat exchange surface calculation	Once Through
C-LRHX2	Heat exchange surface calculation	Once Through
C-LRHX3	Heat exchange surface calculation	Once Through
C-VSEP4	Separator volume calculation	Once Through
C-VSEP5	Separator volume calculation	Once Through
C-VSEP6	Separator volume calculation	Once Through
C-DPME1	Pressure Drop across the unit calculation	Once Through/Recirculation
C-DPHREF	Pressure Drop across the unit calculation	Once Through/Recirculation

Table A.12: *List of all calculators implemented in the Aspen simulation*

Acronyms

AD	*Anaerobic Digestion*
ATR	*Auto-Thermal Reforming*
BASF	*Baden Aniline and Soda Factory*
BGTL	*Biogas to liquid*
CEPCI	*Chemical Engineering Plant Cost Index*
CGE	*Cold Gas efficiency*
CIS	*Commonwealth of Independent States*
CAGR	*Compound Annual Growth Rate*
COM	*Cost of manufacturing*
DME	*Di-methyl-ether*
DMFC	*Direct Methanol Fuel cell*
DDB	*Double Declining Balance*
DR	*Dry Reforming*
EoS	*Equations of State*
EU	*European Union*
EDR	*Exchanger Desing and Rating*
FTR	*Fired Tubular Reformer*
GHSV	*Gas hourly space velocity*
GHG	*Greenhouse gases*
GDP	*Gross Domestic Product*
HRSG	*Heat Recovery Steam Generator*
IMPCA	*International Methanol Producers and Consumers Association*
KPI	*Key Performance Indicators*
LHHW	*Langmuir-Hinshelwood-Hougen-Watson*
LNG	*Liquid Natural Gas*
LPG	*Liquid Petroleum Gas*
LHV	*Lower Heating Value*
MTG	*Methanol to gasoline*
MTO	*Methanol to olefine*
MTP	*Methanol to propylene*
MDEA	*Methyl-Di-Ethanol-Amine*
MEA	*Methyl-Ethanol-amine*
MTBE	*Methyl-tertiary-butyl-ether*
NPV	*net present value*
NRTL	*Non Random Two Liquid*

PBP	*Pay Back period*
PSA	*Pressure Swing Absorption*
PFD	*Process Flow Diagram*
ROROI	*rate of return on investment*
RR	*Recycle Ratio*
RK	*Redlich - Kwong*
RKS	*Redlich - Kwong - Soave*
RON	*Research Octane Number*
RWGS	*Reverse Water Gas Shift*
SMR	*Steam Methane Reforming*
SR	*Steam Reforming*
SF	*Stream Factor*
TAnD	*Thermophilic Anaerobic Digestion*
TR	*Tri Reforming*
TEMA	*Tubular Exchanger Manufacturers' Association*
US	*United States*
VLE	*Vapour Liquid equilibrium*
VFA	*Volatile Fatty Acids*
WGS	*Water Gas Shift*

REFERENCES

[1] L. Riva, I. Martinez, M. Martini, F. Gallucci, M. Van Sint Annaland, M.C. Romano, "Techno-economic analysis of the Ca-Cu process integrated in hydrogen plants with CO2 capture", 2018;

[2] Jhonson Matthey, “Technology Review” pp 172-182 “Methanol production – A technical history”, 2017;

[3] A. Vita, C. Italiano, D. Previtali, C. Fabiano, A. Palella, F. Freni, G. Bozzano, L. Pino, F. Manetti, “Methanol synthesis from biogas: a thermodynamic analysis”, 2018;

[4] Silje Kreken Almeland, Knut Åge Meland and Daniel Greiner Edvardsen, "Process Design and Economical Assessment of a Methanol Plant", Norwegian University of Science and Technology, Department of Chemical Engineering, Process Desing course project, 2009;

[5] Kim Winther, "Methanol as motor fuel", Danish Technological Institute 2019;
[6] A. A. Kiss, J. J. Pragt, H. J. Vos, G. Bargeman, M. T. de Groot, " Novel efficient process for methanol synthesis by CO2 hydrogenation", 2015;

[7] Jhonson Matthey, “Technology Review”, 61(4) pp 297-307, "Reducing the carbon intensity of methanol for use as a transport fuel", 2017;

[8] D. Seddon, Duncan Seddon & Associates Pty. Ltd, Australia, "Methanol and dimethyl ether (DME) production from synthesis gas" 12, 2011;

[9] Methanol Safe Handling Technical Bulletin, Methanol Institute, "Compatibility of Metals & Alloys in Neat Methanol Service", " https://www.methanol.org/";

[10] Elton Amirkhas, Raj Bedi, Steve Harley,Trevor Lango, "Methanol Production in Trinidad e Tobago", Final report, University of California, Davis, 2006;

[11] L. R. Clausen, N. Houbak, B. Elmegaard, "Technoeconomic analysis of a methanol plant based on gasification of biomass and electrolysis of water", 2010;

[12] "Electricity Currents: A Survey of Current Industry News and Developments" The Electricity Journal 30, pp 65-68, 2017 ;

[13] I. Dimitriou, H. Goldingway, A. V. Bridgewater," Techno-economic and uncertainty analysis of Biomass to Liquid (BTL) systems for transport fuel production", 2018;

[14] H. Zang, L. Wang, M. Perez-Fortes, J. Van Herle, F. Maréchal, U. Desideri, "Techno-economic optimization of biomass-to-methanol with solid-oxide electrolyzer", 2020;

[15] "Learn How to Optimize Heat Exchanger Designs using Aspen Shell & Tube Exchanger.", Aspentech, 2015;

[16] "Water electrolysis & renewable energy systems", Fuel cell Today, Orchard Road, Royston, UK, 2013.

[17] Donald E. Garrett, "Chemical Engineering Economics", Van Nostrand Reinhold, New York, 1989;

[18] H. P. Loh, Jennifer Lyons, Charles W. White, "Process Equipment Cost Estimation", Final Report, 2002;

[19] Herib Blanco, Wouter Nijs, Johannes Ruf, André Faaij, "Potential for hydrogen and Power-to-Liquid in a low-carbon EU energy system using cost optimization", 2018;

[20] Richard A. Turton, Joseph A. Shaeiwitz, Debangsu Bhattacharyya, Wallace B. Whiting, "Analysis, synthesis and desing of chemical processes", 5th edition, 2018;

[21] G. de Guido, notes from the course of "Chemical Processes and Technologies" 2019;

[22] Cooling Tower Products, How much do a cooling tower cost, "https://www.coolingtowerproducts.com/cooling-tower-cost/";

[23] A. Brenna, notes from course of "Corrosion and Material Protection" 2020;

[24] "Biogas Cost Reductions to Boost Sustainable Transport", Irena "https://www.irena.org/newsroom/articles/2017/Mar/Biogas-Cost-Reductions-to-Boost-Sustainable-Transport", 2017;

[25] Statistical Review of World Energy - CO2 emissions, British Petroleum, "https://www.bp.com/en/global/corporate/energy-economics/statistical-review-of-world-energy/co2-emissions.htm", 2020;

[26] P. Chiesa, notes from course of "Sistemi Energetici Avanzati" 2019.
[27] Statistical Review of World Energy - Primary Energy, British Petroleum," https://www.bp.com/en/global/corporate/energy-economics/statistical-review-of-world-energy/primary-energy.html", 2020;

[28] Johannes W. A. Langeveld and Eric C. Peterson, "Biofuel and Biorefinery Technologies" vol.6, 2, "Feedstocks for Biogas Production: Biogas and Electricity Generation Potentials" pp 35-49;

[29] A. Bordoni, E. Romagnoli, E. Foppa Pedretti, G. Toscano, G. Rossini, E. Cozzolino, G. Riva, "La filiera del biogas", ASSAM - Agenzia Serv. Sett. Agroaliment. delle Marche;

[30] S. Rasi, A. Veijanen, J. Rintala, "Trace compounds of biogas from different biogas production plants", Energy 32, 1375-1380, 2007;

[31] W.M. Budzianowski, "A review of potential innovations for production, conditioning and utilization of biogas with multiple-criteria assessment", Renew. Sust. Energy Rev. 54 1148 - 1171, 2016;

[32] C. Yao, W. Pan, A. Yao, "Methanol fumigation in compression-ignition engines: A critical review of recent academic and technological developments", 2017;

[33] A. Onorati, notes from the course of "Internal Combustion Engines", 2019;

[34] "The essential chemical industry online", Methanol, "https://www.essentialchemicalindustry.org/chemicals/methanol.html", 2017;
[35] Research and Markets, "The global methanol market 2019-2027", " http://www.globenewswire.com", 2019;

[36] Wikipedia, " Methyl tert-butyl ether", " https://en.wikipedia.org/wiki/Methyl_tert-butyl_ether";

[37] Methanol Institute, "Dimethyl Ether", " https://www.methanol.org/dimethyl-ether-dme/#:~:text=Synthesis%20gas%20is%20then%20converted,in%20the%20production%20of%20DME.";

[38] G. A. Olah, A. Geoppert, G. K. Surya Prakash, " Beyond Oil and Gas: The Methanol Economy", 2009;

[39] S. Soundarajan, A.K. Dalai, F. Berruti, "Modeling of methanol to olefins (MTO) process in a circulating fluidized bed reactor", 2000;

[40] C. Cremers, M. Scholz,W. Seliger, A. Racz,W. Knechtel, J. Rittmayr, F. Grafwallner, H. Peller, and U. Stimming, "Developments for Improved Direct Methanol Fuel Cell Stacks for Portable Power", 2006;

[41] PubChem, "Formaldehyde", "https://pubchem.ncbi.nlm.nih.gov/compound/Formaldehyde";

[42] G. Iaquaniello, G. Centi, A. Salladini, E. Palo, "Methanol", 22, pp 595-612, "Methanol Economy: Environment, Demand, and Marketing With a Focus on the Waste-to-Methanol Process", 2018;

[43]"Chemical Economics handbook - Methanol", "https://ihsmarkit.com/products/methanol-chemical-economics-handbook.html";

[44] Mansur M. Masih, Khaled Albinali, Lurion De Mello, "Price dynamics of natural gas and the regional methanol markets", 2009;

[45] X. Xu, Y. Liu, F. Zhang, "Clean coal technologies in China based on methanol platform", 2017;

[46] "Global Energy review 2020", IEA, "https://www.iea.org/reports/global-energy-review-2020";

[47] Chicago, Author-Date, 15th ed. Rounsaville, and Fritz Ullmann. 1985. "Ullmann's Encyclopedia of industrial chemistry". Weinheim, Federal Republic of Germany: VCH (6,11);

[48] S. Lee, J. G. Speight, and S. K. Loyalka, "Handbook of alternative fuel technologies", 2018;

[49] Benjamín Cañete, Carlos E. Gigola, Nélida B. Brignole, "Synthesis Gas Processes for Methanol Production via CH4 Reforming with CO2, H2O, and O2", 2014;

[50] Preeti Gangadharan, Krishna C. Kanchi, Helen H. Lou, "Evaluation of the economic and environmental impact of combining dry reforming with steam reforming of methane", 2012;

[51] Treccani, "Enciclopedia degli Idrocarburi," vol. 2, 2006;

[52] S. D. Angeli, G. Monteleone, A. Giaconia and A. A. Lemonidou, "State of the art of catalysts for CH4 steam reforming at low temperature," International Journal of Hydrogen Energy, vol. 39, (5), pp. 1979-1997, 2014;

[53] K. Aasberg-Petersen, I. Dybkjær, C. V. Ovesen, N. C. Schjødt, J. Sehested and S. G. Thomsen, "Natural gas to synthesis gas – Catalysts and catalytic processes," Journal of Natural Gas Science and Engineering, vol. 3, (2), pp. 423-459, 2011;

[54] Muhammad Usman, W.M.A. Wan Daud, Hazzim F.Abbas, "Dry reforming of methane: Influence of process parameters-A review", 2015;

[55] Chunshan Song, Wei Pan, "Tri-reforming of methane: a novel concept for catalytic production of industrially useful synthesis gas with desired H2/CO ratios", 2004;

[56] Jay J. Cheng, "Biomass to renewable energy process", 2nd edition, 2018;

[57] P. Silva, notes from the course of "Power Production from Renewable sources", 2019;

[58] Juntao Zhang, Shengrong Liang, Xiao Feng, "A novel multi effect methanol distillation process", 2010;

[59] Angelo Basile, Francesco Dalena, "Methanol Science and Engineering", 2018;

[60] Carlo N. Hamelinck, André P.C. Faaij, "Production of methanol from biomass", 2006;

[61] Xiaochen Xue, Qianfeng Gu, Habimana Pascal, Osama M. Darwesh, Bing Zhang, Zhiqiang Li,"Simulation and optimization of three-column triple-effect methanol distillation scheme", 2020;

[62] "Scheda dati di sicurezza, metanolo > 99% per sintesi" https://www.carlroth.com/com/en/;

[63] Ning Gao, Chi Zhai,Wei Sun, X. Zhang "Equation oriented method for Rectisol wash modelling and analysis", 2015;

[64] K. M. Kim, J. C. Kim, M. Cheong, J. S. Lee, Y. G. Kim, "Chemical equilibria in methanol synthesis from methyl formate", 1990;

[65] J. G. van Bennekom, J. G. M. Winkelman, R. H. Venderbosch, S.D.G.B. Nieland, and H. J. Heeres, "Modeling and Experimental Studies on Phase and Chemical Equilibria in High-Pressure Methanol Synthesis", 2012;

[66] G. H. Graaf and J. G. M. Winkelman, "Chemical Equilibria in Methanol Synthesis Including the Water Gas Shift Reaction: A Critical Reassessment", 2016;

[67] G. Groppi, notes from the course of "Fundamental of chemical processes", 2018

[68] N. Bouneb, A. H. Meniai, W. Louaer, " Introdcution of the group contribution concept into the NRTL model", 2012;

[69] Petar Dijinovic, Ferdi Schüth, " Electrochemical Energy Storage for Renewable Sources and Grid Balancing", chapter 12 "Energy carriers made from hydrogen", 2015;

[70] T.A. Adams, M. Eden "Learn Aspen Plus in 24h", 2017;

[71] K. M. Vanden Bussche, G. F. Froment "A Steady-State Kinetic Model for Methanol Synthesis and the Water Gas Shift Reaction on a Commercial Cu/ZnO/Al2O3 Catalyst", 1996;

[72] Aspentech, “Aspen Plus Methanol Synthesis Model,” vol. 12, 2011;

[73] G. Herz, E. Reichelt, J. Mathias "Design and evaluation of a Fischer-Tropsch process for the production of waxes from biogas", 2017;

[74] J. Palonen, P. Huttenhuis, G. Rexwinkel, M. Astolfi, C. Elsido"Flexible Dimethyl ether prodcution from biomass gasification with sorption enhanced process", 2016;

[75] U.S Bureau of Labour Statistics, "Occupational Employment and Wages, May 2019", 2019;

[76] D.E. Garrett "Chemical Engineering Economics", 1987;

[77] K. A. G. Schmidt, Y. Maham and A. E. Mather "Use of the NRTL equation for simultaneous correlation of vapour-liquid equilibria and excess enthalpy Applications to aqueous alkanolamine systems", 2007;

[78] B. K. Mondal, S. S. Bandyopadhyay, A. N. Samanta "Vapor–liquid equilibrium measurement and ENRTL modelling of CO2 absorption in aqueous hexamethylenediamine", 2015;

[79]Chemical engineering essentials for the CPI professional, https://www.chemengonline.com/pci-home;

[80] Andrea Montebelli, Carlo GiorgioVisconti, Gianpiero Groppi, EnricoTronconi, Cristina Ferreira, Stefanie Kohler "Enabling small-scale methanol synthesis reactors through the adoption of highly conductive structured catalysts", 2013;

[81] Andrea Montebelli, Carlo GiorgioVisconti, Gianpiero Groppi, EnricoTronconi, Cristina Ferreira, Stefanie Kohler "Optimization of compact multitubular fixed-bed reactors for the methanol synthesis loaded with highly conductive structured catalysts", 2014;